CHAPTER 7

SELECTED TOPICS IN BIFURCATION THEORY

This chapter introduces some basic ideas in bifurcation theory and gives a few examples of current interest. This subject is very large and the chapter cannot pretend to cover anything but a sampling. For this reason two sections—7.2 and 7.5—are written in the nature of surveys; we hope these will alert the reader to some of the important current literature. Sections 7.1 and 7.4 introduce basic ideas in the static and dynamic theory, respectively, and Sections 7.3 and 7.6 select a nontrivial example from each theory to work in detail. These examples are biased towards the authors' interests, so readers may wish to substitute one of their own choosing from the literature.

7.1 BASIC IDEAS OF STATIC BIFURCATION THEORY

This section presents a few sample results in static bifurcation theory. The reader should understand that there are many different points of view in this subject and that the results can be refined in several directions. Some of the books that the serious reader should consult after reading this section are Keller and Antman [1969], Sattinger [1973], Nirenberg [1974], Berger [1977], Iooss and Joseph [1980], and Antman [1983].

We begin with a few introductory remarks. Consider a beam free to move in a plane, distorted from its natural state by the application of a load λ, as shown in Figure 7.1.1. For small λ, the beam slightly compresses, but after a critical load λ_c is reached, it buckles into one of two possible states. The compressed state is still there, but it has become unstable; the stability has been transferred from the original trivial solution to the stable buckled solutions. The situation

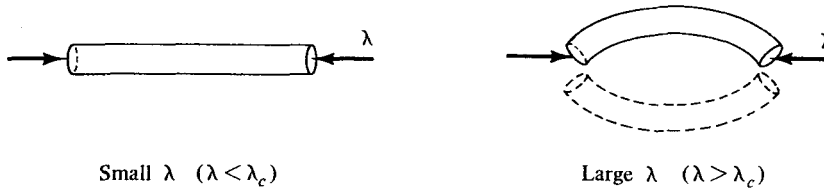

Figure 7.1.1

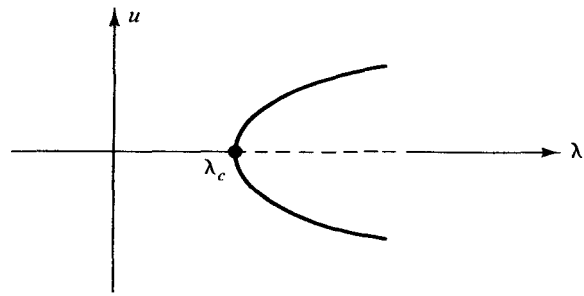

Figure 7.1.2

can be summarized by drawing the pitchfork bifurcation diagram, as in Figure 7.1.2. The vertical axis u represents the displacement of the center line of the beam. In this diagram, stable solutions are drawn with a solid line and unstable ones with a dashed line. One usually concentrates on stable solutions since these are the only ones one will "see."

There are many ways one can model the beam depicted in Figure 7.1.1. First, one could use a full model of three-dimensional elasticity. Second, one could use a rod-model and take into account shearing and extensibility. Perhaps the simplest, however, is the original model adopted by Euler in 1744, which effectively started the subject of bifurcation theory. He assumed the beam is an "elastica"; inextensible and unshearable. If s, ranging from 0 to 1, represents arc length along the beam (so s is a material variable) and $\theta(s)$ is the angle of deflection of the tangent at s, Euler derived the equation

$$EI\theta'' + \lambda \sin\theta = 0, \qquad \theta(0) = \theta(1) = 0,$$

where EI is a constant. There is extensive literature on this equation; we recommend the introductory article in Keller and Antman [1969] for an account. The problem was largely solved by Euler and one gets a bifurcation diagram as shown in Figure 7.1.3. As we shall see shortly, the points of bifurcation $\lambda/EI = k^2\pi^2$ $(k = 1, 2, 3, \ldots)$ on the λ-axis can be readily computed; they are the eigenvalues of the linearized problem about the trivial solution $\theta = 0$; that is,

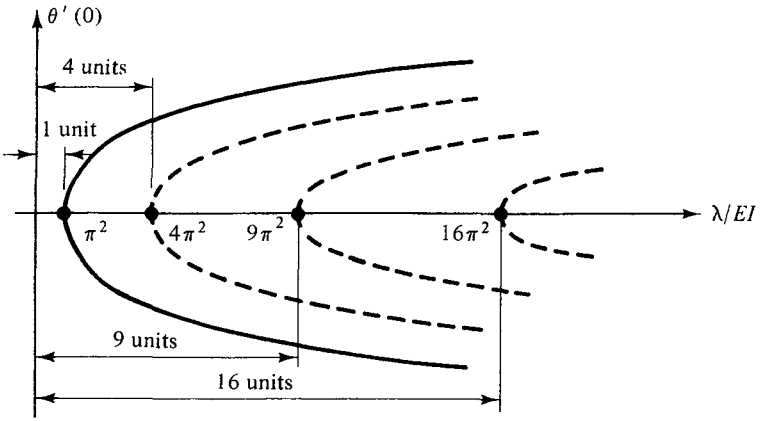

Figure 7.1.3

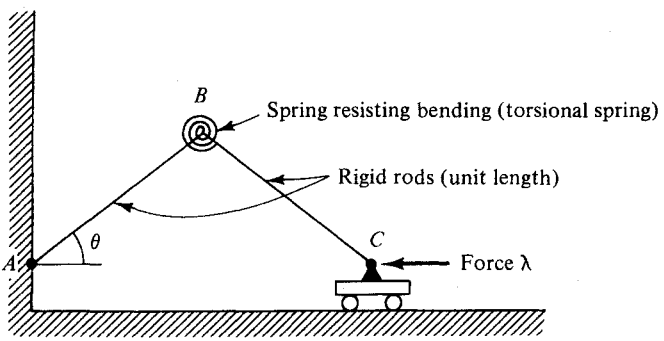

Figure 7.1.4

$EI\phi'' + \lambda\phi = 0$, $\phi(0) = \phi(1) = 0$. See Love [1927], §263 for the actual configurations of the elastica.

A "simpler" model that has the same buckling features as in Figure 7.1.2 is obtained by restricting to a "one mode" model, as in Figure 7.1.4. If the torsional spring has a spring constant κ, the potential energy is $V = \kappa\theta^2/2 + 2\lambda(\cos\theta - 1)$. The equilibria are the critical points of V:

$$\kappa\theta - 2\lambda \sin\theta = 0.$$

Near $\lambda/\kappa = \frac{1}{2}$, the trivial solution $\theta = 0$ bifurcates into two solutions, as in Figure 7.1.2. Note that this can be predicted by the inverse function theorem; if $F(\theta, \lambda) = \kappa\theta - 2\lambda \sin\theta$, then $(\partial F/\partial\theta)(0, \lambda) = \kappa - 2\lambda\cos 0 = \kappa - 2\lambda$, which vanishes when $\kappa - 2\lambda = 0$; that is, $\lambda/\kappa = \frac{1}{2}$. Thus it is near this point that the

implicit function theorem fails to show that $\theta = 0$ is the unique solution. In terms of a series,

$$F(\theta, \lambda) = \kappa\theta - 2\lambda\left(\theta - \frac{\theta^3}{3!} + \frac{\theta^5}{5!} - \cdots\right)$$

and the first term vanishes if $\kappa = 2\lambda$. For $\lambda/\kappa > \frac{1}{2}$ there are two solutions, $\theta = 0$ and the solutions of

$$(\kappa - 2\lambda) + \frac{2\lambda\theta^2}{3!} - \frac{2\lambda\theta^4}{4!} + \cdots = 0.$$

Clearly, if θ is a solution, so is $-\theta$, and so θ is approximately the solution of

$$(\kappa - 2\lambda) + \frac{2\lambda}{3!}\theta^2 = 0,$$

that is,

$$\theta = \pm[3(2\lambda - \kappa)]^{1/2} + \text{higher-order terms.}$$

Graphically, we see the two solutions in Figure 7.1.5. From this graph we can also obtain the *global* bifurcation picture, as in Figure 7.1.6. Note the differences with Figure 7.1.3. The stability of solutions can be examined by looking at whether or not the solution is a maximum or minimum of V. For example, as λ/κ is increased beyond $\frac{1}{2}$, what happens to V in a neighborhood of $\theta = 0$ is depicted in Figure 7.1.7.

Before beginning the theory, we summarize a few things that examples like this teach us.

1.1 Remarks

(a) The problem of static bifurcation may be stated abstractly as that of solving an equation $f(x, \lambda) = 0$, where λ denotes one or more param-

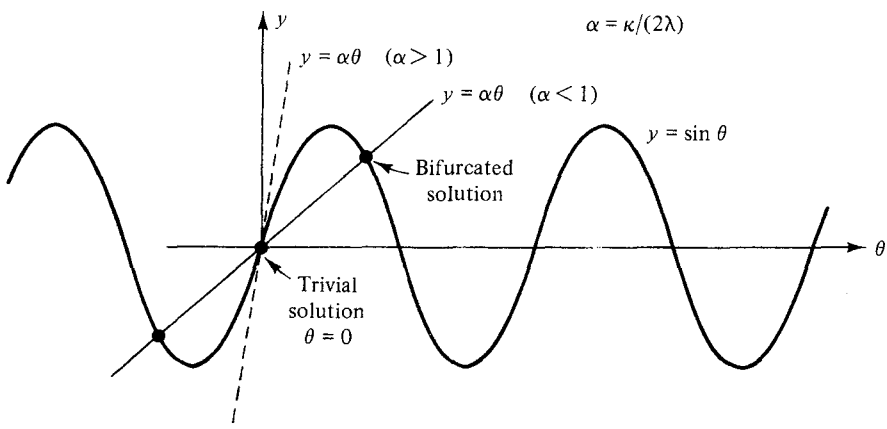

Figure 7.1.5

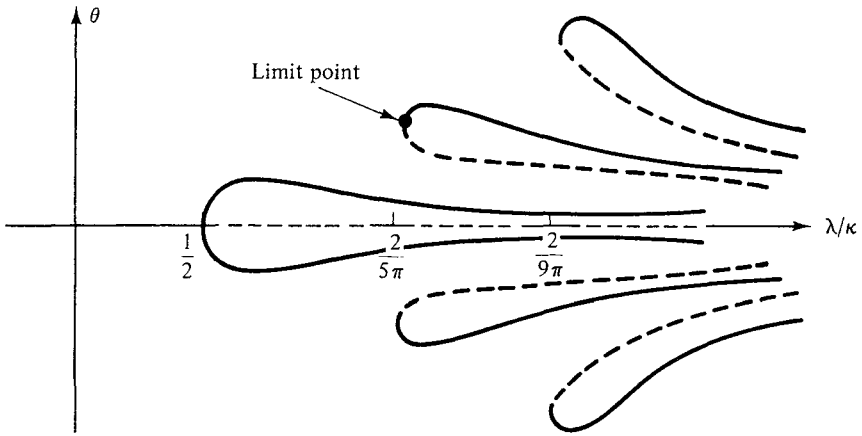

Figure 7.1.6

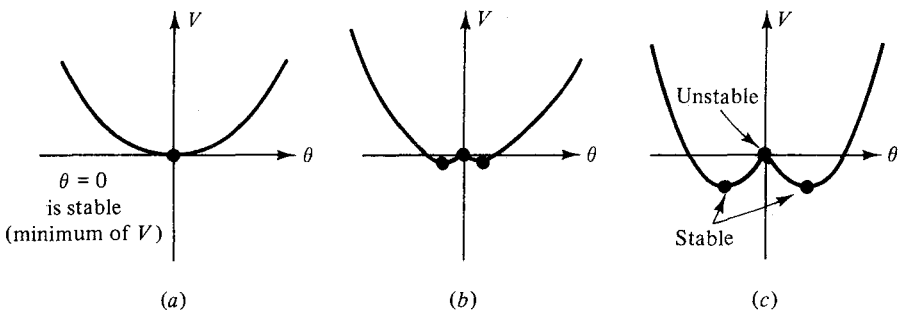

Figure 7.1.7 (a) $\lambda/\kappa < \frac{1}{2}$. (b) $\lambda/\kappa = \frac{1}{2}+$. (c) $\lambda/\kappa > \frac{1}{2}$.

eters to be varied and x is a variable representing the state of the system.

(b) When solutions are located, it is important to decide which are stable and which are unstable; this may be done by determining the spectrum of the linearization or by testing for maxima or minima of a potential.

(c) Is the bifurcation diagram sensitive to small perturbations of the equations or the addition of further parameters? A bifurcation diagram that is insensitive to such changes is called *structurally stable*.

(d) Before any declaration is made that "the complete global bifurcation diagram is obtained," the following criteria should be fulfilled: (i) Are you sure you have *all* the essential parameters (see (c))? (ii) Does the model you have chosen remain a good one for large values of the parameter and the variable?

Let us comment briefly on (c) and (d). The bifurcation diagram in 7.1.6 near $\theta = 0$, $\lambda/\kappa = \frac{1}{2}$ is *structurally unstable*. If an additional imperfection parameter is included, the bifurcation diagram changes. For example, in Figure 7.1.4, let ϵ be the distance between the direction of λ and the point A—that is, the vertical distance between A and C. If the solutions are plotted in ϵ, θ space, where $\mu = (\lambda/\kappa) - \frac{1}{2}$, we get the situation shown in Figure 7.1.8. This is generally

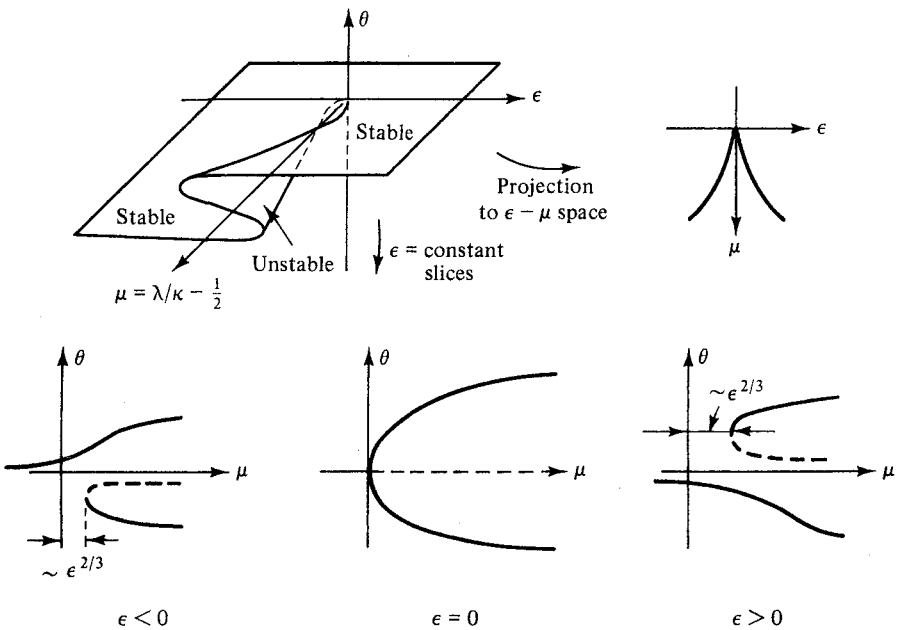

Figure 7.1.8

called an *imperfection-sensitivity diagram*. (The $\frac{2}{3}$ power law of Koiter [1945] is noted.) We discuss these points in greater depth in Box 1.1, and especially the important point: is one extra parameter like ϵ sufficient to completely capture all possible perturbations? (It is not, even for this basic example.)

Comment d(ii) is also relevant; suppose one goes to the trouble to produce the global bifurcation diagram in Figure 7.1.6. Are these extra branches meaningful? They correspond to θ beyond the range $[0, 2\pi]$, where the torsional spring has been "wound up" a number of extra times. For very large windings the linear spring law presumably breaks down, or, due to other constraints, large windings may be prohibited (the mechanism may not allow it). It then requires some work to decide which portions of Figure 7.1.6 are actually relevant to the problem at hand.

Now we begin the mathematical development of static bifurcation theory. Let us start with the simplest situation in which we have a trivial solution available and have one parameter. Thus, let $\mathfrak{X}$ and $\mathfrak{Y}$ be Banach spaces and let $f\colon \mathfrak{Y} \times \mathbb{R} \longrightarrow \mathfrak{X}$ be a given C^∞ mapping; assume that $f(0, \lambda) = 0$ for all λ.

1.2 Definition We say that $(0, \lambda_0)$ is a *bifurcation point* of the equation $f(x, \lambda) = 0$ if every neighborhood of $(0, \lambda_0)$ contains a solution (x, λ) with $x \neq 0$.

The following gives a necessary condition for bifurcation.

1.3 Proposition *Suppose that $A_\lambda = D_x f(0, \lambda)$ (the derivative with respect to x) is an isomorphism from $\mathfrak{Y}$ to $\mathfrak{X}$. Then $(0, \lambda)$ is* not *a bifurcation point.*

Proof By the implicit function theorem (see Section 4.1) $f(x, \lambda) = 0$ is uniquely solvable for $x(\lambda)$ near $(0, \lambda)$; since $x = 0$ is a solution, no others are possible in a neighborhood of $(0, \lambda)$. ∎

1.4 Example Suppose $f(x, \lambda) = Lx - \lambda x + g(x, \lambda)$, where $g(0, \lambda) = 0$ and $D_x g(0, \lambda) = 0$. For this to make sense, we assume L is a linear operator in a Banach space $\mathfrak{X}$ and let $\mathfrak{Y}$ be its domain. Here $A_\lambda = D_x f(0, \lambda) = L - \lambda I$, so this is an isomorphism precisely when λ is not in the spectrum of L. (This is the definition of the spectrum.) Thus, loosely speaking (and this is correct if A_λ has discrete spectrum), *bifurcation can occur only at eigenvalues of L.*

> ***Problem 1.1*** Verify that this criterion correctly predicts the bifurcation points in Figure 7.1.3.

It is desirable to have a more general definition of bifurcation point than 1.2, for bifurcations do not always occur off a known solution. The *limit point* in Figure 7.1.6 is an example; limit points also occur in Figure 7.1.8. Limit points are sometimes called *fold points*, *turning points*, or *saddle-node bifurcations* in the literature.

A general definition of bifurcation point suitable for our purposes is this: we call (x_0, λ_0) a *bifurcation point* of f if for every neighborhood $\mathfrak{U}$ of λ_0, and $\mathfrak{V}$ of (x_0, λ_0), there are points λ_1 and λ_2 in $\mathfrak{U}$ such that the sets $\Sigma_{\lambda_1} \cap \mathfrak{V}$ and $\Sigma_{\lambda_2} \cap \mathfrak{V}$, where $\Sigma_\lambda = \{x \in \mathfrak{Y} \mid f(x, \lambda) = 0\}$, are not homeomorphic (e.g., contain different numbers of points). However, there is a sense in which even this is not general enough; for example, consider $f(x, \lambda) = x^3 + \lambda^2 x = 0$. According to the above definitions this does not have a bifurcation point at $(0, 0)$. However, bifurcations do occur in slight perturbations of f (such as imperfections). For these reasons, some authors may wish to call any point where $D_x f$ is not an isomorphism a bifurcation point. It may be useful, however, to call it a *latent bifurcation point*.

We will now give a basic bifurcation theorem for $f\colon \mathbb{R} \times \mathbb{R} \to \mathbb{R}$. Below we shall reduce a more general situation to this one. This theorem concerns the simplest case in which $(0, \lambda_0)$ could be a bifurcation point [so $(\partial f/\partial x)(0, \lambda_0)$ must vanish], $x = 0$ is a trival solution [$f(0, \lambda) = 0$ for all λ, so $(\partial f/\partial \lambda)(0, \lambda_0) = 0$], and in which f has some symmetry such as $f(x, \lambda) = -f(-x, \lambda)$, which forces $f_{xx}(0, \lambda) = 0$.

There are many proofs of this result available and the theorem has a long history going back to at least Poincaré. See Nirenberg [1974] for an alternative proof (using the Morse lemma) and Crandall and Rabinowitz [1971] and Iooss and Joseph [1980] for a "bare hands" proof. The proof we have selected is based on the method of Lie transforms—that is, finding a suitable coordinate change by integrating a differential equation. These ideas were discussed in Section 1.7 (see the proof of the Poincaré lemma in Box 7.2, Chapter 1). This method turns out to be one that generalizes most easily to complex situations.[1]

1.5 Theorem *Let $f\colon \mathbb{R} \times \mathbb{R} \to \mathbb{R}$ be a smooth mapping and satisfy the following conditions:*

(i) $f(x_0, \lambda_0) = 0$, $f_x(x_0, \lambda_0) = 0$, $f_\lambda(x_0, \lambda_0) = 0$, *and* $f_{xx}(x_0, \lambda_0) = 0$; *and*
(ii) $f_{xxx}(x_0, \lambda_0) \neq 0$ *and* $f_{x\lambda}(x_0, \lambda_0) \neq 0$.

Then (x_0, λ_0) is a bifurcation point. In fact, there is a smooth change of coordinates in a neighborhood of (x_0, λ_0) of the form

$$x = \phi(\bar{x}, \lambda) \quad \text{with} \quad \phi(0, \lambda_0) = x_0$$

and a smooth nowhere zero function $T(\bar{x}, \lambda)$ with $T(0, \lambda_0) = +1$ such that[2]

$$T(\bar{x}, \lambda) f(\phi(\bar{x}, \lambda), \lambda) = \bar{x}^3 \pm \lambda \bar{x}$$

with $\pm$ depending on the sign of $[f_{x\lambda}(x_0, \lambda_0) \cdot f_{xxx}(x_0, \lambda_0)]$. See Figure 7.1.9.

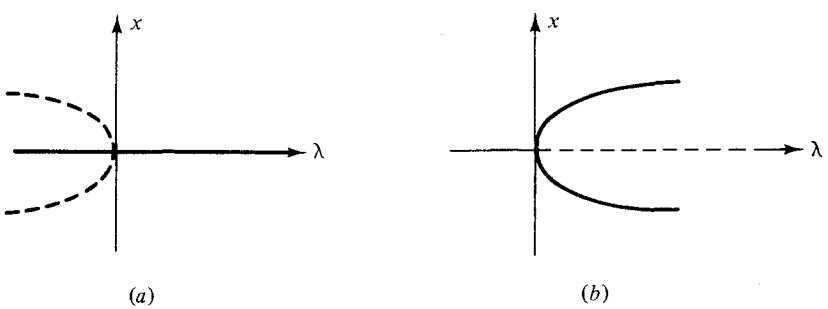

Figure 7.1.9 (a) The "+" case: $x^3 + \lambda x = 0$. (b) The "−" case: $x^3 - \lambda x = 0$.

[1]We thank M. Golubitsky for suggesting this proof.

[2]This kind of coordinate change (called *contact equivalence*), suggested by singularity theory, is the most general coordinate change preserving the structure of the zero set of f. See Box 1.1 for the general definitions.

Proof We can assume that $(x_0, \lambda_0) = (0, 0)$. By an initial rescaling and multiplication by -1 if necessary, we can assume that $f_{xxx}(0, 0) = 6$ and $f_{x\lambda}(0, 0) = \pm 1$, say $+1$. We seek a time-dependent family of coordinate transformations $\phi(\bar{x}, \lambda, t)$ and $T(\bar{x}, \lambda, t)$ $(0 \leq t \leq 1)$ such that

$$T(\bar{x}, \lambda, t)h(\phi(\bar{x}, \lambda, t), \lambda, t) = \bar{x}^3 + \lambda\bar{x} \equiv g(\bar{x}, \lambda), \tag{1}$$

where $h(x, \lambda, t) = (1 - t)g(x, \lambda) + tf(x, \lambda)$. If (1) can be satisfied, then at $t = 1$ it is the conclusion of the theorem. To solve (1), differentiate it in t:

$$\dot{T}h + T\dot{h} + Th_x\dot{\phi} = 0,$$

that is,

$$\frac{\dot{T}}{T}h + [f - g] + \dot{\phi}h_x = 0. \tag{2}$$

Now we need the following:

1.6 Lemma *Let $k(x, \lambda)$ be a smooth function of x and λ satisfying $k(0, 0) = 0$, $k_x(0, 0) = 0$, and $k_{xx}(0, 0) = 0$ and $k_\lambda(0, 0) = 0$. Then there are smooth functions $A(x, \lambda)$ and $B(x, \lambda)$ with B vanishing at $(0, 0)$ satisfying*

$$k(x, \lambda) = A(x, \lambda)(x^3 + \lambda x) + B(x, \lambda)(3x^2 + \lambda).$$

Moreover, if $k_{xxx}(0, 0) = 0$ and $k_{x\lambda}(0, 0) = 0$, then $A(0, 0) = 0$ and $B_x(0, 0) = 0$.

Proof By Taylor's theorem we can write

$$k(x, \lambda) = \lambda^2 a_1(x, \lambda) + x^3 b_1(x, \lambda) + x\lambda c_1(x, \lambda).$$

But

$$x^3 = \tfrac{1}{2}[x(3x^2 + \lambda) - (x^3 + \lambda x)],$$

$$\lambda x = \tfrac{1}{2}[3(x^3 + \lambda x) - x(3x^2 + \lambda)],$$

and

$$\lambda^2 = \lambda(3x^2 + \lambda) - 3x(\lambda x).$$

Substituting these expressions into the Taylor expansion for k gives the desired form for k. We have $B(0, 0) = k_\lambda(0, 0) = 0$ by assumption. If, in addition, $k_{xxx}(0, 0) = 0$ and if $k_{x\lambda}(0, 0) = 0$, then we can use Taylor's theorem to write

$$k(x, \lambda) = \lambda^2 a_2(x, \lambda) + x^4 b_2(x, \lambda) + x^2\lambda c_2(x, \lambda).$$

Substituting the above expressions for x^3 and $x\lambda$ into $x^4 = x \cdot x^3$ and $x^2\lambda = x \cdot x\lambda$ we get the desired form of k with $A(0, 0) = 0$ and $B(0, 0) = 0$. We then compute that $k_{xxx}(0, 0) = 6B_x(0, 0)$ and so $B_x(0, 0) = 0$ as well. ∎

1.7 Lemma (*Special Case of Nakayama's Lemma*) *Let $g(x, \lambda) = x^3 + \lambda x$ and $h(x, \lambda, t) = g(x, \lambda) + tp(x, \lambda)$, where $p(x, \lambda) = f(x, \lambda) - g(x, \lambda)$. Then for $0 \leq t \leq 1$ and (x, λ) in a neighborhood of $(0, 0)$, we can write $p(x, \lambda) = a(x, \lambda, t)h(x, \lambda, t) + b(x, \lambda, t)\, h_x(x, \lambda, t)$, where $a(0, 0, t) = 0$, $b(0, 0, t) = 0$ and $b_x(0, 0, t) = 0$.*

Proof By 1.6 we can write $p(x, \lambda) = A(x, \lambda)g(x, \lambda) + B(x, \lambda)g_x(x, \lambda)$. Thus $h = (1 + tA)g + tBg_x$ and hence $h_x = tA_xg + (1 + tA + tB_x)g_x + tBg_{xx}$. Since

$B = B_x = 0$ at $(0, 0)$, 1.6 can be used to write $6xB = Bg_{xx} = Eg + Fg_x$. Thus, h_x has the form $h_x = tCg + (1 + tD)g_x$, where $D(0, 0) = 0$. Hence

$$\begin{pmatrix} h \\ h_x \end{pmatrix} = \begin{pmatrix} 1 + tA & tB \\ tC & 1 + tD \end{pmatrix} \begin{pmatrix} g \\ g_x \end{pmatrix}$$

At $(x, \lambda) = (0, 0)$ this matrix has the form $\begin{pmatrix} 1 & 0 \\ tC(0, 0) & 1 \end{pmatrix}$, so it is invertible in a neighborhood of $(0, 0)$. Hence g and g_x can be written as a linear combination of h and h_x. Substitution gives the result claimed. ∎

Let us now use 1.7 to solve (1) and (2). First find ϕ by solving the ordinary differential equation

$$\dot{\phi}(\bar{x}, \lambda, t) = -b(\phi(\bar{x}, \lambda, t), \lambda, t), \qquad \phi(x, \lambda, 0) = x.$$

This can be integrated for the whole interval $0 \leq t \leq 1$ in a neighborhood of $(0, 0)$ because b vanishes at $(0, 0)$. Next solve

$$\dot{T}(\bar{x}, \lambda, t) = -a(\phi(\bar{x}, \lambda, t), \lambda, t)T(\bar{x}, \lambda, t), \qquad T(x, \lambda, 0) = 1.$$

This is linear, so can be integrated to $t = 1$. This produces ϕ, T satisfying (2) and so, by integration, (1). Moreover, $a(0, 0, t) = 0$, so $T(0, 0, t) = 1$ and $b(0, 0, t) = 0$, $b_x(0, 0, t) = 0$ so $\phi(0, 0, t) = 0$, $\phi_x(0, 0, t) = 1$. Thus, the transformation is of the form $T(x, \lambda) = 1 +$ higher order terms and $\phi(x, \lambda) = x +$ higher order terms. ∎

One calls the function $g(x, \lambda) = x^3 \pm \lambda x$ into which f has been transformed, a *normal form*. The transformation of coordinates allowed preserves all the qualitative features we wish of bifurcation diagrams (note that the λ-variable was unaltered). Furthermore, once a function has been brought into normal form, the stability of the branches can be read off by a direct computation (stability in the context of the dynamical theory is discussed in Section 7.3 below). In Figure 7.1.9 note that the *subcritical* branch in (a) is unstable, while the *supercritical* branch in (b) is stable.

Problem 1.2 Let $f(0, 0) = 0$, $f_x(0, 0) = 0$ and $f_{xx}(0, 0) \neq 0$, $f_\lambda(0, 0) \neq 0$. Show that f has the normal form $x^2 \pm \lambda$ (limit point).

These techniques lead to the results shown in Table 7.1.1 classifying some of the simple cases in one variable. (The "index" equals the number of negative eigenvalues.) Methods of singularity theory, a special case of which was given in 1.5, allow one to do the same analysis for more complex bifurcation problems.

In Box 1.1 we describe the imperfection-sensitivity analysis of the pitchfork. Next, however, we shall describe how many bifurcation problems can be reduced to one of the above cases by means of the *Liapunov–Schmidt procedure*.

Suppose f: $\mathcal{Y} \times \Lambda \to \mathcal{X}$ is a smooth (or C^1) map of Banach spaces. Let $f(x_0, \lambda_0) = 0$ and suppose that (x_0, λ_0) is a candidate bifurcation point; thus the linear operator $A = A_{x_0} = D_x f(x_0, \lambda_0)$: $\mathcal{Y} \to \mathcal{X}$ will in general have a

Table 7.1.1

Definining Conditions at (0, 0)	Nondegeneracy Conditions at (0, 0)	Normal Form	Picture (+ case)
(1) $f = f_x = 0$	$f_{xx} \neq 0, f_\lambda \neq 0$	$x^2 \pm \lambda$	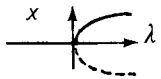 (limit point)
(2) $f = f_x = f_\lambda = 0$	$f_{xx} \neq 0$, $D^2 f$ has index 0 or 2	$x^2 + \lambda^2$	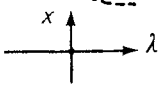 (isola)
(3) $f = f_x = f_\lambda = 0$	$f_{xx} \neq 0$, $D^2 f$ has index 1	$x^2 - \lambda^2$	 (trans-critical bifurcation)
(4) $f = f_x = f_{xx} = 0$	$f_{xxx} \neq 0, f_\lambda \neq 0$	$x^3 \pm \lambda$	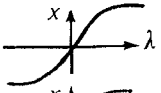 (hysteresis)
(5) $f = f_x = f_\lambda = f_{xx} = 0$	$f_{xxx} \neq 0, f_{x\lambda} \neq 0$	$x^3 \pm \lambda x$	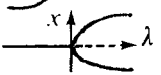 (pitchfork)

kernel Ker $A \neq \{0\}$ and a range Range $A \neq \mathfrak{X}$. Assume these spaces have closed complements. Keeping in mind the Fredholm alternative discussed in Section 6.1, let us write the complements in terms of adjoints even though they could be arbitrary at this point:

$$\mathfrak{Y} = \text{Ker } A \oplus \text{Range } A^*,$$
$$\mathfrak{X} = \text{Range } A \oplus \text{Ker } A^*.$$

Recall that A is Fredholm when Ker A and Ker A^* are finite dimensional, for example, this is the case for the operator A of linear elastostatics; then A is actually self-adjoint: $A = A^*$.

Now let $\mathbb{P}: \mathfrak{X} \longrightarrow$ Range A denote the orthogonal projection to Range A and split up the equation $f(x, \lambda) = 0$ into two equations:

$$\mathbb{P}f(x, \lambda) = 0 \quad \text{and} \quad (I - \mathbb{P})f(x, \lambda) = 0.$$

The map $\mathbb{P}f(x, \lambda)$ takes $\mathfrak{Y} \times \Lambda$ to Range A and has a surjective derivative at (x_0, λ_0). Therefore, by the implicit function theorem the set of solutions of $\mathbb{P}f(x, \lambda) = 0$ form the graph of a smooth mapping ψ: (a neighborhood of 0 in Ker A translated to x_0) $\times$ (a neighborhood of λ_0 in Λ) $\longrightarrow$ Range A^* (translated to x_0). See Figure 7.1.10. By construction, $\psi(x_0, \lambda_0) = (x_0, \lambda_0)$ and $D_u\psi(x_0, \lambda_0) = 0$ (u is the variable name in Ker A). This information can be substituted into the equation $(I - \mathbb{P})f(x, \lambda) = 0$ to produce the following theorem.

1.8 Theorem *The set of solutions of $f(x, \lambda) = 0$ equals, near (x_0, λ_0), the set of solutions of the bifurcation equation:*

$$(I - \mathbb{P})f((u, \psi(u, \lambda)), \lambda) = 0,$$

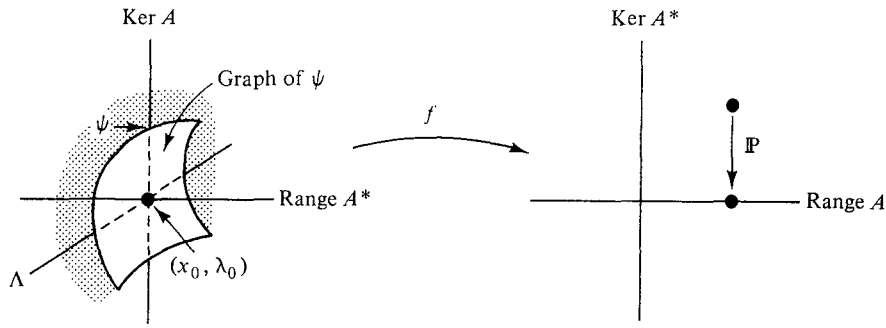

Figure 7.1.10

where ψ is implicitly defined by $\mathbb{P}f((u, \psi(u, \lambda)), \lambda) = 0$ and where $(u, \psi(u, \lambda)) \in \mathcal{Y} = \operatorname{Ker} A \oplus \operatorname{Range} A^* + \{x_0\}$.

Sometimes it is convenient to think of the Liapunov–Schmidt procedure this way: the equation $\mathbb{P}f(x, \lambda) = 0$ defines a smooth submanifold $\Sigma_{\mathbb{P}}$ of $\mathcal{Y} \times \Lambda$ (with tangent space $\operatorname{Ker} A \oplus \operatorname{Ker} \mathbb{P}D_\lambda f(x_0, \lambda_0)$ at (x_0, λ_0)); the bifurcation equation is just the equation $(I - \mathbb{P})f \mid \Sigma_{\mathbb{P}} = 0$. For computations it is usually most convenient to actually realize $\Sigma_{\mathbb{P}}$ as a graph, as in 1.7, but for some abstract considerations the manifold picture can be useful (such as the following: if the original equation has a compact symmetry group, so does the bifurcation equation). Sometimes f is to be thought of as a vector field, depending parametrically on λ. This suggests replacing $\Sigma_{\mathbb{P}}$ by a manifold C tangent to Ker A and such that f is everywhere tangent to C. The bifurcation equation now is just $f \mid C = 0$. This has the advantage that if f is a gradient, so is the bifurcation equation. The manifold C is called a *center manifold* and is discussed in Section 7-4. The relationship between the center manifold and Liapunov–Schmidt approaches is discussed there and in Chow and Hale [1982] and in Schaeffer and Golubitsky [1981]. In Rabinowitz [1977a] it is shown how to preserve the gradient character directly in the Liapunov–Schmidt procedure. Another closely related procedure is the "splitting lemma" of Gromoll and Meyer; cf. Golubitsky and Marsden [1983].

Let us now apply the Liapunov–Schmidt procedure to the pitchfork. This is called *bifurcation at a simple eigenvalue* for reasons that will be explained below. (See Golubitsky and Schaeffer [1984], Ch. 4 for a generalization.)

1.9 Proposition *Assume $f: \mathcal{Y} \times \mathbb{R} \to \mathcal{X}$ is smooth, $f(x_0, \lambda_0) = 0$, and:*

(i) $\dim \operatorname{Ker} A = 1$, $\dim \operatorname{Ker} A^* = 1$;
(ii) $D_\lambda f(x_0, \lambda_0) = 0$, *and* $D_x^2 f(x_0, \lambda_0)\cdot(u_0, u_0) = 0$, *where u_0 spans* Ker A;

(iii)[3] $\langle (D_x^3 f(x_0, \lambda_0)(u_0, u_0, u_0)), v_0 \rangle \neq 0$ *and* $\langle (D_x D_\lambda f(x_0, \lambda_0) \cdot u_0), v_0 \rangle \neq 0$, *where* v_0 *spans* Ker A.

Then near $(x_0 . \lambda_0)$, *the set of solutions of* $f(x, \lambda) = 0$ *consists of a pitchfork lying in a two-dimensional submanifold of* $\mathcal{Y} \times \mathbb{R}$.

Proof We can suppose that $x_0 = 0$ and $\lambda_0 = 0$. Identify Ker A and Ker A^* with $\mathbb{R}$ by writing elements of Ker A as $u = zu_0$, $z \in \mathbb{R}$ and elements of Ker A^* as wv_0, $w \in \mathbb{R}$. Define $F: \mathbb{R} \times \mathbb{R} \to \mathbb{R}$ by $F(z, \lambda) = \langle f(zu_0 + \psi(zu_0, \lambda), \lambda), v_0 \rangle$. By the Liapunov-Schmidt procedure, it suffices to verify the hypotheses of 1.5 for F. Since $\psi(0, 0) = 0$ and $f(0, 0) = 0$, clearly $F(0, 0) = 0$. Also

$$F_z(z, \lambda) = \langle (D_x f(zu_0 + \psi(zu_0, \lambda), \lambda) \cdot (u_0 + D_u \psi(zu_0, \lambda) \cdot u_0), v_0 \rangle,$$

which vanishes at (0, 0) since v_0 is orthogonal to the range of $D_x f$. Similarly,

$$F_\lambda(z, \lambda) = \langle D_\lambda f(zu_0 + \psi(zu_0, \lambda), \lambda), v_0 \rangle + \langle D_x f(zu_0 + \psi(zu_0, \lambda), \lambda) \cdot D_x \psi(zu_0, \lambda), v_0 \rangle \tag{3}$$

vanishes at (0, 0) since $\langle D_\lambda f(0, 0), v_0 \rangle = 0$ and v_0 is orthogonal to the range of $D_x f(0, 0)$. Next,

$$F_{zz}(z, \lambda) = \langle D_x^2 f(zu_0 + \psi(zu_0, \lambda), \lambda) \cdot [u_0 + D_u \psi(zu_0, \lambda) \cdot u_0]^2, v_0 \rangle + \langle D_x f(zu_0 + \psi(zu_0, \lambda), \lambda) \cdot D_u^2 \psi(zu_0, \lambda) \cdot u_0^2, v_0 \rangle \tag{4}$$

At (0, 0) the first term vanishes since $D_u \psi(0, 0) = 0$ and by our hypothesis on $D_x^2 f$. The second term vanishes since v_0 is orthogonal to the range of $D_x f(0, 0)$. By implicit differentiation, note that

$$\mathbb{P} D_x f(u + \psi(u, \lambda), \lambda) \cdot (w + D_u \psi(u, \lambda) \cdot w) = 0$$

so differentiating in u again,

$$\mathbb{P} D_x^2 f(u + \psi(u, \lambda), \lambda) \cdot [w + D_u \psi(u, \lambda) \cdot w]^2 + \mathbb{P} D_x f(u + \psi(u, \lambda), \lambda) \cdot D_u^2 \psi(u, \lambda) \cdot [w]^2 = 0.$$

Thus, $D_u^2 \psi(0, 0) = 0$ since $D_x^2 f(0, 0) = 0$ by assumption. Similarly from $D_\lambda f(0, 0) = 0$ we get $D_\lambda \psi(0, 0) = 0$. Therefore, we compute from (3) and (4),

$$F_{z\lambda}(0, 0) = \langle D_{z\lambda} f(0, 0) \cdot u_0, v_0 \rangle \neq 0$$

and

$$F_{xxx}(0,) = \langle D_x^3 f(0, 0) \cdot [u_0]^3, v_0 \rangle \neq 0. \blacksquare$$

Condition (ii) is sometimes associated with the assumption of $\mathbb{Z}_2$-symmetry $f(-x, \lambda) = -f(x, \lambda)$.

1.10 Example Suppose $f(x, \lambda) = Lx - \lambda x + g(x, \lambda)$, as in 1.4. Suppose $L^* = L$ and λ_0 is a *simple* non-zero eigenvalue of L. Then Ker A = Ker A^* =

---

[3] In the abstract context, $\langle \alpha, v \rangle = (I - \mathbb{P})\alpha$, but in actual problems, where A is an elliptic operator, $\mathbb{P}$ is the L^2-orthogonal projection and $\langle , \rangle$ is the L^2-inner product.

span u_0, where u_0 satisfies $Lu_0 = \lambda u_0$. Then condition (i) of 1.9 holds. Condition (ii) holds if, for example, $g(-x, \lambda) = -g(x, \lambda)$, and condition (iii) holds if $\langle D_x^3 g(0, \lambda_0)\cdot[u_0^3], u_0\rangle \neq 0$ (i.e., the leading term in g is a nontrivial cubic term). Note that $\langle D_x D_\lambda f(0, \lambda_0)\cdot u_0, v_0\rangle = -\lambda_0 \| u_0 \|^2 \neq 0$ automatically. For instance, these conditions apply to the problem

$$\Delta\phi - \lambda\phi + \lambda\phi^3 = 0$$

on a region $\Omega \subset \mathbb{R}^3$, where Dirichlet boundary conditions hold, choosing $\mathfrak{X} = L^2(\Omega)$, $\mathfrak{Y} = H_0^2(\Omega)$, provided λ_0 is a simple eigenvalue for Δ on Ω.[4]

Problem 1.3 For the Euler beam, prove that a pitchfork bifurcation occurs at $\lambda/EI = k^2\pi^2$ ($k = 1, 2, \ldots$); see Figure 7.1.3.

Problem 1.4 Derive criteria for a transcritical bifurcation in a Banach space under condition (i) of 1.9 by imposing conditions (3) of Table 7.1.1 on the bifurcation equation.

For bifurcation at multiple eigenvalues one can in principle go through similar procedures, although the algebra becomes more complex. There are a number of observations to be made concerning multiple eigenvalues.

1.11 Remarks

(a) Bifurcation at multiple eigenvalues is often associated with symmetries of f and of the bifurcation point, just as the pitchfork is associated with the reflection symmetry $f(-x, \lambda) = -f(x, \lambda)$. When studying the bifurcation problem or imperfection-sensitivity analysis of it, this symmetry group must be taken into account. (See Golubitsky and Schaeffer [1979b] and Box 1.1 for more information.)

(b) Many problems of *secondary bifurcation* (further branching, appearance of limit points, etc.) can be dealt with by perturbing a bifurcation problem with a multiple eigenvalue (see, e.g., Bauer, Keller and Reiss [1975], Chow, Hale, and Mallet-Paret [1975], and Golubitsky and Schaeffer [1979a, b]; some examples are sketched in Section 7.2).

(c) Simple rules for the pitchfork such as "supercritical branches are stable" do not necessarily apply at multiple eigenvalues (see, e.g., McLeod and Sattinger [1973]). However, this information can usually be filled in using symmetries, considering the perturbed situation and applying the simple rules (from Table 7.1.1) to its component parts; see Schaeffer and Golubitsky [1981] and Section 7.2 for examples.

(d) See Nirenberg [1974] for a simple example of a problem with a double eigenvalue for which no bifurcation occurs; it is, however, a "latent" bifurcation point. Using degree theory, Krasnoselskii [1964] has shown, under some hypotheses, that an eigenvalue of *odd* multiplicity

[4]The first eigenvalue of a self-adjoint elliptic operator on scalars is always simple.

of a problem of the form

$$f(x, \lambda) = x - \lambda Tx + g(x, \lambda),$$

where T and g are compact, is a bifurcation point. This applies to Example 1.9 if L has a compact inverse by rewriting $Lx - \lambda x + g(x, \lambda) = 0$ as $x - \lambda L^{-1}x + L^{-1}g(x, \lambda) = 0$. Notice, however, that the details of the bifurcation (how many branches, their stability and structural stability) require further analysis. Krasnoselskii's theorem is discussed in Box 1.2. Conditions for an eigenvalue of *even* multiplicity to be a bifurcation point are given in Buchner, Marsden, and Schechter [1982] and references therein.

For problems in elasticity, most applications have been made to rods, plates, and shells as we shall outline in Section 7.2. Three-dimensional elasticity problems for pure displacement can be dealt with by the techniques outlined above, although no seminal examples have been computed. Most interesting examples are pure traction or have mixed boundary conditions. The mixed case is complicated by technical problems (with function spaces). Some basic examples for the pure traction problem are, however, available. Rivlin's example of homogeneous deformations of an incompressible cube will be given in Section 7.2 and the Signorini–Stoppelli problem of a natural state subjected to small loads will occupy the whole of 7.3. These problems both require great care with the symmetry group.

Box 1.1 ***Imperfection-Sensitivity Analysis of the Pitchfork***

That small imperfections can perturb a bifurcation diagram and, for example, bring about the onset of buckling significantly earlier than that predicted by the ideal theory has a long history in the engineering literature, going back at least to Koiter [1945]. For accounts in the engineering literature, Ziegler [1968] and references therein may be consulted.

Recent history developed along three more or less separate lines; in pure mathematics, the subject of catastrophe theory and more generally singularity theory was developed, starting with R. Thom around 1955, and is now a large subject; see, for example, Golubitsky and Guillemin [1973]. Secondly, in applied mathematics, the subject of perturbed bifurcation theory was developed by many authors, such as Keener and Keller [1973] and Benjamin [1978]. Thirdly, in engineering the subject was developed by Roorda [1965], Sewell [1966b], and Thompson and Hunt [1973], [1975]. These three lines of development are now merging through the works of people in all these branches; the papers of Chow,

Hale, and Mallet-Paret [1975] and Golubitsky and Schaeffer [1979a] have been especially important in making the unification. We shall present a few ideas of Golubitsky and Schaeffer [1979a] to indicate how the modern theory goes. Their theory differs from previous works in that they distinguish between bifurcation parameters and imperfection parameters; for example, catastrophe theory does not make this distinction explicit. This important point was already hinted at in the work of Thompson and Hunt.

The mathematical theory centers around two notions, called *contact equivalence* and *universal unfolding*. Let $f\colon \mathbb{R}^n \times \mathbb{R} \to \mathbb{R}^m$ be given and suppose f is C^∞ and $f(0, 0) = 0$. For example, f may be the map obtained from the bifurcation equation in the Liapunov–Schmidt procedure. Everything will be restricted to a small neighborhood of (0, 0) without explicit mention.

1.12 Definition We say f_1 and f_2 are *contact equivalent* at (0, 0) if there is a (local) diffeomorphism of $\mathbb{R}^n \times \mathbb{R}$ to itself of the form $(x, \lambda) \mapsto (\phi(x, \lambda), \Lambda(\lambda))$ such that $\phi(0, 0) = 0$, $\Lambda(0) = 0$, and a (smooth, local) map $(x, \lambda) \mapsto T(x, \lambda)$ from $\mathbb{R}^n \times \mathbb{R}$ to the invertible $m \times m$ matrices[5] such that

$$f_1(x, \lambda) = T(x, \lambda) \cdot f_2(\phi(x, \lambda), \Lambda(\lambda)).$$

Notice that the change of coordinates on $\mathbb{R}^n \times \mathbb{R}$ maps sets on which $\lambda =$ constant, to themselves. In this sense, this notion of equivalence recognizes the special role played by the bifurcation parameter, λ. It should be clear that the zero sets of f_1 and f_2 can then be said to have the "same" bifurcation diagram. See Figure 7.1.11.

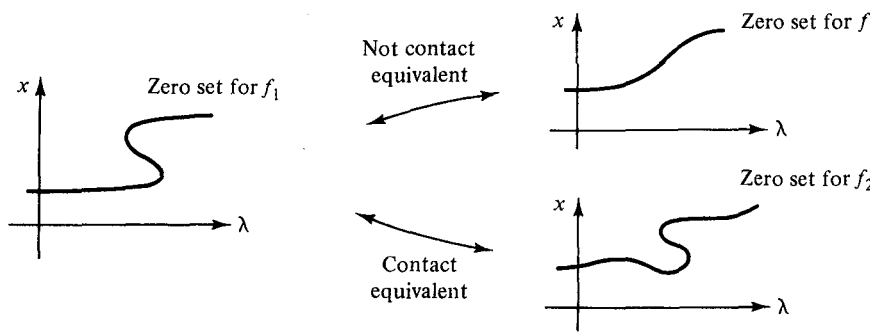

Figure 7.1.11

[5]Allowing *nonlinear* changes of coordinates on the range turns out not to increase the generality (cf. Golubitsky and Schaeffer [1979a], p. 23).

We can rephrase Theorem 1.5 by saying that if $n = m = 1$ and $f(0, 0) = 0$, $f_x(0, 0) = 0$, $f_\lambda(0, 0) = 0$, $f_{xx}(0, 0) = 0$, and $f_{xxx}(0, 0) \times f_{x\lambda}(0, 0) \neq 0$, then f is contact equivalent to $g(x, \lambda) = x^3 \pm \lambda x$.

Now we consider perturbations (or imperfections) of f.

1.13 Definition Let $f: \mathbb{R}^n \times \mathbb{R} \longrightarrow \mathbb{R}^m$ be smooth and $f(0, 0) = 0$. An l-parameter *unfolding* of f is a smooth map $F: \mathbb{R}^n \times \mathbb{R} \times \mathbb{R}^l \longrightarrow \mathbb{R}^m$ such that $F(x, \lambda, 0) = f(x, \lambda)$ for all x, λ (in a neighborhood of $(0, 0)$).

Let F_1 be an l_1-parameter unfolding of f and F_2 be an l_2-parameter unfolding. We say that F_1 *factors through* F_2 if there is a smooth map $\psi: \mathbb{R}^{l_1} \longrightarrow \mathbb{R}^{l_2}$ such that for every $\beta \in \mathbb{R}^{l_1}$, $F_1(\cdot, \cdot, \beta)$ (i.e., β is held fixed) is contact equivalent to $F_2(\cdot, \cdot, \psi(\beta))$.

An l-parameter unfolding F of f is called a *universal unfolding of* f if every unfolding of f factors through F.

Roughly speaking, a universal unfolding F is a perturbation of f with l extra parameters that captures *all* possible perturbations of the bifurcation diagram of f (up to contact equivalence). Thus, if one can find F, one has solved the problem of imperfection-sensitivity of the bifurcation diagram for f. The number of *extra* parameters l required is unique and is called the *codimension* of f.

The complete theory for how to compute the universal unfolding would require too much space for us to go into here; see Golubitsky and Schaeffer [1979a]. However, we can indicate what is going on for the pitchfork. If we return to the proof of 1.5, we see that a general unfolding of $g(x, \lambda) = x^3 \pm \lambda x$ will have a Taylor expansion of the form

$$F(x, \lambda, \alpha_1, \ldots, \alpha_l) = x^3 \pm \lambda x + \alpha_1 + \alpha_2 x + \alpha_3 \lambda + \alpha_4 x^2 + \alpha_5 \lambda^2 + \alpha_6 x^2 \lambda + \alpha_7 x \lambda^2 + \alpha_8 \lambda^3 + \text{Remainder}.$$

A more difficult argument than the one given in the proof of 1.5 (though similar in spirit) shows that under contact equivalence, we can transform away all the terms except $\alpha_4 x^2$ and α_1 (these, roughly, correspond to the fact that before, we had $f(0, 0) = 0$ and $f_{xx}(0, 0) = 0$, so these terms were absent in its Taylor expansion).[6] This is the idea of the method behind the proof of the following.

1.14 Proposition

(a) *A universal unfolding of* $x^3 \pm \lambda x$ *is* $F(x, \lambda, \alpha, \beta) = x^3 + \beta x^2 \pm \lambda x + \alpha$.

[6]A subtlety is that after transformation the new α_4 will depend on the old α_4 and α_3. To properly deal with the Taylor expansion in this case requires the "Malgrange preparation theorem."

(b) *Let $f(x, \lambda)$ satisfy the hypotheses of* 1.5 *and let $F(x, \lambda, a, b)$ be a two-parameter unfolding of f. Then F is universal if*

$$\det \begin{bmatrix} 0 & 0 & f_{x\lambda} & f_{xxx} \\ 0 & f_{\lambda x} & f_{\lambda\lambda} & f_{\lambda xx} \\ F_a & F_{ax} & F_{a\lambda} & F_{axx} \\ F_b & F_{bx} & F_{b\lambda} & F_{bxx} \end{bmatrix} \neq 0,$$

Problem 1.5 Show that another universal unfolding of the pitchfork is $x^3 - \lambda x + \beta\lambda + \alpha$.

Part (b) of 1.14 is useful since one may wish to put on a variety of imperfections. For example, in the buckling of a beam one may wish to give it slight inhomogeneities, a slight transverse loading, and so on. The criterion above guarantees that one has enough extra parameters.

The perturbed bifurcation diagrams that go with the universal unfolding F in 1.14(a) are shown in Figure 7.1.12. Note that transcritical bifurcations and hysteresis are included, unlike Figure 7.1.8.

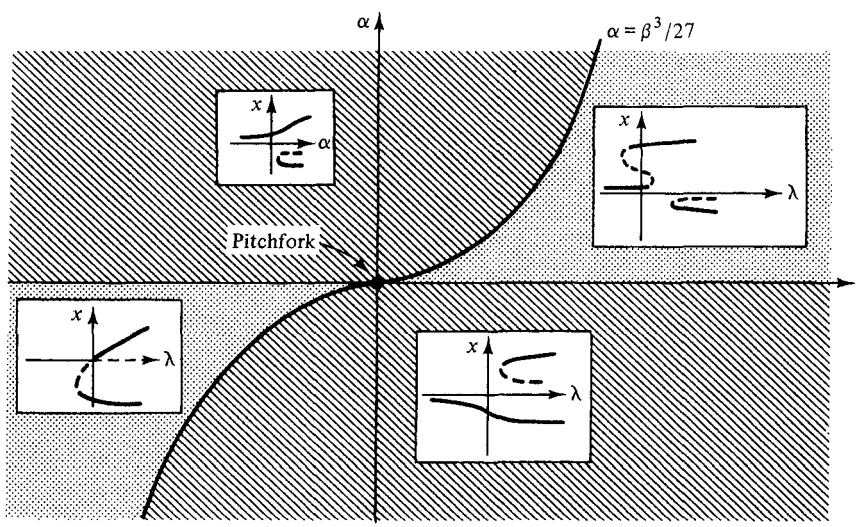

Figure 7.1.12

Problem 1.6 Show that the hysteresis in Figure 7.1.12 can be obtained by passing through the cusp (Fig. 7.1.8) along various lines for 1.14(a) and straight lines through the origin in Problem

1.5. (See Golubitsky and Schaeffer [1979a], p. 53 for the answer to the first part.)

Problem 1.7 Write an essay on imperfection-sensitivity analysis of the Euler beam using Zeeman [1976] and Golubitsky and Schaeffer [1979a]. Utilize the function spaces from Chapter 6.

Box 1.2 ***Remarks on Global Bifurcation***

There are some results on global bifurcation available that are useful in elasticity. The main result is a globalization of Krasnoselski's theorem mentioned above due to Rabinowitz [1971]. There have been important variants (useful for operators preserving positivity) due to Dancer [1973] and Turner [1971]. Most of the applications in elasticity under realistic global assumptions are due to Antman and are described in the next section. However, there are also a number of other intersting applications to, for instance, solitary water waves by Keady and Norbury [1978] and by Amick and Toland [1981].

We shall just state the results; the works of Nirenberg [1974] and Ize [1976] should be consulted for proofs. It is to be noted that *global* imperfection-sensitivity results are not available (to our knowledge).

One considers mappings of $\mathfrak{X} \times \mathbb{R}$ to $\mathfrak{X}$ of the form

$$f(x, \lambda) = x - \lambda Tx + g(x, \lambda),$$

where $T: \mathfrak{X} \longrightarrow \mathfrak{X}$ is compact, g is compact and $g(x, \lambda) = o(\|x\|)$, uniformly on compact λ-intervals. The proof of the following theorem is based on the notion of topological degree.

1.15 Theorem (*Krasnoselskii* [1964]) *If* $1/\lambda_0$ *is an eigenvalue of* T *of odd multiplicity, then* $(0, \lambda_0)$ *is a bifurcation point.*

Let $\mathcal{S} = \{(x, \lambda) \mid f(x, \lambda) = 0 \text{ and } x \neq 0\} \cup (0, 1/\lambda_0)$ (the nontrivial solutions) and let $\mathcal{C}$ be the maximal connected subset of $\mathcal{S}$ containing $(0, 1/\lambda_0)$. The theorem of Rabinowitz basically states that $\mathcal{C}$ cannot "end in mid-air."

1.16 Theorem (*Rabinowitz* [1971]) *Let* λ_0 *and* $\mathcal{C}$ *be as above. Then either* $\mathcal{C}$ *is unbounded or it intersects the* λ*-axis at a finite number of points* $0, 1/\lambda_j$, *where* λ_j *are eigenvalues of* T*; the number of* λ_j *with odd multiplicity is even.*

The two alternatives are shown schematically, in Figure 7.1.13.

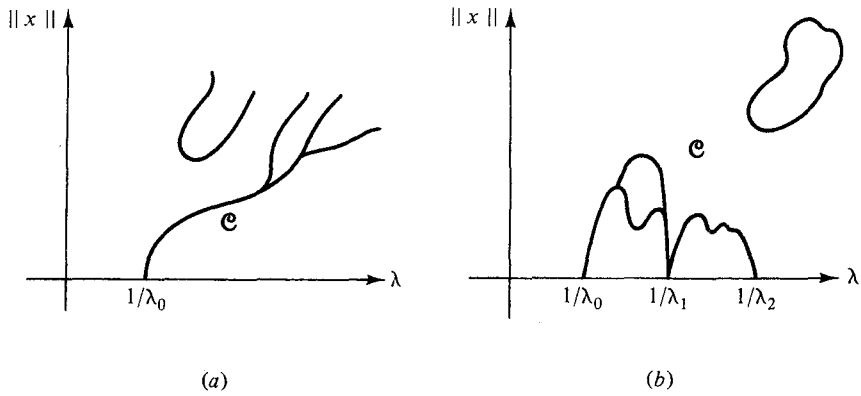

Figure 7.1.13 (a) $\mathcal{C}$ unbounded. (b) $\mathcal{C}$ returns to λ-axis.

Similar results for dynamic bifurcations (see Section 7.3) have been obtained by Alexander and Yorke [1978] and Chow and Mallet-Paret [1978].

Box 1.3 ***Summary of Important Formulas for Section 7.1***

Necessary Condition for Bifurcation

The necessary condition for bifurcation of $f(x, \lambda) = 0$ from a trivial solution $x = 0$ at λ_0 is that $D_x f(0, \lambda_0)$ not be an isomorphism.

Pitchfork Bifurcation

If $f(x, \lambda)$, $x \in \mathbb{R}$, $\lambda \in \mathbb{R}$ satisfies $f(x_0, \lambda_0) = 0$, $f_x(x_0, \lambda_0) = 0$, $f_\lambda(x_0, \lambda_0) = 0$, $f_{xx}(x_0, \lambda_0) = 0$, and $f_{xxx}(x_0, \lambda_0) \cdot f_{x\lambda}(x_0, \lambda_0) \neq 0$, then the zero set of f near (x_0, λ_0) is a pitchfork: f looks like $x^3 \pm \lambda x$ near $(0, 0)$.

Imperfection Sensitivity

The imperfection sensitivity analysis of $x^3 \pm \lambda x$ requires two extra imperfection parameters and is completely described by $F(x, \lambda, \alpha, \beta) = x^3 \pm \lambda x + \beta x^2 + \alpha$.

Liapunov Schmidt Procedure

If $\mathbb{P}$ is the projection onto Range $D_x f(x_0, \lambda_0)$, then solve $f(x, \lambda) = 0$ by solving $\mathbb{P} f(x, \lambda) = 0$ implicitly for $x = u + \phi(u, \lambda)$, $u \in$ Ker

$D_x f(x_0, \lambda_0)$, and substituting into $(I - \mathbb{P})f(x, \lambda) = 0$. The resulting equation, $(I - \mathbb{P})f(u + \phi(u, \lambda), \lambda)) = 0$ is the bifurcation equation. The pitchfork criterion may be applied to this if dim Ker $D_x f(x_0, \lambda_0) = 1$ and if $D_x f(x_0, \lambda_0)$ is self-adjoint.

7.2 A SURVEY OF SOME APPLICATIONS TO ELASTOSTATICS

This section is divided into three parts. First of all we present a basic example due to Rivlin. This concerns bifurcations that occur in an incompressible cube subject to a uniform tension on its faces. This is of interest because it is one of the few *three*-dimensional examples that can be computed explicitly. Furthermore, it is a seminal example for seeing how imperfection-sensitivity and symmetry can affect examples. We recommend reading Section 4 of the introductory chapter to review the context of the example. Secondly, we shall review *some* of the literature on the buckling of rods, plates, and shells. This literature is vast and our review is selective and biased towards the papers relevant to those current theoretical research directions that we know about and think are the most promising. Thirdly, we discuss (in Boxes 2.1 to 2.3) the following three points in conjunction with examples:

1. global versus local bifurcation analyses and exact verses approximate theories;
2. imperfection-sensitivity (Are there enough parameters?);
3. the role of symmetry.

In the next section we give a relatively detailed discussion of an important example: the traction problem near an unstressed state. This example was chosen for its interest to us and because it is in line with our emphasis in this book on *three*-dimensional problems. However, it might be of benefit to some readers to replace it by one of the examples mentioned in this section's survey, depending on interest.

We begin now with a discussion of Rivlin's [1948b] example of homogeneous deformations of a cube of incompressible neo-Hookean material. We thank John Ball and David Schaeffer for their help with this problem. The (dead load) traction problem is considered. The prescribed traction $\boldsymbol{\tau}$ is normal to each face of the cube with a magnitude τ, the same for each face, as in Figure 7.2.1.

We take a stored energy function for a homogeneous isotropic hyperelastic material; that is, of the form

$$W(\boldsymbol{F}) = \Phi(\lambda_1, \lambda_2, \lambda_3),$$

where $\lambda_1, \lambda_2, \lambda_3$ are the principal stretches and Φ is a symmetric function of

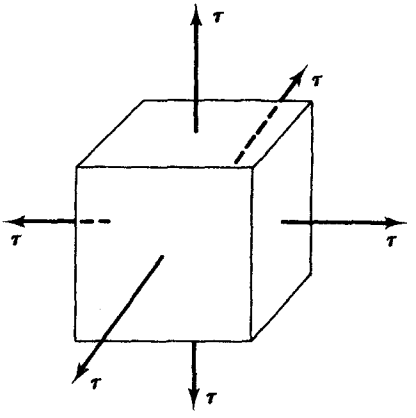

Figure 7.2.1

$\lambda_1, \lambda_2, \lambda_3$. Recall that the first Piola–Kirchhoff stress tensor $\boldsymbol{P}$ is given by

$$P_a{}^A = \rho_{\text{Ref}} \frac{\partial W}{\partial F^a{}_A}.$$

We shall choose $\rho_{\text{Ref}} = 1$.

Place the center of the cube at the origin and consider homogeneous deformations; that is, $\boldsymbol{x} = \boldsymbol{F} \cdot \boldsymbol{X}$, where $\boldsymbol{F}$ is a constant 3×3 matrix. In particular, we seek solutions with $\boldsymbol{F} = \text{diag}(\lambda_1, \lambda_2, \lambda_3)$ relative to a rectangular coordinate system whose axes coincide with the axes of the block; the spatial and material coordinate systems are coincident. (This turns out to be the most general homogeneous solution; cf. Problem 2.2 below.)

> ***Problem 2.1*** Introduce an off diagonal entry δ into $\boldsymbol{F}$ and show that the new principal stretches $\bar{\lambda}_1, \bar{\lambda}_2, \bar{\lambda}_3$ satisfy $\bar{\lambda}_1^2 + \bar{\lambda}_2^2 + \bar{\lambda}_3^2 = \lambda_1^2 + \lambda_2^2 + \lambda_3^2 + \delta^2$. Show that $\partial\bar{\lambda}_i/\partial\delta = 0$ at $\delta = 0$ $(i = 1, 2, 3)$. Conclude that $\boldsymbol{P}$ is diagonal.

Since $\boldsymbol{P}$ is diagonal by this problem, we find that

$$\boldsymbol{P} = \text{diag}\left(\frac{\partial\Phi}{\partial\lambda_1}, \frac{\partial\Phi}{\partial\lambda_2}, \frac{\partial\Phi}{\partial\lambda_3}\right).$$

For a neo-Hookean material,

$$\Phi = \alpha(\lambda_1^2 + \lambda_2^2 + \lambda_3^2 - 3), \quad \alpha > 0 \text{ a constant.}$$

The equilbrium equations for an incompressible material are obtained from the usual ones by replacing $\boldsymbol{P}$ by $\boldsymbol{P} - p\boldsymbol{F}^{-1}$, where p is the pressure, to be determined from the incompressibility condition $J = 1$; that is, $\lambda_1\lambda_2\lambda_3 = 1$. Thus we must have

$$\text{DIV}(\boldsymbol{P} - p\boldsymbol{F}^{-1}) = \boldsymbol{0} \quad \text{in} \quad \mathcal{B}$$

and

$$(\boldsymbol{P} - p\boldsymbol{F}^{-1}) \cdot \boldsymbol{N} = \boldsymbol{\tau} \quad \text{on} \quad \partial\mathcal{B}.$$

We must solve these for the unknowns $\lambda_1, \lambda_2, \lambda_3$. For $W = \Phi$, these equations read

$$\frac{\partial}{\partial X^i}\left(\frac{\partial \Phi}{\partial \lambda_i} - \frac{p}{\lambda_i}\right) = 0 \quad \text{in} \quad \mathcal{B}$$

and

$$\frac{\partial \Phi}{\partial \lambda_i} - \frac{p}{\lambda_i} = \tau \text{ on the face along the } i\text{th axis} \quad (i = 1, 2, 3).$$

For a neo-Hookean material, $\partial\Phi/\partial\lambda_i = 2\alpha\lambda_i$, a constant, so the first equation is equivalent to the assertion that p is a constant in $\mathcal{B}$. The second equation becomes

$$2\alpha\lambda_1^2 - p = \tau\lambda_1,$$
$$2\alpha\lambda_2^2 - p = \tau\lambda_2,$$
$$2\alpha\lambda_3^2 - p = \tau\lambda_3.$$

Eliminating p gives

$$[2\alpha(\lambda_1 + \lambda_2) - \tau](\lambda_1 - \lambda_2) = 0, \tag{1}$$
$$[2\alpha(\lambda_2 + \lambda_3) - \tau](\lambda_2 - \lambda_3) = 0, \tag{2}$$
$$[2\alpha(\lambda_3 + \lambda_1) - \tau](\lambda_3 - \lambda_1) = 0. \tag{3}$$

Case 1 The λ_i's are distinct. Then (1), (2), and (3) yield $\tau = 2\alpha(\lambda_1 + \lambda_2) = 2\alpha(\lambda_2 + \lambda_3) = 2\alpha(\lambda_3 + \lambda_1)$, which implies $\lambda_1 = \lambda_2 = \lambda_3$, a contradiction. Thus, *there are no solutions with the* λ_i's *distinct.*

Case 2 $\lambda_1 = \lambda_2 = \lambda_3$. Since $\lambda_1\lambda_2\lambda_3 = 1$, we get $\lambda_i = 1$ $(i = 1, 2, 3)$ (and $p = 2\alpha - \tau$). This is a solution for all α, the trivial one.

Case 3 Two λ_i's equal. Suppose $\lambda_2 = \lambda_3 = \lambda$, so $\lambda_1 = \lambda^{-2}$. Then (1) and (3) coincide, giving

$$2\alpha(\lambda^{-2} + \lambda) - \tau = 0.$$

Thus, we need to find the positive roots of the cubic

$$f(\lambda) = \lambda^3 - \frac{\tau}{2\alpha}\lambda^2 + 1 = 0.$$

Since $f(0) = 1$ and $f'(\lambda) = 3\lambda(\lambda - \tau/3\alpha)$, a positive root requires $\tau > 0$. There will be none if $f(\tau/3\alpha) > 0$, one if $f(\tau/3\alpha) = 0$, and two if $f(\tau/3\alpha) < 0$; see Figure 7.2.2.

Since $f(\tau/3\alpha) = -\frac{1}{2}(\tau/3\alpha)^3 + 1$, there are no positive roots if $\tau < 3\sqrt[3]{2}\,\alpha$, one if $\tau = 3\sqrt[3]{2}\,\alpha$, and two if $\tau > 3\sqrt[3]{2}\,\alpha$. The larger of these two positive roots is always greater than unity; the smaller is greater than unity or less than unity according as $3\sqrt[3]{2}\,\alpha < \tau < 4\alpha$ or $4\alpha < \tau$, respectively. These solutions are graphed in Figure 7.2.3, along with the trivial solution $\lambda_i = 1$, τ artibrary. Thus taking permutations of $\lambda_1, \lambda_2, \lambda_3$ into account, we get:

(a) *One solution*, namely, $\lambda_1 = \lambda_2 = \lambda_3 = 1$ *if* $\tau < 3\sqrt[3]{2}\,\alpha$.

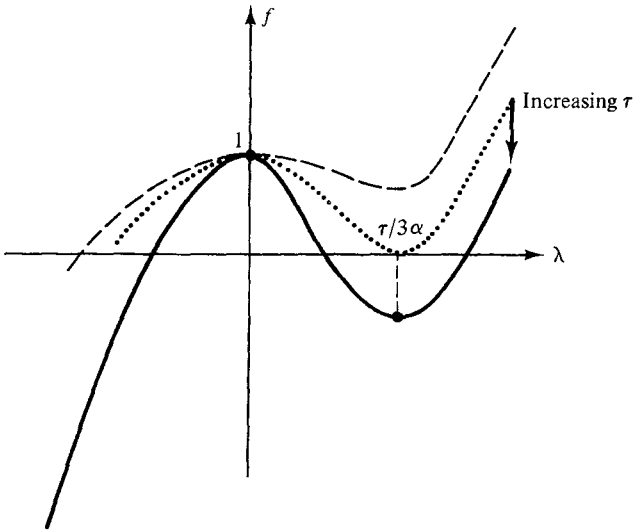

Figure 7.2.2

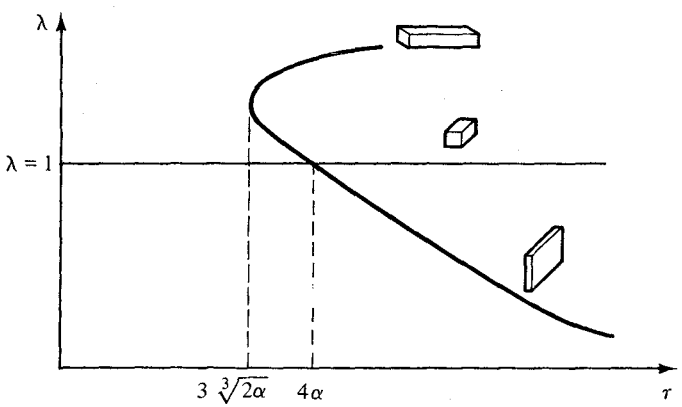

Figure 7.2.3

(b) *Four solutions* if $\tau = 3\sqrt[3]{2}\,\alpha$ or $\tau = 4\alpha$.
(c) *Seven solutions* if $\tau > 3\sqrt[3]{2}\,\alpha$, $\tau \neq 4\alpha$.

If we regard τ as a bifurcation parameter, we see that six new solutions are produced in "thin air" as τ crosses the critical value $\tau = 3\sqrt[3]{2}\,\alpha$. This is clearly a bifurcation phenomenon. Bifurcation of a more traditional sort occurs at $\tau = 4\alpha$. For unequal forces, see Sect. 7.3 and Sawyers [1976].

Rivlin [1948b], [1974b] shows that the trivial solution is stable for $0 \leq \tau/\alpha < 4$ and unstable for $\tau/\alpha > 4$; the trivial solution loses its stability when it is crossed

by the nontrivial branch at $\tau = 4\alpha$. The three solutions corresponding to the larger root of f are always stable, and the three solutions corresponding to the smaller root are never stable. Beatty [1967b] established instability for $\tau < 0$.

Symmetry plays a crucial role in this problem. The two solutions found above led to six solutions when permutations of λ_1, λ_2, λ_3 were considered. This suggests that the basic symmetry group for the problem is S_3, and this is essentially correct—although the cube admits a much larger group of symmetries, most elements act trivially in the problem at hand, leaving only the group S_3. The same group and similar mathematics occurs in a convection problem studied by Golubitsky and Scheaffer [1981].

Because of the presence of this symmetry group, the transcritical bifurcation in Figure 7.2.3 at $\tau = 4\alpha$ is structurally stable. Without the symmetry the bifurcation would be imperfection sensitive; that is, a generic small perturbation would split the diagram into two distinct components. However, the bifurcation *cannot* be destroyed by a small perturbation that preserves the symmetry. Moreover, the usual rules about exchange of stability are completely modified by the symmetry. In particular, the nontrivial branch of solutions that crosses the trivial solution at $\tau = 4\alpha$ is *unstable both below and above* the bifurcation point.

Interesting new phenomena appear if a more general stored energy function is considered. Consider the Mooney–Rivlin material for which

$$\Phi(\lambda_1, \lambda_2, \lambda_3) = \alpha(\lambda_1^2 + \lambda_2^2 + \lambda_3^2 - 3) + \beta(\lambda_1^{-2} + \lambda_2^{-2} + \lambda_3^{-2} - 3),$$

where α and β are positive constants. (This reduces to the neo-Hookean case if $\beta = 0$.) If $0 < \beta/\alpha < \frac{1}{3}$, there are new fully asymmetric solutions of the equations (corresponding to Case 1 above) that bifurcate from the nontrivial symmetric solutions (Case 3). These new bifurcations cause some surprising changes of stability of the symmetric branches. As $\beta/\alpha \longrightarrow \frac{1}{3}$ from below, the fully asymmetric solutions collapse into the original bifurcation from the trivial solution, and for $\beta/\alpha > \frac{1}{3}$, they move off into the complex plane. This transition provides an example of a bifurcation problem that itself is structurally unstable but occurs stably in a one-parameter family of bifurcation problems; that is, it is of codimension one. See Ball and Schaeffer [1982] for details.

Problem 2.2 Consider the traction problem with $\boldsymbol{\tau} = \tau \boldsymbol{N}$ for a constant $\boldsymbol{\tau}$ and an isotropic material. (a) Show that if ϕ_0 is a solution, then so is $\boldsymbol{Q} \circ \phi_0 \circ \boldsymbol{Q}^{-1}$ for $\boldsymbol{Q} \in \mathrm{SO}(3)$. (b) Conclude that nontrivial solutions can never be *strict* local minima of the energy (cf. Adeleke [1980]). {Thus, stability in this traction problem refers to neutral or conditional stability; see Ball and Schaeffer [1982] for more information.} (c) If $\phi_0(X) = \mathrm{diag}(\lambda^{-2}, \lambda, \lambda)(X)$ for $\lambda \neq 1$, show that (a) yields a set of solutions identifitable with $\mathbb{RP}^2$, real projective 2-space; i.e. the space of lines in $\mathbb{R}^3$.

Another example that can be worked out fairly explicitly is anti-plane shear, due to Knowles, and is described in Gurtin [1981a]. This example is important

for light it may shed on the role of strong ellipticity and phase transitions. Phase transitions are of current interest in continuum mechanics (see Box 4.1, Chapter 6) but there seems to be a large gap to be bridged to the concepts one hears from physicists on the subject: symmetry breaking, renormalization group, and chaotic dynamics. The only thing one sees in common are energy functions with dimples, as in Figure 7.2.4. It is true that such pictures are common to the pitchfork bifurcation and its attendant symmetry breaking, to a loss of strong ellipticity, to chaotic dynamics, and to the Maxwell rule in thermodynamics. However, such observations are shallow. What are the deeper connections?

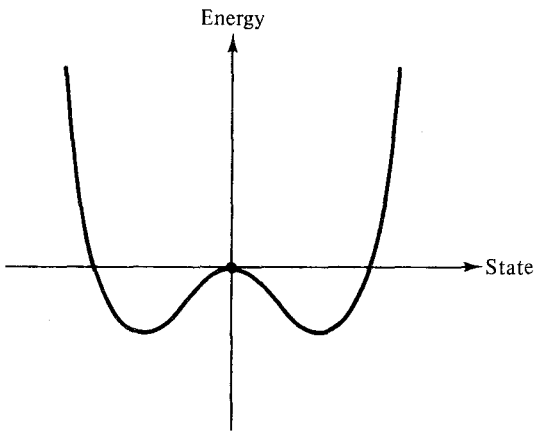

Figure 7.2.4

We turn next to surveying some of the literature on applications of bifurcation theory to elastostatics. Apart from Rivlin's example above, the Signorini–Stoppelli problem treated in the next section, and some semi-inverse methods (see below), virtually all the remaining examples are for rod, shell, and plate theories. The literature is massive and we can pretend to do no more than give a brief indication of some of the papers. We shall simply organize our selections in loosely grouped categories and make a few comments as we proceed. The following boxes discuss a few directions of current research and unifying treads. Of course it is impossible to be sure exactly in what directions current research will become most active.

Warning: Our list is not comprehensive, and many important papers are left out. We apologize for this, but a selection was necessary because of the massive undertaking involved.

Mathematical Theory. This in itself is a vast topic. The methods range from analytical to very geometric. Stackgold [1971], Sattinger [1973], Nirenberg

[1974], Berger [1977], Stuart [1979], and Iooss and Joseph [1980] are good places to begin. There the basic theorems on bifurcation at simple eigenvalues are proved by various methods, all different from ours in the previous section. Crandall and Rabinowitz [1971], [1973] is a standard reference, noted for clean and complete proofs. Nirenberg and Berger also discuss Kransoselski's [1964] basic results and methods based on topological degree. Nirenberg [1974] and Ize [1976] are good references for the global theory of Rabinowitz [1971].

The literature for bifurcation at multiple eigenvalues is more specialized, but still large. Some samples are McLeod and Sattinger [1973], Magnus [1976b], Shearer [1976, 7] and Marsden [1978], and Buchner, Marsden, and Schechter [1982].

Imperfection-sensitivity questions spawned a whole series of papers, especially recent ones using singularity theory. Three papers using classical methods that were among the first to exploit the fact that multiple eigenvalue problems can be very sensitive unless enough parameters are included and that including them can yield new solutions and explanations, are Keener and Keller [1973], Keener [1974], and Bauer, Keller, and Reiss [1975]. These new solutions are called "secondary bifurcations." Examples were given in the previous section. The first papers to attempt to systematically use singularity theory in bifurcation problems are those of Chow, Hale, and Mallet-Paret [1975], [1976]. See also Hale [1977]. This theory was advanced considerably by Golubitsky and Schaeffer [1979a, b], whose methods were outlined in the previous section.

Applications Using Analytic Methods. Again the literature here is massive. We shall only discuss some of the recent references. First, the collections Keller and Antman [1969] and Rabinowitz [1977b] contain many valuable articles. Also, there are numerous papers that were very important for the recent history such as Friedrichs [1941], Keller, Keller, and Reiss [1962] and Bauer and Reiss [1965].

Sturmian theory is used in Kolodner [1955] who analyzed the states of a rotating string. This was improved considerably by exploiting Rabinowitz' global theory as well as Sturmain theory by Antman [1980a].

For plate theory, Yanowitch [1956] is important for it is one of the first to discuss symmetry breaking. The von Karman and related equations are often used to model plates, and many papers are written on this, such as Knightly [1967], Wolkowski [1967] (circularly symmetric bifurcations), Berger and Fife [1967] (global analysis using calculus of variations and degree theory; see also Berger [1974]), Bauer, Keller, and Reiss [1970], Knightly and Sather [1970], [1974], [1975] (local analysis using the Liapunov–Schmidt procedure), and Matkowsky and Putnik [1974]. There are a number of similar papers for shell models, such as Knightly and Sather [1975], [1980], Sather [1977], and Shearer [1977].

In a series of important papers—Antman [1977], [1978a], [1979a], [1980c], Antman and Rosenfeld [1978], Antman and Nachman [1979], and Antman and Dunn [1980]—use Sturmian theory together with Rabinowitz' global theory to

prove global bifurcation and preservation of nodal structure for geometrically exact models; see Box 2.1 below. This extends earlier work of, for example, Greenberg [1967]. Antman and Kenney [1981] use an extension of the Rabinowitz theory due to Alexander and Antman [1981] to study a two-parameter problem. Antman and Carbone [1977] show that shear- and necking-type bifurcations with hysteresis can occur within the context of hyperelasticity without plasticity-type assumptions. Maddocks [1982] considers non-planar configurations of the elastica.

A number of three-dimensional problems can be done by semi-inverse methods—that is, assuming symmetry and looking for solutions of a particular form. Perhaps the most famous is Antman [1978b], [1979b], where it is shown that thick spherical shells admit everted solutions (a tennis ball cut in half and then pushed inside out). Some barelling solutions in three dimensions for a traction displacement problem of a compressed cylinder were found by Simpson and Spector [1982].

Applications Using Imperfection-Sensitivity or Singularity Theory. Historically this really started with Koiter [1945], Roorda [1965], Sewell [1966b], and Thompson and Hunt [1973]. More systematic, but still "bare hands" methods were applied in Keener and Keller [1972] and Keller [1973].

Singularity theory was applied to the von Karman equations in Chow, Hale, and Mallet-Paret [1975]. Papers in a similar spirit are Mallet-Paret [1977] (inspired by Knightly and Sather [1975]), Magnus and Poston [1977], Vanderbauwhede [1978], Potier-Ferry [1979], Hunt [1982] and Golubitsky, Marsden and Schaeffer [1983].

A paper that explains mode jumping in the buckling of a rectangular plate is Schaeffer and Golubitsky [1980]. This is one of the most interesting uses of the imperfection-sensitivity approach in the previous section to a hard concrete example; see Box 2.2 below. For a survey of many other applications of a similar type, see Stewart [1981] and Thompson [1982].

Box 2.1 ***Global Bifurcation Analysis: Buckling of a Rod***

Usually a bifurcation analysis is called *global* when the structure of the solutions set is determined for all values of the parameter (or parameters) λ and the full range of the state variable x. If this determination is made only in a neighborhood of a given solution (x_0, λ_0), then the analysis is called *local.* In Section 7.1 we described some methods used in local bifurcation analysis and in Box 1.2 we mentioned some global techniques. Here we make a few additional remarks.

1. In the papers of Antman quoted above it is made clear that before one attempts a global bifurcation analysis, one should have a model

that is valid for large deformations. In particular, this is not the case for the von Karman equations and global results for them are of limited interest in the region of large deflections. In Antman's work geometrically exact models are used that are valid for large deformations.

2. For example, we briefly consider the deformations of nonlinearly elastic rods (Antman and Rosenfeld [1978], Antman [1980c]). The reference configuration is an interval $[s_1, s_2]$ on $\mathbb{R}$. A *configuration* is a map $\phi: [s_1, s_2] \longrightarrow \mathbb{R}^3 \times S^2$ denoted $\phi(s) = (\boldsymbol{r}(s), \boldsymbol{d}_3(s))$. Here S^2 is the two-sphere and $\boldsymbol{d}_3 \in S^2$ represents the normal to a plane in $\mathbb{R}^3$ that describes shearing in the rod. See Figure 7.2.5, where we draw the rod with a thickness that has been suppressed in the mathematical model. Thus, we are considering rods that are capable of bending, elongating and shearing. One can also contemplate more complex situations allowing twisting

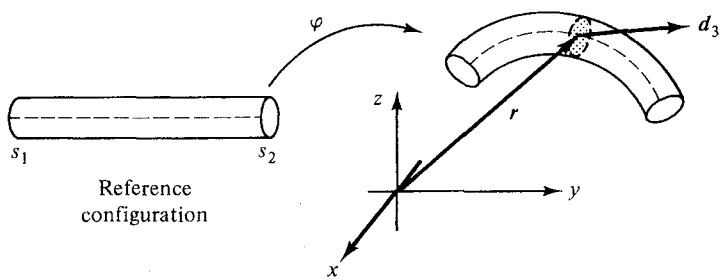

Figure 7.2.5

and necking. Note that bodies of this type fall into the general class of Cosserat continua, considered in Box 2.3, Chapter 2 with a reference $\boldsymbol{d}_3$ being $\boldsymbol{d}_3 = \boldsymbol{i}$, say. If we wished to take into account twisting, for example, it is not enough to specify $\boldsymbol{d}_3$, but we also need to specify twisting about $\boldsymbol{d}_3$ through some angle. For this situation one convenient way is to take a configuration to be a map $\phi: [s_1, s_2] \longrightarrow \mathbb{R}^3 \times \mathbb{F}_3$, the oriented 3-frame bundle on $\mathbb{R}^3$; that is, $\phi(s)$ consists of a base point $\boldsymbol{r}(s)$ and an oriented orthonormal frame $(\boldsymbol{d}_1, \boldsymbol{d}_2, \boldsymbol{d}_3)$ at $\boldsymbol{r}(s)$. The plane of $\boldsymbol{d}_1$ and $\boldsymbol{d}_2$ (normal to $\boldsymbol{d}_3$) gives the shearing and the orientation of $\boldsymbol{d}_1$ and $\boldsymbol{d}_2$ within this plane gives the twisting. (Again the Cosserat theory requires a reference section of the frame bundle, which we can take to be the standard frame $(\boldsymbol{i}, \boldsymbol{j}, \boldsymbol{k})$.) In that notation, $\mathcal{B} = [s_1, s_2]$ and $\mathcal{S} = \mathbb{R}^3 \times \mathbb{F}_3$. The equation $\boldsymbol{d}_3 = \boldsymbol{d}_1 \times \boldsymbol{d}_2$ of course means we can write the equations just in terms of $\boldsymbol{r}$, $\boldsymbol{d}_1$, and $\boldsymbol{d}_2$. Analogous to the requirement $J > 0$ in three-dimensional elasticity, here we require that $\boldsymbol{r}$ be an embedding and that $\boldsymbol{r}' \cdot \boldsymbol{d}_3 > 0$; that is, the shearing is not infinitely severe.

The equilibrium equations for the rod are obtained by balancing forces and moments. One assumes there is a traction vector $\boldsymbol{n}(s)$ corresponding to contact forces in the rod. The balance equation for an external force $\boldsymbol{f}$ per unit length is then

$$\boldsymbol{n}' + \boldsymbol{f} = 0.$$

Likewise, one assumes a couple force field $\boldsymbol{m}(s)$ and an external couple $\boldsymbol{g}$ and derives the equation

$$\boldsymbol{m}' + \boldsymbol{r}' \times \boldsymbol{n} + \boldsymbol{g} = 0$$

by balancing torque.

Problem 2.3 Show that these balance equations are a special case of the Cosserat equations in Box 2.3, Chapter 2.

These equations together with boundary conditions and constitutive equations (i.e., $\boldsymbol{n}$, $\boldsymbol{m}$ as functions of $\boldsymbol{r}'$, $\boldsymbol{d}_1$, $\boldsymbol{d}_2$, $\boldsymbol{d}_1'$, $\boldsymbol{d}_2'$) are the equations for the rod. These are in general quasi-linear *ordinary* differential equations.

Antman's program for planar deformations and buckling of straight rods goes something like the following:

(a) introduce new variables ν, η, μ by writing

$$\begin{aligned} \boldsymbol{d}_3 &= \cos\theta\boldsymbol{i} + \sin\theta\boldsymbol{j}, & \boldsymbol{r}' &= (1+\nu)\boldsymbol{d}_3 + \eta\boldsymbol{d}_1, \\ \boldsymbol{d}_1 &= -\sin\theta\boldsymbol{i} + \cos\theta\boldsymbol{j}, & \boldsymbol{n} &= N\boldsymbol{d}_3 + H\boldsymbol{d}_1, \\ \boldsymbol{d}_2 &= \boldsymbol{k}, & \boldsymbol{m} &= M\boldsymbol{k}. \end{aligned}$$

Thus a configuration is specified by $\boldsymbol{r}(s)$ and $\theta(s)$. Let $\mu = \theta' - \theta_{\text{Ref}}$, so μ would be a curvature if s were arc length. The constitutive hypothesis is that N, H, M are functions $(\hat{N}, \hat{H}, \hat{M})$ of (ν, η, μ); the analogue of strong ellipticity is that the Jacobian matrix be positive-definite. Under suitable growth conditions one can globally invert this relationship to obtain

$$\nu = \hat{\nu}(N, H, \mu), \qquad \eta = \hat{\eta}(N, H, \mu).$$

With $f = 0$, $g = 0$, $s_1 = 0$, $s_2 = 1$, $\theta_{\text{Ref}} = 0$ and the boundary conditions $\theta(0) = 0$, $\theta(1) = 0$, $\boldsymbol{r}(0) = 0$, $\boldsymbol{n}(1) = -\lambda\boldsymbol{i}$, one gets $\hat{N} = -\lambda\cos\theta$ and $\hat{H} = \lambda\sin\theta$, so the problem reduces to the quasi-linear equation

$$[\hat{M}(\hat{\nu}, \hat{\eta}, \theta')]' + \lambda[(1+\hat{\nu})\sin\theta + \hat{\eta}\cos\theta] = 0, \qquad \text{(A)}$$

where $\hat{\nu}$ and $\hat{\eta}$ become functions of $-\lambda\cos\theta$, $\lambda\sin\theta$, and θ'.

For an inextensible ($\hat{\nu} = 0$) and unshearable ($\hat{\eta} = 0$) rod, with $\hat{M}(\mu) = EI\mu$, this equation becomes the Euler elastica equation:

$$EI\theta'' + \lambda\sin\theta = 0. \qquad \text{(E)}$$

(b) One analyzes (A) using Rabinowitz' global bifurcation theorem. One way to do this is to convert this quasi-linear equation to a semilinear one like (E). This can be done by regarding the basic variables as (λ, θ, M) and replacing (A) by the first-order semilinear system consisting of (A) and $\theta' = \mu$, a function of $(-\lambda \cos \theta, \lambda \sin \theta, M)$.

(c) Finally, one invokes elementary Sturmian theory to deduce that along the global solution branches found, the nodal properties do not change. Unlike the elastica, however, the bifurcated branch could rejoin the trivial solution at another eigenvalue. See Antman and Rosenfeld [1978] for details. For work related to Kirchhoff's problem on the loading and twisting of columns, where the geometrically exact theory produces quite different results from Kirchhoff's, see Antman [1974b] and Antman and Kenney [1981].

3. A major open problem connected with such global analyses is to see how they behave under an imperfection sensitivity analysis. As we indicated in the previous section, it is for such questions that the local theory is much more developed. In fact, often a complete local analysis can produce results that are in some sense global. For example, if a multiple eigenvalue bifurcation point is unfolded or perturbed, secondary bifurcations occur nearby and can be located quite precisely. Such things could be very difficult using currently known global techniques.

4. Even geometrically exact models can be criticized along the lines that approximate models such as the von Karman equations are criticized. Obviously for very severe deformations, the assumption that the rod can be realistically modeled in the manner indicated above is only an approximation, so is misleading unless it can be shown to be structurally stable. It also seems clear that the situation is much better for geometrically exact models than for geometrically approximate ones. Probably one should carefully investigate the range of validity for any model as part of the problem in any global bifurcation study. For example, the von Karman equations *do* successfully model many interesting bifurcation problems.

Box 2.2 ***Imperfection Sensitivity: Mode Jumping in the Buckling of a Plate***

In the previous section we indicated that singularity theory is a very powerful tool in an analysis of imperfection sensitivity. Such analyses, when fully done, produce bifurcation diagrams that are insensitive to

further perturbations. It is therefore consistent to use any reasonable approximation to an exact model, valid near the bifurcation point of interest. Therefore, unlike the previous box, the use of approximate models such as the von Karman equations here is justified.

Carrying out a substantial singularity analysis can involve a variety of issues, some of which we wish to point out. We shall make some comments in the context of the beautiful paper of Schaeffer and Golubitsky [1980]. (Related work is found in Matkowsky and Putnik [1974], Chow, Hale and Mallet-Paret [1976], and Magnus and Poston [1977].)

The problem concerns the buckling of a rectangular plate (Figure 7.2.6). The aspect ratio l (i.e., length/width) used in experiments of

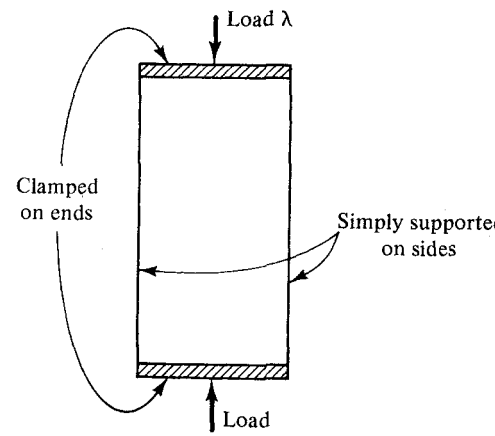

Figure 7.2.6

Stein [1959] was about 5.36. For the load λ exceeding a certain value λ_0, the plate buckles to a state with wave number 5. As λ increases further the plate undergoes a sudden and violent snap buckling to wave number 6. The phenomenon is called "mode jumping" and the problem is to explain it.

Parameterizing the plate by $\Omega = \{(z_1, z_2) | 0 \leq z_1 < l\pi \text{ and } 0 \leq z_2 \leq \pi\}$, the von Karman equations for w, the z_3 component of the deflection and ϕ, the Airy stress function, are

$$\Delta^2 w = [\phi, w] - \lambda w_{z_1 z_1},$$
$$\Delta^2 \phi = -\tfrac{1}{2}[w, w].$$

where Δ^2 is the biharmonic operator and [,] is the symmetric bilinear

form defined by

$$[u, v] = u_{z_1z_1}v_{z_2z_2} + u_{z_2z_2}v_{z_1z_1} - 2u_{z_1z_2}v_{z_1z_2}.$$

The boundary conditions for w are $w = \partial w/\partial n = 0$ on the ends (clamped) and $w = \Delta w = 0$ on the sides (simply supported).

A few of the highlights of the procedures followed are given next:

(a) Bauer, Keller, and Riess [1975] used a spring model without boundary conditions. Matkowsky and Putnik [1974] and Matkowsky, Putnik and Reiss [1980] use simply supported boundary conditions. The type of boundary conditions used makes an important difference. Schaeffer and Stein noted that the clamped conditions for the ends makes more sense physically. In the present case, at $l_k = \sqrt{k(k+2)}$ there is a double eigenvalue λ_0. For $k = 5$, this is actually fairly close to the situation near wave numbers 5 and 6. Thus the strategy is to unfold the bifurcation near this double eigenvalue and see what secondary bifurcations arise.

(b) The Liapunov–Schmidt procedure is now done to produce a function $G: \mathbb{R}^2 \times \mathbb{R} \to \mathbb{R}^2$.

(c) There is a symmetry in the problem that is exploited. This symmetry on the $\mathbb{R}^2$ obtained in the Liapunov–Schmidt procedure is $\mathbb{Z}_2 \oplus \mathbb{Z}_2$, generated by $(x, y) \mapsto (-x, -y)$ and $(x, y) \mapsto (x, -y)$. These correspond to 2 of the 3 obvious symmetries of the original problem (the other gives no extra information). Also, G is the gradient (for each $\lambda \in \mathbb{R}$) of a function invariant under this action.

(d) The symmetry in (a) greatly simplifies the unfolding procedure, where now unfolding is done under the assumption of a symmetry group for the equations. The general theory for this is described in Golubitsky and Shaeffer [1979b].

(e) Mode jumping does not occur with all the boundary conditions simply supported. There one gets a bifurcation diagram like that in Figure 7.2.7(a); the wave number 5 solution never

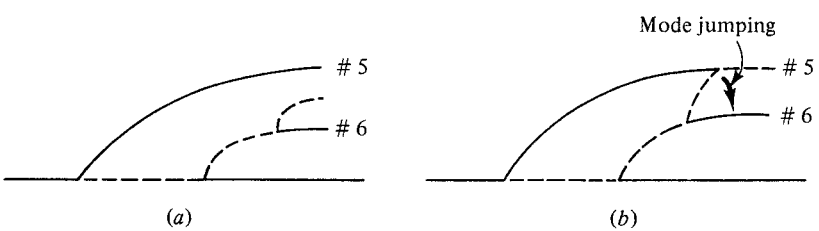

Figure 7.2.7

loses stability. With the boundary conditions above, the bifurcation diagram is like Figure 7.2.6(b); the wave number 5 solution loses stability and wave number 6 picks it up by way of a jump. These figures only show the orbits; to get all solutions one acts on the orbits by the symmetry group.

Examples like this show that the local analysis using singularity theory can produce rather sophisticated bifurcation diagrams. This kind of detailed explanation and computable complexity is beyond the reach of most global results known at present. The blending of techniques like this with those of the previous box represents a considerable challenge.

Box 2.3 ***The Role of Symmetry in Bifurcation Problems***

When studying bifurcation problems, questions of symmetry arise in many guises. This box discusses some of the ways symmetry can be exploited, and some of the tantalizing questions it raises.

If a bifurcation problem has a multiple eigenvalue, then the problem is usually non-generic. Sometimes this non-genericity is due to the invariance of the problem under a symmetry group. We indicated in the previous box that a bifurcation analysis including imperfection-sensitivity results can be obtained for such problems. If a (real) problem is anywhere near such a special point, it is often wise to regard it as an imperfection in a more ideal model. In fact, some otherwise simple eigenvalue problems may be better treated as belonging to a perturbation of a double eigenvalue problem. This whole philosophy of symmetrizing to bring eigenvalues together seems to be frutiful.

When we say a bifurcation problem has a certain symmetry group, we mean that it is covariant under the action of this group. For example, if $F\colon \mathfrak{X} \times \mathbb{R} \longrightarrow \mathfrak{Y}$ is a map whose zeros we wish to study and $\mathcal{G}$ is a group acting on $\mathfrak{X}$ and $\mathfrak{Y}$, we say F is *covariant* when

$$F(gx, \lambda) = gF(x, \lambda)$$

for $g \in \mathcal{G}$, $x \in \mathfrak{X}$, $\lambda \in \mathbb{R}$, and where gx is the action of g on x. The *symmetry group* of a point $x \in \mathfrak{X}$ is defined by

$$\mathcal{G}_x = \{g \in \mathcal{G} \mid gx = x\}.$$

When a bifurcation occurs, often the trivial solution has symmetry group $\mathcal{G}$, but the bifurcating solution has a smaller symmetry group. We say that the bifurcation has *broken the symmetry*.

It is an important problem to study how symmetries are so broken and how they relate to pattern formation and related questions. If $\mathcal{G}_x$ gets smaller, the solution gets less symmetric, or more complex. What, if anything, does this have to do with entropy?

If $\mathcal{G}$ acts on $\mathfrak{X}$ linearly, methods of group representations can be used to analyze which "modes" go unstable and hence how the symmetry is broken. The idea is to break up $\mathfrak{X}$ into a direct sum (like a Fourier decomposition) on each piece of which $\mathcal{G}$ acts irreducibly and determine in which piece the eigenvalue crosses. Two basic references for this method are Ruelle [1973] and Sattinger [1979]. There are numerous related papers as well. (For example, Rodrigues and Vanderbauwhede [1978] give conditions under which the bifurcating solutions do not break symmetry.) This kind of phenomenon actually is abundant. It occurs in Taylor cells between rotating cylinders, in hexagonal cells in convection problems, and in many problems of chemical kinetics. For example, the breaking of S^1 symmetry to a discrete symmetry occurs in the Taylor problem in fluid muchanics (Rand [1982]) and the breaking of SO(3) to S^1 symmetry occurs in the blowing up of a balloon (Haughton and Ogden [1980]) and in convection in a spherical shell (Chossat [1979]). See, Sattinger [1980], Haken [1979], Buzano and Golubitsky [1982], and Golubitsky, Marsden and Schaeffer [1983] for more examples and references.

A much more serious kind of symmetry breaking is to allow imperfections that break the symmetry in various ways; that is, the equations themselves rather than the solutions break the symmetry. Here, not only is the mathematics difficult (it is virtually non-existent), but it is not as clear what one should allow physically.

In Arms, Marsden, and Moncrief [1981], a special class of bifurcation problems is studied where the structure of the bifurcation and its connection with symmetry can be nailed down. The problems studied are of the form $F(x, \lambda) = J(x) - \lambda = 0$, where J is the Noether conserved quantity for a symmetry group acting on phase space. It is shown that bifurcations occur precisely at points with symmetry; how the symmetry is broken is determined.

In the next section we shall see how symmetry in the form of SO(3) and material frame indifference comes into the analysis of the traction problem in an essential way. We shall see that bifurcation points are those with a certain symmetry, in accordance with the general philosophy exposed here. However the detailed way symmetry enters the problem is different from the examples mentioned so far since the trivial solutions are not fixed by the group and the group also acts on parameter space.

For more information on these points, see Golubitsky and Schaeffer [1982] and [1984].

7.3 THE TRACTION PROBLEM NEAR A NATURAL STATE (Signorini's Problem)[7]

In the 1930s Signorini discovered an amazing fact: the traction problem in nonlinear elasticity can have non-unique solutions even for small loads and near a natural state. Here non-unique means unequal up to a rigid body motion of the body and loads. What is even more amazing is that this non-uniqueness depends, in many cases, not on the whole stored energy function, but only on the elasticity tensor c_{abcd} for linearized elasticity, even though the traction problem for linearized elasticity has uniqueness up to rigid body motions, as we proved in Section 6.1. For example, the loads shown in Figure 7.3.1 can produce

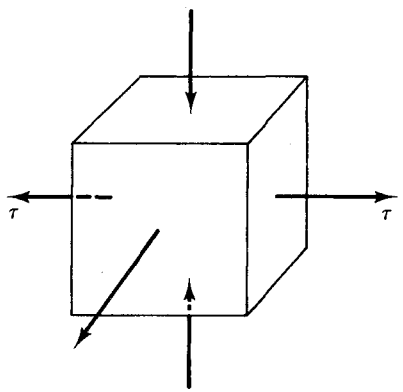

Figure 7.3.1

more than one solution, even for a (compressible) neo-Hookean material, and (arbitrarily small) loads near the one shown. The occurence of these extra solutions in the nonlinear theory and yet their absence in the linearized theory is not easy (for us) to understand intuitively, although it may be related to bulging or barelling solutions. Experiments for such situations are not easy to carry out; cf. Beatty and Hook [1968].

This state of affairs led to much work—much of it in the Italian school—and was the subject of some controversy concerning the validity of linearized elasticity. Some of the main contributions after Signorini were by Tolotti [1943], Stoppelli [1958], Grioli [1962], and Capriz and Podio-Guidugli [1974]. The problem is discussed at length and additional contributions given in Truesdell and Noll [1965]; see also Wang and Truesdell [1973] and Van Buren [1968].

---

[7]This section was done in collaboration with D. Chillingworth and Y. H. Wan and is based on Chillingworth, Marsden, and Wan [1982a, b].

Nowadays we do not see any contradictions, but rather we see a *bifurcation* in the space of solutions of the equations of elastostatics. Whenever there is a bifurcation, the correspondence with the linearized problem becomes singular; that is, the problem is *linearization unstable* in the sense of Section 4.4. In the framework of elastodynamics there is clearly no bifurcation or linearization instability, but this makes the bifurcation in the elastostatic problem no less interesting. This bifurcation in the space of solutions then takes its place alongside similar phenomena in other classical field theories such as general relativity and gauge theory (see Arms, Marsden, and Moncrief [1981], and references therein).

The most complete results in the literature before now are those of Stoppelli [1958]. His results are stated (without proof, but in English) in Grioli [1962]. However, this analysis is incomplete for three reasons. First, the load is varied only by a scalar factor. In a full neighborhood of loads with axes of equilibrium there are additional solutions missed by their analysis; thus, an imperfection-sensitivity-type analysis reveals more solutions. Second, their analysis is only local in the rotation group, so additional nearly stress-free solutions are missed by restricting to rotations near the identity. Third, some degenerate classes of loads were not considered. However, singularity theory can deal with these cases as well. The complexity of the problem is indicated by the fact that for certain types of loads one can find up to 40 geometrically distinct solutions that are nearly stress free, whereas Stoppelli's analysis produces at most 3.

These problems have recently been solved by Chillingworth, Marsden, and Wan [1982a]. This section gives a *brief introduction* to their methods. The paper should be consulted for the complete analysis. However, we do go far enough to include a complete and considerably simplified proof of the first basic theorem of Stoppelli. Apart from Van Buren [1968], whose proof is similar to Stoppelli's, a complete proof has not previously appeared in English.

3.1 Notation Let the reference configuration be a bounded region $\mathcal{B} = \Omega \subset \mathbb{R}^3$ with smooth boundary.[8] As we saw in Section 6.1, the linearized equations have a kernel consisting of infinitesimal rigid body motions. We can readily eliminate translations by assuming $0 \in \Omega$ and working with the configuration space $\mathcal{C}$ consisting of all deformations $\phi: \Omega \to \mathbb{R}^3$ that are of class $W^{s,p}$, $s > 3/p + 1$ and satisfy $\phi(0) = 0$. (Recall that such ϕ's are necessarily C^1.) The central difficulty of the problem is then the presence of the rotational covariance of the problem (material frame indifference).

Let $W(X, C)$ be a given smooth stored energy function, where C is, as usual,

[8] We believe that our results also hold when Ω has piecewise smooth boundary. This program depends on elliptic regularity for such regions. Except in special cases, this theory is nonexistent (as far as we know) and seems to depend on a modification of the usual Sobolev spaces near corners. However for simple shapes like cubes, where the linearized elastostatic equations can be solved explicitly, the necessary regularity can be checked by hand. See pp. 318 and 371.

the Cauchy–Green tensor. Let $\boldsymbol{P} = \partial W/\partial \boldsymbol{F}$ and $\boldsymbol{S} = 2\,\partial W/\partial \boldsymbol{C}$ be the first and second Piola–Kirchhoff stress tensors and $\mathbf{A} = \partial \boldsymbol{P}/\partial \boldsymbol{F}$ the elasticity tensor.

We make the following two assumptions.

3.2 Assumptions

(H1) When $\phi = I_\Omega$ (identity map on Ω), $\boldsymbol{P} = \mathbf{0}$; that is, the undeformed state is stress free, or natural.

(H2) Strong ellipticity holds at (and hence near) $\phi = I_\Omega$.

Since the undeformed state is stress free, the classical elasticity tensor for elasticity linearized about $\phi = I_\Omega$ is $\mathbf{c} = 2\,\partial^2 W/\partial \boldsymbol{C}\,\partial \boldsymbol{C}$ evaluated at $\phi = I_\Omega$.

Let $\boldsymbol{B}\colon \Omega \longrightarrow \mathbb{R}^3$ denote a given body force (per unit volume) and $\boldsymbol{\tau}\colon \partial\Omega \longrightarrow \mathbb{R}^3$ a given surface traction (per unit area). These are dead loads; in other words, the equilibrium equations for ϕ that we are studying are:

$$\left.\begin{aligned} \operatorname{DIV} \boldsymbol{P}(X, \boldsymbol{F}(X)) + \boldsymbol{B}(X) &= 0 \qquad \text{for} \quad X \in \Omega, \\ \boldsymbol{P}(X, \boldsymbol{F}(X))\cdot \boldsymbol{N}(X) &= \boldsymbol{\tau}(X) \qquad \text{for} \quad X \in \partial\Omega, \end{aligned}\right\} \tag{E}$$

where $\boldsymbol{N}(X)$ is the outward unit normal to $\partial\Omega$ at $X \in \partial\Omega$.

3.3 Definition Let $\mathcal{L}$ denote the space of all pairs $l = (\boldsymbol{B}, \boldsymbol{\tau})$ of loads (of class $W^{s-2,p}$ on Ω and $W^{s-1-1/p,p}$ on $\partial\Omega$) such that

$$\int_\Omega \boldsymbol{B}(X)\, dV(X) + \int_{\partial\Omega} \boldsymbol{\tau}(X)\, dA(X) = 0.$$

That is, the total force on Ω vanishes, where dV and dA are the respective volume and area elements on Ω and $\partial\Omega$.

Observe that if $(\boldsymbol{B}, \boldsymbol{\tau})$ are such that (E) holds for some $\phi \in \mathcal{C}$, then $(\boldsymbol{B}, \boldsymbol{\tau}) \in \mathcal{L}$.

The group $\mathrm{SO}(3) = \{\boldsymbol{Q} \in \boldsymbol{L}(\mathbb{R}^3, \mathbb{R}^3) \mid \boldsymbol{Q}^T\boldsymbol{Q} = I_{\mathbb{R}^3} \text{ and } \det \boldsymbol{Q} = +1\}$ of proper orthogonal transformations will play a key role. By (H1), $\phi = I_\Omega$ solves (E) with $\boldsymbol{B} = \boldsymbol{\tau} = \mathbf{0}$. By material frame indifference, $\phi = \boldsymbol{Q}|\Omega$ ($\boldsymbol{Q}$ restricted to Ω) is also a solution for any $\boldsymbol{Q} \in \mathrm{SO}(3)$. The map $\boldsymbol{Q} \mapsto \boldsymbol{Q}|\Omega$ embeds SO(3) into $\mathcal{C}$ and we shall identify its image with SO(3). Thus, the "trivial" solutions of (E) are elements of SO(3).

Our basic problem is as follows:

(*P1*) *Describe the set of all solutions of* (*E*) *near the trivial solutions* SO(3) *for various loads* $l \in \mathcal{L}$ *near zero.* Here, "describe" includes the following objectives:

(a) counting the solutions;
(b) determining the stability of the solutions;
(c) showing that the results are insensitive to small perturbations of the stored energy function and the loads; that is, the bifurcation diagram produced is structurally stable.

3.4 Notations and Facts about the Rotation Group SO(3) Let $\mathfrak{M}_3 = L(\mathbb{R}^3, \mathbb{R}^3)$ = linear transformations of $\mathbb{R}^3$ to $\mathbb{R}^3$; sym $= \{A \in \mathfrak{M}_3 \mid A^T = A\}$; skew $= \{A \in \mathfrak{M}^3 \mid A^T = -A\}$.

We identify skew with so(3), the Lie algebra of SO(3). $\mathbb{R}^3$ and skew are isomorphic by the mapping $\boldsymbol{v} \in \mathbb{R}^3 \mapsto \boldsymbol{W}_v \in$ skew, where $\boldsymbol{W}_v(\boldsymbol{w}) = \boldsymbol{w} \times \boldsymbol{v}$; relative to the standard basis, the matrix of $\boldsymbol{W}_v$ is

$$\boldsymbol{W}_v = \begin{bmatrix} 0 & r & -q \\ -r & 0 & p \\ q & -p & 0 \end{bmatrix}, \quad \text{where} \quad \boldsymbol{v} = (p, q, r).$$

The Lie bracket is $[\boldsymbol{W}_v, \boldsymbol{W}_w] = \boldsymbol{v} \otimes \boldsymbol{w} - \boldsymbol{w} \otimes \boldsymbol{v} = -\boldsymbol{W}_{v \times w}$, where $\boldsymbol{v} \otimes \boldsymbol{w} \in \mathfrak{M}_3$ is given by $(\boldsymbol{v} \otimes \boldsymbol{w})(\boldsymbol{u}) = \boldsymbol{v}\langle \boldsymbol{w}, \boldsymbol{u}\rangle$. The standard inner product on $\mathbb{R}^3$ is $\langle \boldsymbol{v}, \boldsymbol{w}\rangle = \frac{1}{2}\operatorname{trace}(\boldsymbol{W}_v^T \boldsymbol{W}_w)$, called the *Killing form* on SO(3). Finally, $\exp(\boldsymbol{W}_v)$ is the rotation about the vector $\boldsymbol{v}$ in the positive sense, through the angle $\|\boldsymbol{v}\|$.

Now we turn to some preliminary facts about $\mathcal{L}$ and $\mathcal{C}$.

3.5 Definition Let $\boldsymbol{\phi} \in \mathcal{C}$ and $l \in \mathcal{L}$. We say that l is *equilibrated relative to* $\boldsymbol{\phi}$ if the total torque in the configuration $\boldsymbol{\phi}$ vanishes:

$$\int_\Omega \boldsymbol{\phi}(X) \times \boldsymbol{B}(X)\, dV(X) + \int_{\partial\Omega} \boldsymbol{\phi}(X) \times \boldsymbol{\tau}(X)\, dA(X) = 0,$$

where $l = (\boldsymbol{B}, \boldsymbol{\tau})$. Let $\mathcal{L}_e$ denote the loads that are equilibrated relative to the identity.

> ***Problem 3.1*** Show that if $l = (\boldsymbol{B}, \boldsymbol{\tau})$ satisfies (E) for some $\boldsymbol{\phi} \in \mathcal{C}$, then l is equilibrated relative to $\boldsymbol{\phi}$. (*Hint*: Use the Piola identity.)

3.6 Definition Define the *astatic load map* $\boldsymbol{k}: \mathcal{L} \times \mathcal{C} \longrightarrow \mathfrak{M}_3$ by

$$\boldsymbol{k}(l, \boldsymbol{\phi}) = \int_\Omega \boldsymbol{B}(X) \otimes \boldsymbol{\phi}(X)\, dV(X) + \int_{\partial\Omega} \boldsymbol{\tau}(X) \otimes \boldsymbol{\phi}(X)\, dA$$

and write $\boldsymbol{k}(l) = \boldsymbol{k}(l, I_\Omega)$.

We have actions of SO(3) on $\mathcal{L}$ and $\mathcal{C}$ given by:

***Action of* SO(3) *on* $\mathcal{L}$:** $\boldsymbol{Q}l(X) = (\boldsymbol{Q}\boldsymbol{B}(X), \boldsymbol{Q}\boldsymbol{\tau}(X))$.
***Action of* SO(3) *on* $\mathcal{C}$:** $\boldsymbol{Q}\boldsymbol{\phi} = \boldsymbol{Q} \circ \boldsymbol{\phi}$.

Note that $\boldsymbol{Q}l$ means "the load arrows are rotated, keeping the body fixed." We shall write $\mathcal{O}_l$ and $\mathcal{O}_\phi$ for the SO(3) orbits of l and $\boldsymbol{\phi}$; that is,

$$\mathcal{O}_l = \{\boldsymbol{Q}l \mid \boldsymbol{Q} \in \mathrm{SO}(3)\} \quad \text{and} \quad \mathcal{O}_\phi = \{\boldsymbol{Q}\boldsymbol{\phi} \mid \boldsymbol{Q} \in \mathrm{SO}(3)\}.$$

Thus, $\mathcal{O}_{I_\Omega}$ consists of the trivial solutions corresponding to $l = 0$.

The following is a list of basic observations about the astatic load map, each of which may be readily verified.

3.7 Proposition

(A1) *l is equilibrated relative to ϕ if and only if $\boldsymbol{k}(l, \phi) \in$ sym. In particular, $l \in \mathcal{L}_e$ if and only if $\boldsymbol{k}(l) \in$ sym.*

(A2) (*Equivariance*) *For $l \in \mathcal{L}$, $\phi \in \mathcal{C}$, and $\boldsymbol{Q}_1, \boldsymbol{Q}_2 \in$ SO(3),*

$$\boldsymbol{k}(\boldsymbol{Q}_1 l, \boldsymbol{Q}_2\phi) = \boldsymbol{Q}_1\boldsymbol{k}(l, \phi)\boldsymbol{Q}_2^{-1}.$$

In particular, $\boldsymbol{k}(\boldsymbol{Q}l) = \boldsymbol{Q}\boldsymbol{k}(l)$.

(A3) (*Infinitesimal Equivariance*) *For $l \in \mathcal{L}$, $\phi \in \mathcal{C}$, $\boldsymbol{W}_1, \boldsymbol{W}_2 \in$ skew,*

$$\boldsymbol{k}(\boldsymbol{W}_1 l, \phi) = \boldsymbol{W}_1\boldsymbol{k}(l, \phi), \qquad \boldsymbol{k}(l, \boldsymbol{W}_2\phi) = -\boldsymbol{k}(l, \phi)\boldsymbol{W}_2.$$

In particular, $\boldsymbol{k}(\boldsymbol{W}l) = \boldsymbol{W}\boldsymbol{k}(l)$.

Problem 3.2 Prove each of these assertions.

Later on, we shall be concerned with how the orbit of a given $l \in \mathcal{L}$ meets $\mathcal{L}_e$. The most basic result in this direction is the following.

3.8 DaSilva's Theorem Let $l \in \mathcal{L}$. Then $\mathcal{O}_l \cap \mathcal{L}_e \neq \varnothing$.

Proof By the polar decomposition, we can write $\boldsymbol{k}(l) = \boldsymbol{Q}^T\boldsymbol{A}$ for some $\boldsymbol{Q} \in$ SO(3) and $\boldsymbol{A} \in$ sym. By (A2), $\boldsymbol{k}(\boldsymbol{Q}l) = \boldsymbol{Q}\boldsymbol{k}(l) = \boldsymbol{A} \in$ sym, so by (A1), $\boldsymbol{Q}l \in \mathcal{L}_e$. ∎

Similarly, any load can be equilibrated relative to any chosen configuration by a suitable rotation.

Solutions of (E) with an "axis of equilibrium" will turn out to coincide with the bifurcation points. The idea is to look for places where $\mathcal{O}_l$ meets $\mathcal{L}_e$ in a degenerate way.

3.9 Definition Let $l \in \mathcal{L}_e$ and $\boldsymbol{v} \in \mathbb{R}^3$, $\|\boldsymbol{v}\| = 1$. We say that $\boldsymbol{v}$ is an *axis of equilibrium* for l when $\exp(\theta\boldsymbol{W}_v)l \in \mathcal{L}_e$ for all real θ—that is, when rotations of l through any angle θ about the axis $\boldsymbol{v}$ do not destroy equilibration relative to the identity.

There are a number of useful ways of reformulating the condition that $\boldsymbol{v}$ be an axis of equilibrium. These are listed as follows.

3.10 Proposition *Let $l \in \mathcal{L}_e$ and $\boldsymbol{A} = \boldsymbol{k}(l) \in$ sym. The following conditions are equivalent:*

(1) *l has an axis of equilibrium $\boldsymbol{v}$.*

(2) *There is a $\boldsymbol{v} \in \mathbb{R}^3$, $\|\boldsymbol{v}\| = 1$ such that $\boldsymbol{W}_v l \in \mathcal{L}_e$.*

(3) *$\boldsymbol{W} \mapsto \boldsymbol{A}\boldsymbol{W} + \boldsymbol{W}\boldsymbol{A}$ fails to be an isomorphism of skew to itself.*

(4) Trace($\boldsymbol{A}$) *is an eigenvalue of $\boldsymbol{A}$.*

Proof

(1) $\Rightarrow$ (2) Differentiate $\exp(\theta\boldsymbol{W}_v)l$ in θ at $\theta = 0$.

(2) $\Rightarrow$ (1) Note that by (A2)

$$k(\exp(\theta W_v)l) = [I + W_{\theta v} + \tfrac{1}{2}(W_{\theta v})^2 + \cdots]\, k(l).$$

Since $k(W_v l) = W_v k(l)$ is symmetric, this is symmetric, term by term.

(2) $\Rightarrow$ (3) Since $k(W_v l) = W_v A$ is symmetric, $W_v A + A W_v = 0$, so $W \mapsto AW + WA$ is not an isomorphism.

(3) $\Rightarrow$ (2) There exists a $v \in \mathbb{R}^3$, $\|v\| = 1$ such that $W_v A + A W_v = \mathbf{0}$, so $k(W_v l) = W_v A$ is symmetric.

(3) $\Rightarrow$ (4) Define $L \in \mathfrak{M}_3$ by $L = (\text{trace } A)I - A$. Then one has the relationship

$$W_{Lv} = A W_v + W_v A,$$

as may be verified by considering a basis of eigenvectors for A. Therefore, $A W_v + W_v A = \mathbf{0}$ if and only if $Lv = \mathbf{0}$; that is, v is an eigenvector of A with eigenvalue trace(A). ∎

3.11 Corollary *Let $l \in \mathfrak{L}_e$ and $A = k(l) \in$ sym. Let the eigenvalues of A be denoted a, b, c. Then l has no axis of equilibrium if and only if*

$$(a + b)(a + c)(b + c) \neq 0.$$

Proof This condition is equivalent to saying that trace(A) is not an eigenvalue of A. ∎

3.12 Definition We shall say that $l \in \mathfrak{L}_e$ is a *type 0* load if l has no axis of equilibrium and if the eigenvalues of $A = k(l)$ are distinct.

The following shows how the orbits of type 0 loads meet $\mathfrak{L}_e$.

3.13 Proposition *Let $l \in \mathfrak{L}_e$ be a type 0 load. Then $\mathcal{O}_l \cap \mathfrak{L}_e$ consists of four type 0 loads.*

Proof We first prove that the orbit of A in $\mathfrak{M}_3$ under the action $(Q, A) \mapsto QA$ meets sym in four points. Relative to its basis of eigenvectors, we can write $A = \text{diag}(a, b, c)$. Then $\mathcal{O}_A \cap$ sym contains the four points

$$\begin{aligned}
&\text{diag}(a, b, c) && (Q = I),\\
&\text{diag}(-a, -b, c) && (Q = \text{diag}(-1, -1, 1)),\\
&\text{diag}(-a, b, -c) && (Q = \text{diag}(-1, 1, -1)),\\
&\text{diag}(a, -b, -c) && (Q = \text{diag}(1, -1, -1)).
\end{aligned}$$

These are distinct matrices since $(a + b)(a + c)(b + c) \neq 0$. Now suppose a, b, and c are distinct. Suppose $QA = S \in$ sym. Then $S^2 = A^2$. Let μ_i be an eigenvalue of S with eigenvector u_i. Then $S^2 u_i = \mu_i^2 u_i = A^2 u_i$, so μ_i^2 is an eigenvalue of A^2. Thus, as the eigenvectors of A^2 with a given eigenvalue are unique, u_i is an eigenvector of A and $\pm\mu_i$ is the corresponding eigenvalue. Since $\det Q = +1$, $\det S = \det A$, so we must have one of the four cases above.

By equivariance, $\boldsymbol{k}(\mathcal{O}_l) \cap \text{sym} = \mathcal{O}_{\boldsymbol{k}(l)} \cap \text{sym}$ consists of four points. Nov $\mathcal{O}_l \cap \mathcal{L}_e = \boldsymbol{k}^{-1}(\mathcal{O}_{\boldsymbol{k}(l)} \cap \text{sym})$, so it suffices to show that $\boldsymbol{k}$ is one-to-one on $\mathcal{O}_l$ This is a consequence of the following and Property (A2) of 3.7.

3.14 Lemma *Suppose* $\boldsymbol{A} \in \text{sym}$ *and* $\dim \operatorname{Ker} \boldsymbol{A} \leq 1$. *Then* $\boldsymbol{A}$ *has no iso tropy; that is,* $\boldsymbol{QA} = \boldsymbol{A}$ *implies* $\boldsymbol{Q} = \boldsymbol{I}$.

Proof Every $\boldsymbol{Q} \neq \boldsymbol{I}$ acts on $\mathbb{R}^3$ by rotation through an angle θ about a uniqu axis; say $l \subset \mathbb{R}^3$ (l is a line through the origin in $\mathbb{R}^3$). Now $\boldsymbol{QA} = \boldsymbol{A}$ means that $\boldsymbol{Q}$ is the identity on the range of $\boldsymbol{A}$. Therefore, if $\boldsymbol{Q} \neq \boldsymbol{I}$ and $\boldsymbol{QA} = \boldsymbol{A}$, the range o $\boldsymbol{A}$ must be zero or one dimensional; that is, $\dim \operatorname{Ker} \boldsymbol{A} > 2$. ∎

The next proposition considers the range and kernel of $\boldsymbol{k}: \mathcal{L} \longrightarrow \mathfrak{M}_3$.

3.15 Proposition

1. Ker $\boldsymbol{k}$ *consists of those loads in* $\mathcal{L}_e$ *for which every axis is an axis of equilibrium.*
2. $\boldsymbol{k}: \mathcal{L} \longrightarrow \mathfrak{M}_3$ *is surjective.*

Proof For 1, let $l \in \operatorname{Ker} \boldsymbol{k}$. For $\boldsymbol{W} \in \text{skew}$, $\boldsymbol{k}(\boldsymbol{W}l) = \boldsymbol{W}\boldsymbol{k}(l) = \boldsymbol{0}$, so $\boldsymbol{W}l \in \mathcal{L}_e$; by 3.10 every axis is an axis of equilibrium. Conversely, if $\boldsymbol{W}l \in \mathcal{L}_e$ for all $\boldsymbol{W} \in \text{skew}$, then $\boldsymbol{k}(\boldsymbol{W}l) = \boldsymbol{W}\boldsymbol{k}(l)$ is symmetric for all $\boldsymbol{W}$; that is, $\boldsymbol{k}(l)\boldsymbol{W} + \boldsymbol{W}\boldsymbol{k}(l) = \boldsymbol{0}$ for all $\boldsymbol{W}$. From $\boldsymbol{W}_{\boldsymbol{L}v} = \boldsymbol{A}\boldsymbol{W}_v + \boldsymbol{W}_v\boldsymbol{A}$, where $\boldsymbol{A} = \boldsymbol{k}(l)$ and $\boldsymbol{L} = (\text{trace } \boldsymbol{A})\, \boldsymbol{I} - \boldsymbol{A}$, we see that $\boldsymbol{L} = \boldsymbol{0}$. This implies trace $\boldsymbol{A} = \boldsymbol{0}$ and hence $\boldsymbol{A} = \boldsymbol{0}$.

To prove 2, introduce the following SO(3)-invariant inner product on $\mathcal{L}$:

$$\langle l, \bar{l} \rangle = \int_\Omega \langle \boldsymbol{B}(X), \bar{\boldsymbol{B}}(X) \rangle \, dV(X) + \int_{\partial\Omega} \langle \boldsymbol{\tau}(X), \bar{\boldsymbol{\tau}}(X) \rangle \, dA(X).$$

Relative to this and the inner product $\langle \boldsymbol{A}, \boldsymbol{B} \rangle = \text{trace}(\boldsymbol{A}^T\boldsymbol{B})$ on $\mathfrak{M}_3$, the adjoint $\boldsymbol{k}^T: \mathfrak{M}_3 \longrightarrow \mathcal{L}$ of $\boldsymbol{k}$ is given by

$$\boldsymbol{k}^T(\boldsymbol{A}) = (\boldsymbol{B}, \boldsymbol{\tau}), \quad \text{where} \quad \boldsymbol{B}(X) = \boldsymbol{A}X - \boldsymbol{G}, \boldsymbol{\tau}(X) = \boldsymbol{A}X,$$

and

$$\boldsymbol{G} = \int_\Omega \boldsymbol{A}X \, dV(X) + \int_{\partial\Omega} \boldsymbol{A}X \, dA(X).$$

If $\boldsymbol{k}^T(\boldsymbol{A}) = (\boldsymbol{0}, \boldsymbol{0})$, then it is clear that $\boldsymbol{A} = \boldsymbol{0}$. It follows that $\boldsymbol{k}$ is surjective. ∎

3.16 Corollary

1. Ker $\boldsymbol{k}$ *is the largest subspace of* $\mathcal{L}_e$ *that is* SO(3) *invariant.*
2. $\boldsymbol{k} \,|\, (\operatorname{Ker} \boldsymbol{k})^\perp : (\operatorname{Ker} \boldsymbol{k})^\perp \longrightarrow \mathfrak{M}_3$ *is an isomorphism.*

Let $\boldsymbol{j} = (\boldsymbol{k} \,|\, (\operatorname{Ker} \boldsymbol{k})^\perp)^{-1}$ and write

$$\text{Skew} = \boldsymbol{j}\,\text{skew}, \qquad \text{Sym} = \boldsymbol{j}\,\text{sym}.$$

These are linear subspaces of $\mathcal{L}$ of dimension three and six, respectively. Thus we have the decomposition:

$$\mathfrak{L} = \overbrace{\text{Skew}}^{\text{SO(3)-invariant pieces}} \oplus \underbrace{\text{Sym} \oplus \overbrace{\text{Ker}\, \boldsymbol{k}}}_{\mathfrak{L}_e}$$

of $\mathfrak{L}$, corresponding to the decomposition $\mathfrak{M}_3 = \text{skew} \oplus \text{sym}$:

$$\boldsymbol{U} = \tfrac{1}{2}(\boldsymbol{U} - \boldsymbol{U}^T) + \tfrac{1}{2}(\boldsymbol{U} + \boldsymbol{U}^T) \quad \text{of} \quad \mathfrak{M}_3.$$

Now we are ready to reformulate our problem in several ways that will be useful.

Define $\Phi\colon \mathfrak{C} \longrightarrow \mathfrak{L}$ by $\Phi(\phi) = (-\text{DIV}\, \boldsymbol{P}, \boldsymbol{P}\cdot\boldsymbol{N})$; that is,

$$\Phi(\phi)(X) = (-\text{DIV}\, \boldsymbol{P}(X, \boldsymbol{F}(X)), \boldsymbol{P}(X, \boldsymbol{F}(X))\cdot\boldsymbol{N}(X))$$

so the equilibrium equations (E) become $\Phi(\phi) = l$. From material frame indifference, we have equivariance of Φ: $\Phi(\boldsymbol{Q}\phi) = \boldsymbol{Q}\Phi(\phi)$. The results of Boxes 1.1, Chapter 3 and 1.1, Chapter 6, show that Φ is a smooth mapping. The derivative of Φ is given by

$$D\Phi(\phi)\cdot\boldsymbol{u} = (-\text{DIV}(\mathbf{A}\cdot\nabla\boldsymbol{u}), (\mathbf{A}\cdot\nabla\boldsymbol{u})\cdot\boldsymbol{N})$$

and at $\phi = I_\Omega$ this becomes

$$D\Phi(I_\Omega)\cdot\boldsymbol{u} = 2(-\text{DIV}(\mathbf{c}\cdot\boldsymbol{e}), (\mathbf{c}\cdot\boldsymbol{e})\cdot\boldsymbol{N}),$$

where $\boldsymbol{e} = \frac{1}{2}[\nabla\boldsymbol{u} + (\nabla\boldsymbol{u})^T]$.

If $D\Phi(I_\Omega)\colon T_{I_\Omega}\mathfrak{C} \longrightarrow \mathfrak{L}$ were an isomorphism, we could solve $\Phi(\phi) = l$ uniquely for ϕ near I_Ω and l small. The essence of our problem is that $D\Phi(I_\Omega)$ is *not* an isomorphism.

Define $\mathfrak{C}_{\text{sym}} = \{\boldsymbol{u} \in T_{I_\Omega}\mathfrak{C} \mid \boldsymbol{u}(0) = \mathbf{0} \text{ and } \nabla\boldsymbol{u}(0) \in \text{sym}\}$. From (H2) and Section 6.1, we have:

3.17 Lemma *$D\phi(I_\Omega)\,|\,\mathfrak{C}_{\text{sym}}\colon \mathfrak{C}_{\text{sym}} \longrightarrow \mathfrak{L}_e$ is an isomorphism.*

The connection between the astatic load map $\boldsymbol{k}\colon \mathfrak{L} \longrightarrow \mathfrak{M}_3$ and Φ is seen from the following computation of $\boldsymbol{k}\circ\Phi$.

3.18 Lemma *Let $\phi \in \mathfrak{C}$ and $\boldsymbol{P}$ be the first Piola–Kirchhoff stress tensor evaluated at ϕ. Then*

$$\boldsymbol{k}(\Phi(\phi)) = \int_\Omega \boldsymbol{P}\, dV.$$

This follows by an application of Gauss' theorem to

$$\boldsymbol{k}(\Phi(\phi)) = \int_\Omega (-\text{DIV}\, \boldsymbol{P}) \otimes \boldsymbol{X}\, dV(X) + \int_{\partial\Omega} (\boldsymbol{P}\cdot\boldsymbol{N}) \otimes \boldsymbol{X}\, dA(X).$$

This should be compared with the astatic load relative to the configuration ϕ rather than I_Ω; one gets

$$\boldsymbol{k}(\Phi(\phi), \phi) = \int_{\phi(\Omega)} \boldsymbol{\sigma}\, dv.$$

which is symmetric, while $\boldsymbol{k}(\Phi(\phi)) = \boldsymbol{k}(\Phi(\phi), I_\Omega)$ need not be.

To study solutions of $\Phi(\phi) = l$ for ϕ near the trivial solutions and l near a given load l_0, it suffices to take $l_0 \in \mathcal{L}_e$. This follows from DaSilva's theorem and equivariance of Φ.

Let $\mathcal{C}_{\text{sym}}$ be regarded as an affine subspace of $\mathcal{C}$ centered at I_Ω i.e. identify $\mathcal{C}_{\text{sym}}$ and $\mathcal{C}_{\text{sym}} + I_\Omega$. Let $\tilde{\Phi}$ be the restriction of Φ to $\mathcal{C}_{\text{sym}}$. From the implicit function theorem we get:

3.19 Lemma *There is a ball centered at I_Ω in $\mathcal{C}_{\text{sym}}$ whose image $\mathfrak{N}$ under $\tilde{\Phi}$ is a smooth submanifold of $\mathcal{L}$ tangent to $\mathcal{L}_e$ at 0 (see Figure 7.3.2). The manifold $\mathfrak{N}$ is the graph of a unique smooth mapping*

$$F\colon \mathcal{L}_e \longrightarrow \text{Skew}$$

such that $F(0) = 0$ and $DF(0) = 0$.

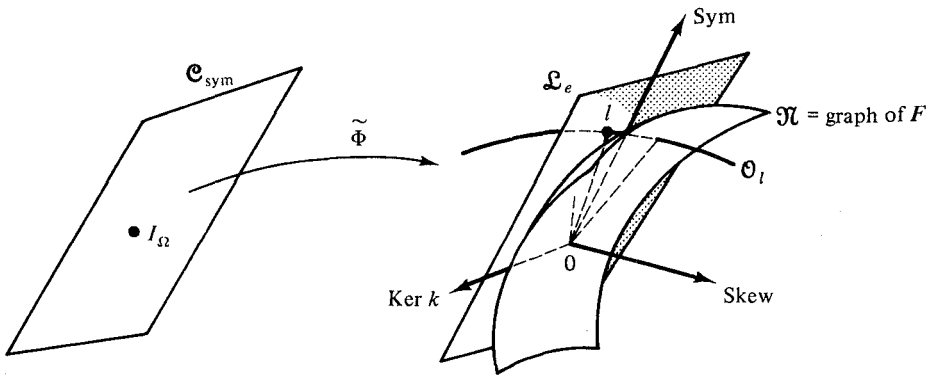

Figure 7.3.2

Later we shall show how to compute $D^2F(0)$ in terms of $D\Phi(I_\Omega)^{-1}$ and $\mathbf{c}$ (see Proposition 3.34).

Now we are ready to reformulate Problem (*P1*).

(*P2*) *For a given $l_0 \in \mathcal{L}_e$ near zero, study how $\mathcal{O}_l$ meets the graph of F for various l near l_0.*

Problems (P1) and (P2) are related as follows. Let ϕ solve (E) with $l \in \mathcal{L}$ and Q be such that $\bar{\phi} = Q\phi \in \mathcal{C}_{\text{sym}}$. Then $\Phi(\bar{\phi}) = Ql$, so the orbit of l meets the graph of F at $\Phi(\bar{\phi})$. Conversely, if the orbit of l meets $\mathfrak{N}$ at $\Phi(\bar{\phi})$, then $\phi = Q^{-1}\bar{\phi}$ solves (E).

We claim that near the trivial solutions, the numbers of solutions to each problem also correspond. This follows from the next lemma.

3.20 Lemma *There is a neighborhood $\mathfrak{U}$ of I_Ω in $\mathcal{C}_{\text{sym}}$ such that $\phi \in \mathfrak{U}$ and $Q\phi \in \mathfrak{U}$ implies $Q = I$.*

Proof Note that $\mathcal{C}_{\text{sym}}$ is transverse to $\mathcal{O}_{I_\Omega}$ at I_Ω and I_Ω has no isotropy. Thus, as SO(3) is compact, $\mathcal{O}_{I_\Omega}$ is closed, so there is a neighborhood $\mathcal{U}_0$ of I_Ω in $\mathcal{C}_{\text{sym}}$ such that $\boldsymbol{Q}|\Omega \in \mathcal{U}_0$ implies $\boldsymbol{Q} = \boldsymbol{I}$. The same thing is true of orbits passing through a small neighborhood of $\boldsymbol{I}$ by openness of transversality and compactness of SO(3). ∎

If $\mathcal{O}_l$ meets $\mathfrak{N}$ in k points $\boldsymbol{Q}_i l = \Phi(\bar{\phi}_i)$ $(i = 1, \ldots, k)$, then $\bar{\phi}_i$ are distinct as Φ is 1-1 on a neighborhood of I_Ω in $\mathcal{C}_{\text{sym}}$. If this neighborhood is also contained in $\mathcal{U}$ of 3.20, then the points $Q_i^{-1}\bar{\phi}_i = \phi_i$ are also distinct.

Hence problems (P1) and (P2) are equivalent.

In connection with the action $(\boldsymbol{Q}, \boldsymbol{A}) \mapsto \boldsymbol{QA}$ of SO(3) on $\mathfrak{M}_3$, we shall require some more notation. Let

$$\text{Skew}(\boldsymbol{QA}) = \tfrac{1}{2}(\boldsymbol{QA} - \boldsymbol{A}^T\boldsymbol{Q}^T) \in \text{skew}$$

and

$$\text{Sym}(\boldsymbol{QA}) = \tfrac{1}{2}(\boldsymbol{QA} + \boldsymbol{A}^T\boldsymbol{Q}^T) \in \text{sym}$$

be the skew-symmetric and symmetric parts of $\boldsymbol{QA}$, respectively.

We shall, by abuse of notation, suppress $\boldsymbol{j}$ and identify Sym with sym and Skew with skew. Thus we will write a load $l \in \mathcal{L}$ as $l = (\boldsymbol{A}, \boldsymbol{n})$, where $\boldsymbol{A} = \boldsymbol{k}(l) \in \mathfrak{M}_3$ and $\boldsymbol{n} \in \ker \boldsymbol{k}$; hence $l \in \mathcal{L}_e$ precisely when $\boldsymbol{A} \in$ sym. The action of SO(3) on $\mathcal{L}$ is given by $\boldsymbol{Q}l = (\boldsymbol{QA}, \boldsymbol{Qn})$.

Using this notation we can reformulate Problem (P2) as follows:

> ***(P3)*** *For a given $l_0 = (\boldsymbol{A}_0, \boldsymbol{n}_0) \in \mathcal{L}_e$ near zero, and $l = (\boldsymbol{A}, \boldsymbol{n})$ near l_0, find $\boldsymbol{Q} \in$ SO(3) such that*
>
> $$\text{Skew}(\boldsymbol{QA}) - \boldsymbol{F}(\text{Sym}(\boldsymbol{A}, \boldsymbol{Q}), \boldsymbol{Qn}) = \boldsymbol{0}.$$

Next define a rescaled map $\bar{\boldsymbol{F}}: \mathbb{R} \times \mathcal{L}_e \longrightarrow$ Skew by

$$\bar{\boldsymbol{F}}(\lambda, l) = \frac{1}{\lambda^2}\boldsymbol{F}(\lambda l).$$

Since $\boldsymbol{F}(0) = \boldsymbol{0}$ and $D\boldsymbol{F}(0) = \boldsymbol{0}$, $\boldsymbol{F}$ is smooth. Moreover, if $\boldsymbol{F}(l) = \frac{1}{2}\boldsymbol{G}(l) + \frac{1}{6}\boldsymbol{C}(l) + \cdots$ is the Taylor expansion of $\boldsymbol{F}$ about zero, then $\bar{\boldsymbol{F}}(\lambda, l) = \frac{1}{2}\boldsymbol{G}(l) + (\lambda/6)\boldsymbol{C}(l) + \cdots$.

In problem (E) let us measure the size of l by the parameter λ. Thus, replace $\Phi(\phi) = l$ for l near zero by $\Phi(\phi) = \lambda l$ for λ near zero. This scaling enables us to conveniently distinguish the size of l from its "orientation." In the literature l has always been fixed and λ taken small. Here we allow l to vary as well. These extra parameters are crucial for the complete bifurcation picture. Thus we arrive at the final formulation of the problem.

> ***(P4)*** *For a given $l_0 = (\boldsymbol{A}_0, \boldsymbol{n}_0) \in \mathcal{L}_e$, for l near l_0 and λ small, find $\boldsymbol{Q} \in$ SO(3) such that*
>
> $$\text{Skew}(\boldsymbol{QA}) - \lambda\bar{\boldsymbol{F}}(\lambda, \text{Sym}(\boldsymbol{QA}), \boldsymbol{Qn}) = \boldsymbol{0}.$$

The left-hand side of this equation will be denoted $H(\lambda, A, n, Q)$ or $H(\lambda, Q)$ if A, n are fixed.

With all these preliminaries at hand, we are ready to give a simple proof of one of the first of Stoppelli's basic theorems.[9]

3.21 Theorem *Suppose $l \in \mathcal{L}_e$ has no axis of equilibrium. Then for λ sufficiently small, there is a unique $\bar{\phi} \in \mathcal{C}_{\text{sym}}$ and a unique Q in a neighborhood of the identity in* SO(3) *such that $\phi = Q^{-1}\bar{\phi}$ solves the traction problem*

$$\Phi(\phi) = \lambda l.$$

Proof Define $H: \mathbb{R} \times \mathrm{SO}(3) \longrightarrow \mathrm{Skew}$ by

$$H(\lambda, Q) = \mathrm{Skew}(QA) - \lambda \bar{F}(\lambda, \mathrm{Sym}(QA), n),$$

where $l = (A, n) \in \mathcal{L}_e = \mathrm{Sym} \oplus \mathrm{Ker}\, k$ is fixed. Note that $D_2H(0, I) \cdot W = \mathrm{Skew}(WA) = \frac{1}{2}(AW + WA)$. By Proposition 3.10, this is an isomorphism. Hence, by the implicit function theorem, $H(\lambda, Q) = 0$ can be uniquely solved for Q near $I \in \mathrm{SO}(3)$ as a function of λ near $0 \in \mathbb{R}$. ∎

The geometric reason "why" this proof works and the clue to treating other cases is the following:

3.22 Lemma *If $l \in \mathcal{L}_e$ has no axis of equilibrium, then $\mathcal{O}_l$ intersects $\mathcal{L}_e$ transversely at l* (i.e., $\mathcal{L} = \mathcal{L}_e \oplus T_l\mathcal{O}_l$), *and conversely.*

Proof The tangent space of $\mathcal{O}_l$ at $l \in \mathcal{L}_e$ is $T_l\mathcal{O}_l = \{Wl \mid W \in \mathrm{Skew}\}$. Transversality means that the projection of $T_l\mathcal{O}_l$ to the complement Skew of $\mathcal{L}_e$ is surjective. The projection is $Wl \mapsto \frac{1}{2}(WA + AW)$ where $A = k(l)$, so the result follows from 3.10, part 3. ∎

We have shown that there is only one solution to $\Phi(\phi) = \lambda l$ near the identity if λ is small and l has no axis of equilibrium. How many solutions are there near the set of all trivial solutions SO(3)? This problem has a complex answer that depends on the *type* of l. We analyze the simplest case now. Recall (see Definition 3.12) that a load $l \in \mathcal{L}_e$ is said to be of type 0 if l has no axis of equilibrium and if $A = k(l)$ has distinct eigenvalues.

Loads with no axis of equilibrium occur for loads other than type 0 (see Box 3.1), and Stoppelli's theorem applies to them. However, the global structure of the corresponding set of solutions is quite different ("global" being relative to SO(3)).

3.23 Theorem *Let $l_0 \in \mathcal{L}_e$ be of type* 0. *Then for λ sufficiently small the equation $\Phi(\phi) = \lambda l_0$ has exactly four solutions in a neighborhood of the trivial solutions* $\mathrm{SO}(3) \subset \mathcal{C}$ (*see Figure 7.3.3*).

---

[9]The only other *complete* proof in English we know of is given in Van Buren [1968], although sketches are available in Grioli [1962], Truesdell and Noll [1965], and Wang and Truesdell [1973]. Our proof is rather different; the use of the rescaled map $\bar{F}$ avoids a series of complicated estimates used by Stoppelli and Van Buren.

Proof By 3.13, $\mathcal{O}_{\lambda l_0}$ meets $\mathcal{L}_e$ in four points. By 3.21, in a neighborhood of 0 in $\mathcal{L}$, $\mathcal{O}_{\lambda l_0}$ meets $\mathfrak{N}$ in exactly four points, the images of $\bar{\phi}_1$, $\bar{\phi}_2$, $\bar{\phi}_3$, and $\bar{\phi}_4$, say. Thus Problem (P2) has four solutions. By the equivalence of (P1) and (P2), so does (P1). ∎

Let $A = k(l_0)$ and $\mathcal{S}_A = \{Q \mid QA \in \text{sym}\}$. From the proof of 3.13 we see that $\mathcal{S}_A$ is a four-element subgroup of SO(3), isomorphic to $\mathbb{Z}_2 \oplus \mathbb{Z}_2$. By our earlier discussions, ϕ_i are obtained from $\bar{\phi}_i$ by applying rotations close to elements of $\mathcal{S}_A$. In particular, as $\lambda \longrightarrow 0$, the solutions $\{\phi_i\}$ converge to the four element set $\mathcal{S}_A$ (regarded as a subset of $\mathcal{C}$).

For l sufficiently close to l_0 in 3.23, the problem $\Phi(\phi) = \lambda l$ will also have four solutions. Indeed by openness of transversality, $\mathcal{O}_{\lambda l}$ will also meet $\mathfrak{N}$ in four points. In other words, the picture for type 0 loads in Figure 7.3.3 is structurally stable under small perturbations of l_0.

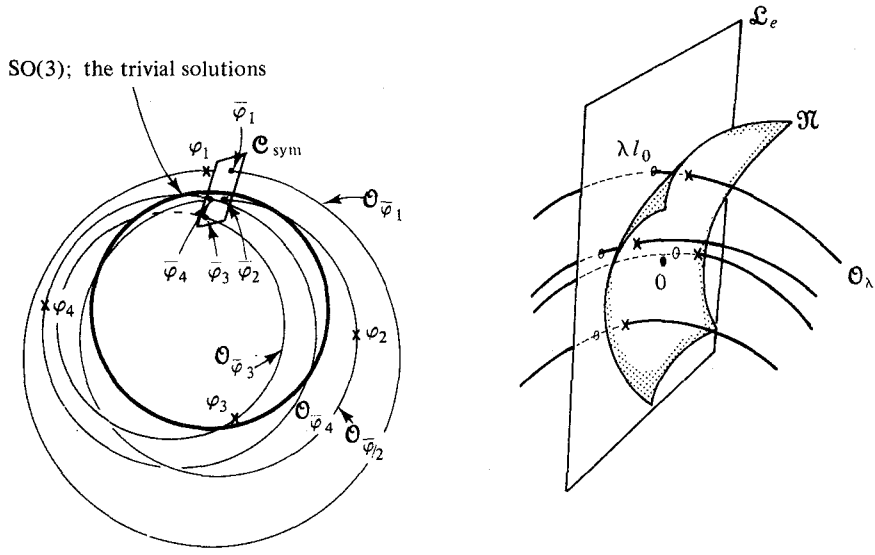

Figure 7.3.3

Next we study the dynamical stability of the four solutions found by Theorem 3.23. This is done under the hypothesis that the classical elasticity tensor is stable: we introduce the following condition.

(H3) *Assume there is an* $\eta > 0$ *such that for all* $e \in \text{Sym}(T_X\Omega, T_X\Omega)$,

$$\epsilon(e) = \tfrac{1}{2}\mathbf{c}(X)(e, e) \geq \eta \| e \|^2, \qquad \| \cdot \| = \text{pointwise norm.}$$

[$\epsilon(e)$ is the stored energy function for linearized elasticity; see Section 4.3.]

Because of the difficulties with potential wells and dynamical stability discussed in Section 6.6, we shall adopt the following "energy criteria" definition of stability.

3.24 Definition A solution ϕ of $\Phi(\phi) = l$ will be called *stable* if ϕ is a loca minimum in $\mathcal{C}$ of the potential function

$$V_l(\phi) = \int_\Omega W(D\phi)\, dV - \langle l, \phi \rangle,$$

where $$\langle l, \phi \rangle = \int_\Omega \boldsymbol{B}(X)\cdot\boldsymbol{\phi}(X)\, dV(X) + \int_{\partial\Omega} \boldsymbol{\tau}(X)\cdot\boldsymbol{\phi}(X)\, dA(X).$$

If ϕ is not stable, its *index* is the dimension of the largest subspace of vectors $\boldsymbol{\iota}$ tangent to $\mathcal{C}$ at ϕ with the property that V_l decreases along some curve tangen to $\boldsymbol{u}$ at ϕ. (Thus, index 0 corresponds to stability.)

3.25 Theorem *Assume (H1)–(H3) and let l_0 be as in 3.23. For λ sufficientl small, exactly one of the four solutions $\phi_1, \phi_2, \phi_3, \phi_4$ is stable; the others have indices 1, 2, and 3. More precisely, suppose ϕ_λ is a solution approaching $\boldsymbol{Q} \in \mathcal{S}_A$ as $\lambda \longrightarrow 0$. Then for λ small, ϕ_l is stable if and only if $\boldsymbol{QA} - \operatorname{tr}(\boldsymbol{QA})\boldsymbol{I} \in \operatorname{sym}$ is positive-definite. In general, the index of ϕ_λ is the number of negative eigenvalues of $\boldsymbol{QA} - \operatorname{tr}(\boldsymbol{QA})\boldsymbol{I}$.*

Proof Let $\phi_0 \in \mathcal{C}$ solve $\Phi(\phi) = \lambda l_0 = l$. Then ϕ_0 is a critical point of $V_{\lambda l_0}$. Consider the orbit $\mathcal{O}_{\phi_0} = \{\boldsymbol{Q}\phi_0 \mid \boldsymbol{Q} \in \mathrm{SO}(3)\}$ of ϕ_0. The tangent space to $\mathcal{C}$ at ϕ_0 decomposes as follows:

$$T_{\phi_0}\mathcal{C} = T_{\phi_0}\mathcal{O}_{\phi_0} \oplus (T_{\phi_0}\mathcal{O}_{\phi_0})^\perp.$$

First consider V_l restricted to $(T_{\phi_0}\mathcal{O}_{\phi_0})^\perp$. Its second derivative at ϕ in the direction of $\boldsymbol{u} \in (T_\phi\mathcal{O}_\phi)^\perp$ is $\int_\Omega (\partial^2 W/\partial \boldsymbol{F}\, \partial \boldsymbol{F})(\phi)\cdot(\nabla \boldsymbol{u}, \nabla \boldsymbol{u})\, dV$. At $\phi_0 = \boldsymbol{Q}\,|\,\Omega$, this becomes

$$\int_\Omega \mathbf{c}(X)\cdot(\boldsymbol{e}(X), \boldsymbol{e}(X))\, dV(X), \quad \text{where} \quad \boldsymbol{e} = \tfrac{1}{2}(\nabla \boldsymbol{u} + (\nabla \boldsymbol{u})^T).$$

This is larger than a positive constant times the L^2-norm of $\boldsymbol{e}$, by (H3). However, since $\boldsymbol{u}$ is in $(T_\phi\mathcal{O}_\phi)^\perp$, $\|\boldsymbol{e}\|_{L^2}^2 \geq$ (const.) $\|\boldsymbol{u}\|_{H^1}^2$ by Korn's inequality (see Box 1.1, Chapter 6). By continuity, if λ is small,

$$D^2 V_{\lambda l_0}(\phi_0)\cdot(\boldsymbol{u}, \boldsymbol{u}) \geq \delta \|\boldsymbol{u}\|_{H^1}^2$$

for all $\boldsymbol{u}$ orthogonal to $\mathcal{O}_{\phi_0}$ at ϕ_0. This implies ϕ_0 is a minimum for $V_{\lambda l_0}$ in directions transverse to $\mathcal{O}_{\phi_0}$ (cf. Section 6.6).

Next, consider $V_{\lambda l_0}$ restricted to $\mathcal{O}_{\phi_0}$. By material frame indifference, W is constant on $\mathcal{O}_{\phi_0}$ and as ϕ_0 must be a critical point for $V_{\lambda l_0}$ restricted to $\mathcal{O}_{\phi_0}$, it is also a critical point for $\lambda l_0 = l$ restricted to $\mathcal{O}_{\phi_0}$ (where l: $\mathcal{C} \longrightarrow \mathbb{R}$ is defined by $l(\phi) = \langle l, \phi \rangle$). It suffices therefore to determine the index of $l\,|\,\mathcal{O}_{\phi_0}$ at ϕ_0. The result is a consequence of continuity and the limiting case $\lambda \longrightarrow 0$ given in the following lemma about type 0 loads.

3.26 Lemma *Let l be type 0 and let $\boldsymbol{A} = \boldsymbol{k}(l)$. Then $\mathcal{S}_A$, regarded as a subset of $\mathcal{C}$ equals the set of critical points of $l\,|\,\mathcal{O}_{I_\Omega}$. These four critical points are nondegenerate with indices 0, 1, 2, and 3; the index of $\boldsymbol{Q}$ is the number of negative eigenvalues of $\boldsymbol{QA} - \operatorname{tr}(\boldsymbol{QA})\boldsymbol{I}$.*

Proof First note that $\mathcal{L}_e = (T_{I_\Omega}\,\mathrm{SO}(3))^\perp$ since $D\Phi(I_\Omega)$ has kernel $T_{I_\Omega}\,\mathrm{SO}(3)$ = skew, has range $\mathcal{L}_e$, and is self-adjoint. Thus $Ql \in \mathcal{L}_e$ if and only if $l \perp T_{Q^T}\,\mathrm{SO}(3)$. It follows that $Ql \in \mathcal{L}_e$ if and only if Q^T is a critical point of $l|\mathcal{O}_{I_\Omega}$. Recall that elements of $\mathcal{S}_A = \{Q \in \mathrm{SO}(3) \mid Ql \in \mathcal{L}_e\}$ are symmetric (see 3.13).

To compute the index of $l|\mathcal{O}_{I_\Omega}$ at $Q \in \mathcal{S}_A$, we compute the second derivative

$$\frac{d^2}{dt^2} l(\exp(tW)Q)\,|_{t=0} = l(W^2Q).$$

Now
$$\begin{aligned} l(W^2Q) &= \operatorname{trace} k(l, W^2Q) = \operatorname{trace} W^2k(l, Q) \\ &= \operatorname{trace} W^2k(Q^Tl) = \operatorname{trace}[W^2QA]. \end{aligned}$$

This quadratic form on skew is represented by the element $QA - \operatorname{tr}(QA)I$ of Sym as is seen by a simple computation. Using the representations for $\{QA\}$ given by Proposition 3.13, namely,

$$\operatorname{diag}(a, b, c), \quad \operatorname{diag}(-a, -b, c), \quad \operatorname{diag}(-a, b, -c), \text{ and } \operatorname{diag}(a, -b, -c)$$

one checks that all four indices occur. ∎

In the following boxes we shall outline, omitting a number of proofs, the methods by which the analysis of the other types proceeds. Again, Chillingworth, Marsden, and Wan [1982a] should be consulted for details and the full results.

Box 3.1 ***Classification of Orbits in $\mathfrak{M}_3$***

The classification of loads depends on a classification of the corresponding astatic loads. This will be done by classifying orbits in $\mathfrak{M}_3$ under the action $(Q, A) \mapsto QA$ of SO(3) on $\mathfrak{M}_3$ by the way the orbits meet sym. By the polar decomposition, we can assume $A \in$ sym. In 3.13 we proved:

3.27 Proposition (*Type 0*) *Suppose $A \in$ sym has no axis of equilibrium and has distinct eigenvalues. Then $\mathcal{O}_A \cap$ sym consists of four points at each of which the intersection is transversal.*

We shall let the eigenvalues of $A \in$ sym be denoted a, b, c; following 3.11 we shall say that A has no axis of equilibrium when $(a+b)(b+c)(a+c) \neq 0$; that is, $a+b+c \neq a, b,$ or c, and in this case $\mathcal{O}_A$ intersects sym transversly at A.

3.28 Definition We shall say A is of *type 1* if A has no axis of equilibrium and if exactly two of a, b, c are equal (say $a = b \neq c$).

3.29 Proposition *If A is type 1, then $\mathcal{O}_A \cap$ sym consists of two points (each with no axis of equilibrium) and an $\mathbb{RP}^1$ . . . or equivalently a circle (each point of which has one axis of equilibrium).*

$\mathbb{RP}^n$ denotes the set of lines through the origin in $\mathbb{R}^{n+1}$. The proof of 3.29 is essentially a straightforward exercise in linear algebra. Likewise, for type 2 we proceed as follows.

3.30 Definition We shall say A is of *type 2* if A has no axis of equilibrium and all three of a, b, c are equal (and so $\neq 0$).

3.31 Proposition *If A is type 2, then $\mathcal{O}_A \cap$ sym consists of one point (A itself) and an $\mathbb{RP}^2$ (each point of which has a whole circle of axes of equilibrium).*

Types 3 and 4 are treated next.

3.32 Definition We say A is *type 3* if dim Ker $A = 2$ and say A is *type* 4 if $A = \mathbf{0}$.

3.33 Proposition *If A is type 3, then $\mathcal{O}_A \cap$ sym consists of two points, A and $-A$. If A is type 4, $\mathcal{O}_A \cap$ sym $= \{\mathbf{0}\}$.*

Thus, orbits in $\mathfrak{M}_3$ fall into exactly five different types; 0, 1, 2, 3, and 4 with the properties above.

Stoppelli partially analyzed only types 0 and 1. We discussed type 0 in the text and shall briefly comment on type 1 in the next box. Types 2, 3, and 4 are also interesting; see Chillingworth, Marsden, and Wan [1982b] for details.

Problem 3.3 Use the results above and 3.21 to prove the existence of at least one solution of the traction problem for a load of types 1 or 2.

Problem 3.4 A load l is called *parallel* if there is a vector $\boldsymbol{a} \in \mathbb{R}^3$ and scalar functions $f\colon \Omega \to \mathbb{R}$, $g\colon \partial\Omega \to \mathbb{R}$ such that $l = (f\boldsymbol{a}, g\boldsymbol{a})$. Show that parallel loads are of type 3.

Problem 3.5 Suppose $\boldsymbol{B} = \mathbf{0}$ and $\boldsymbol{\tau} = \tau \boldsymbol{N}$ for a constant τ. Show that this load is of type 2.

Figure 7.3.4 shows some examples of loads l where $\boldsymbol{k}(l)$ has types 1, 2, 3, and 4.

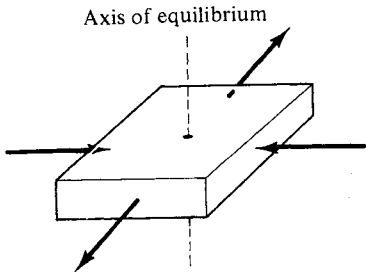

Type 1. Rotation by 180° about one of the horizontal axes produces an equilibrated load with no axis of equilibrium.

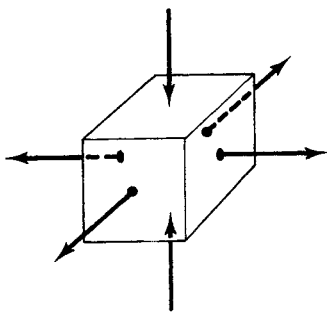

Type 2. Any horizontal axis is an axis of equilibrium; vertical axis is not an axis of equilibrium. Rotation by 180° about the vertical axis gives an equilibrated load with no axis of equilibrium.

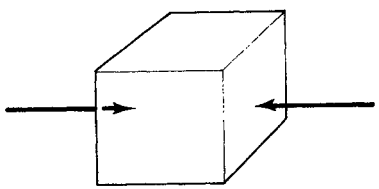

Type 3

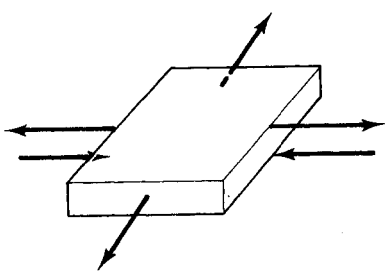

Type 3

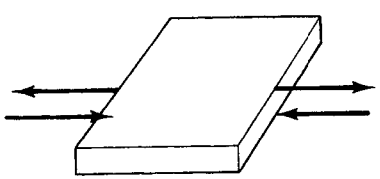

Type 4

Figure 7.3.4

Box 3.2 ***The Bifurcation Equation for Type 1***

We shall now indicate briefly how the bifurcation analysis proceeds. According to the formulation (P4) of our problem, given $(A_0, n_0) \in \mathcal{L}_e$, we wish to solve

$$H(\lambda, A, n, Q) = \mathrm{Skew}(QA) - \lambda \bar{F}(\lambda, \mathrm{Sym}(QA), n) = 0$$

for Q for various (A, n) near (A_0, n_0), and small λ.

Define the vector field X_{A_0} on SO(3) by

$$X_{A_0}(Q) = \mathrm{skew}(QA) \cdot Q$$

(right translation of $\mathrm{Skew}(QA)$ from SO(3) to T_Q SO(3)). Likewise we regard H as a vector field $X(\lambda, A, n, Q)$ on SO(3) depending on the parameters λ, A, n by setting

$$X(\lambda, A, n, Q) = H(\lambda, A, n, Q) \cdot Q.$$

Let $\mathcal{S}_{A_0}$ be the zero set for X_{A_0}. For A_0 of type 1, $\mathcal{S}_{A_0}$ consists of two points and a circle $\mathcal{C}_{A_0}$. One computes that for $Q \in \mathcal{S}_{A_0}$,

$$T_Q\mathcal{S}_{A_0} = \{W_0 Q \mid W_0 \in \text{skew} \quad \text{and} \quad W_0(QA_0) + (QA_0)W_0 = 0\}.$$

From 3.10, $W_0 \mapsto W_0(QA_0)W_0$ corresponds to the linear transformation $QA_0 - \mathrm{tr}(QA_0)I$ under the isomorphism of skew with $\mathbb{R}^3$. Symmetry of this linear transformation when QA_0 is symmetric is a reflection of the fact that X_{A_0} is a gradient field. In fact, X_{A_0} is the gradient of $l_0 \mid \mathcal{O}_{I_\Omega}$—that is, of

$$l_0(Q) = \int_\Omega B_0(X) \cdot Q(X)\, dV(X) + \int_{\partial\Omega} \tau_0(X) \cdot Q(X)\, dA(X)$$

as one sees by a calculation. Thus, by the Fredholm alternative, at each point Q of $\mathcal{S}_{A_0}$, $DX_{A_0}(Q)$: T_Q SO(3) $\longrightarrow T_Q$ SO(3) has range the orthogonal complement of $T_Q\mathcal{S}_{A_0}$. Thus, the range of DX_{A_0} over its zero set $\mathcal{S}_{A_0}$ is the normal bundle of $\mathcal{S}_{A_0}$. The Liapunov–Schmidt procedure now produces a unique section $\phi_{\lambda, A, n}$ of the normal bundle to $\mathcal{S}_{A_0}$ such that the orthogonal projection of $X(\lambda, A, n, Q)$ to the fiber of the normal bundle is zero. Let $\Gamma(\lambda, A, n)$ be the graph of $S_{\lambda, A, n}$ and let $\tilde{X}(\lambda, A, n, Q)$ be the projection of X to $T_Q\Gamma$. Thus, $\tilde{X}$ is a vector field on Γ. The equation $\tilde{X} = 0$ is our bifurcation equation. One can show that, essentially, $\tilde{X}$ is a gradient, so one is looking for critical points of a function on a circle. These can then be described using singularity theory. Cusp bifurcations (see Section 7.1) are, not surprisingly, present, so an isolated solution near the circle can bifurcate into three. Stoppelli [1958] found some of these extra solutions by analyzing a slice of the bifurcation diagram. For type 2 a double cusp occurs and a single solution can bifurcate into 9. These are also new solutions.

Box 3.3 ***Miscellany: Curvature and Linearization Stability***

The manifold $\mathfrak{N}$ was shown to be the graph of a map $\boldsymbol{F}$; see 3.19. Essentially, $\boldsymbol{F}$ is the skew-component of Φ. Now we will demonstrate an almost paradoxical fact: the *second* derivative of this map at I_Ω can be computed knowing only the classical elasticity tensor $\mathbf{c}$. Intuitively one would expect this second derivative to depend on higher nonlinearities. This second derivative tells us, essentially, the curvature of $\mathfrak{N}$.

3.34 Proposition *Let* $\mathfrak{F}\colon \mathcal{C} \to \mathrm{skew}$ *be defined by* $\mathfrak{F}(\phi) = \mathrm{Skew}[\boldsymbol{k}(\Phi(\phi))]$. *Then* $\mathfrak{F}(I_\Omega) = 0$, $D\mathfrak{F}(I_\Omega) = 0$, *and*

$$D^2\mathfrak{F}(I_\Omega)(\boldsymbol{u}, \boldsymbol{u}) = 2\,\mathrm{Skew}\Big(\int_\Omega \nabla\boldsymbol{u}\,\mathbf{c}\cdot\nabla\boldsymbol{u}\,dV\Big) = -2\,\mathrm{Skew}\,\boldsymbol{k}(l_u, \boldsymbol{u}),$$

where $l_u = (\boldsymbol{b}_u, \boldsymbol{\tau}_u)$, $\boldsymbol{b}_u = -\mathrm{DIV}(\mathbf{c}\cdot\boldsymbol{e})$, *and* $\boldsymbol{\tau}_u = (\mathbf{c}\cdot\boldsymbol{e})\cdot\boldsymbol{N}$. *Identifying skew with* $\mathbb{R}^3$, *this reads*

$$-D^2\mathfrak{F}(I_\Omega)(\boldsymbol{u}, \boldsymbol{u}) = \Big(\int_\Omega \boldsymbol{b}_u \times \boldsymbol{u}\,dV + \int_{\partial\Omega} \boldsymbol{\tau}_u \times \boldsymbol{u}\,dA\Big).$$

Proof By 3.17,

$$\mathfrak{F}(\phi) = \mathrm{Skew}\Big(\int_\Omega \boldsymbol{P}\,dV\Big),$$

where $\boldsymbol{P}$ is the first Piola-Kirchhoff stress. We have $\boldsymbol{P}(I_\Omega) = \mathbf{0}$, so $\mathfrak{F}(I_\Omega) = 0$. Also,

$$D\mathfrak{F}(I_\Omega)\cdot\boldsymbol{u} = \mathrm{Skew}\int_\Omega \frac{\partial\boldsymbol{P}}{\partial\boldsymbol{F}}\cdot\nabla\boldsymbol{u}\,dV = \mathrm{Skew}\int_\Omega \mathbf{c}\cdot\nabla\boldsymbol{u}\,dV = 0,$$

as $\mathbf{c}\cdot\nabla\boldsymbol{u}$ is symmetric and $(\partial\boldsymbol{P}/\partial\boldsymbol{F})(I_\Omega) = \mathbf{c}$. Next, to compute $D^2\mathfrak{F}$, we need to use the fact that $\boldsymbol{S}$ is symmetric, so write $\boldsymbol{P} = \boldsymbol{F}\boldsymbol{S}$ and obtain $D_{\boldsymbol{F}}\boldsymbol{P}(\boldsymbol{F})\cdot\nabla\boldsymbol{u} = \nabla\boldsymbol{u}\boldsymbol{S}(\boldsymbol{F}) + \boldsymbol{F}D_{\boldsymbol{F}}\boldsymbol{S}(\boldsymbol{F})\cdot\nabla\boldsymbol{u}$. Thus,

$$\begin{aligned} D^2\boldsymbol{P}(I_\Omega)\cdot(\nabla\boldsymbol{u}, \nabla\boldsymbol{v}) = {} & \nabla\boldsymbol{u}\,D_{\boldsymbol{F}}\boldsymbol{S}(I_\Omega)\cdot\nabla\boldsymbol{v} + \nabla\boldsymbol{v}D_{\boldsymbol{F}}\boldsymbol{S}(I_\Omega)\cdot\nabla\boldsymbol{u} \\ & + D^2_{\boldsymbol{F}}\boldsymbol{S}(I_\Omega)(\nabla\boldsymbol{u}, \nabla\boldsymbol{v}) \end{aligned}$$

Now $D_{\boldsymbol{F}}\boldsymbol{S}(I_\Omega)\cdot\nabla\boldsymbol{u} = D_{\boldsymbol{C}}\boldsymbol{S}(I_\Omega)\cdot(\nabla\boldsymbol{u} + \nabla\boldsymbol{u}^T) = \mathbf{c}\cdot\nabla\boldsymbol{u}$ and $D^2_{\boldsymbol{F}}\boldsymbol{S}(I_\Omega)$ is symmetric, so

$$\begin{aligned} D^2\mathfrak{F}(I_\Omega)\cdot(\boldsymbol{u}, \boldsymbol{v}) &= \mathrm{skew}\int_\Omega D^2_{\boldsymbol{F}}\boldsymbol{P}(I_\Omega)(\nabla\boldsymbol{u}, \nabla\boldsymbol{v})\,dV) \\ &= \mathrm{skew}\Big(2\int_\Omega (\nabla\boldsymbol{u}\,\mathbf{c}\cdot\nabla\boldsymbol{v} + \nabla\boldsymbol{v}\,\mathbf{c}\cdot\nabla\boldsymbol{u})\,dV\Big). \end{aligned}$$

Thus
$$\begin{aligned} D^2\mathfrak{F}(I_\Omega)(\boldsymbol{u}, \boldsymbol{u}) &= 2\,\mathrm{skew}\Big(\int_\Omega \nabla\boldsymbol{u}\,\mathbf{c}\cdot\nabla\boldsymbol{u}\,dV\Big) \\ &= \mathrm{skew}\int_\Omega \boldsymbol{b}\otimes\boldsymbol{u}\,dV + \int_{\partial\Omega} \boldsymbol{\tau}\otimes\boldsymbol{u}\,dA \end{aligned}$$

by the divergence theorem. ∎

3.35 Example For a homogeneous isotropic material, $\mathbf{c}\cdot\boldsymbol{e} = \lambda(\text{trace } \boldsymbol{e})\boldsymbol{I} + 2\mu\boldsymbol{e}$ for constants λ and μ (the Lamé moduli). Thus

$$D^2\mathfrak{F}(I_\Omega)(\boldsymbol{u}, \boldsymbol{u}) = 2 \text{ skew}\left(\int_\Omega [2\mu\nabla\boldsymbol{u}\,\boldsymbol{e} + \lambda \text{ trace}(\boldsymbol{e})\,\nabla\boldsymbol{u}]\,dV\right)$$

$$= 2 \text{ skew} \int_\Omega \{\mu\,\nabla\boldsymbol{u}\,\nabla\boldsymbol{u} + \lambda \text{ trace}(\boldsymbol{e})\,\nabla\boldsymbol{u}\}\,dV$$

Finally we make a few remarks about linearization stability; see Section 4.4.

3.36 Definition Suppose a pair $(\boldsymbol{u}_1, l_1)$ satisfies the equations linearized about our stress free reference state I_Ω; that is,

$$D\Phi(I_\Omega)\cdot\boldsymbol{u}_1 = l_1.$$

Let us call the pair $(\boldsymbol{u}_1, l_1)$ *linearization stable* (*or integrable*) if there exists a curve $(\phi(\lambda), l(\lambda)) \in \mathfrak{C} \times \mathfrak{L}_e$ such that:

(i) $\phi(0) = I_\Omega$, $l(0) = 0$;
(ii) $\phi'(0) - \boldsymbol{u}_1 \in \text{Ker } D\phi(I_\Omega)$, $l'(0) = l_1$; and
(iii) $\Phi(\phi(\lambda)) = l(\lambda)$.

Here $(\phi(\lambda), l(\lambda))$ should be defined in some interval; say $[0, \epsilon)$, $\epsilon > 0$. (We can, of course, do the same about any state, not just I_Ω.)

3.37 Proposition *Suppose $l_1 \in \mathfrak{L}_e$ has no axis of equilibrium and $D\Phi(I_\Phi)\boldsymbol{u}_1 = l_1$. Then $(\boldsymbol{u}_1, l_1)$ is linearization stable.*

Proof Let $l(\lambda) = \lambda l_1$. Then there is a unique smooth curve $\phi(\lambda)$ through I_Ω such that $\Phi(\phi(\lambda)) = l(\lambda)$ by Theorem 3.21. Differentiating at $\lambda = 0$ gives $D\Phi(I_\Omega)\cdot\phi'(0) = l_1$, so $\phi'(0) - \boldsymbol{u}_1 \in \text{Ker } D\Phi(I_\Omega)$. ∎

The following produces a potential obstruction to linearization stability. It is called the "Signorini compatability conditions." Let us use the notation

$$\int_\Omega \boldsymbol{u} \times l \quad \text{for} \quad \int_\Omega \boldsymbol{u}(X) \times \boldsymbol{B}(X)\,dV(X) + \int_{\partial\Omega} \boldsymbol{u}(X) \times \boldsymbol{\tau}(X)\,dA(X).$$

Let us note that linearization stability really just involves l_1; let us say l_1 is *integrable* when there is a curve $(\phi(\lambda), l(\lambda)) \in \mathfrak{C} \times \mathfrak{L}_e$ satisfying (i) and (iii) above with $l'(0) = l_1$. Then $D\Phi(I_\Omega)\cdot\phi'(0) = l_1$ is automatic.

3.38 Proposition *Suppose l_1 is integrable. Then there exists a $\boldsymbol{u}_1$ such that*

$$D\Phi(I_\Omega)\boldsymbol{u}_1 = l_1 \tag{L}$$

and

$$\int_\Omega \boldsymbol{u}_1 \times l_1 = \mathbf{0}. \tag{C}$$

Proof Take $\boldsymbol{u}_1 = \phi'(0)$ and differentiate the identity $\int_\Omega \phi(\lambda) \times l(\lambda) = 0$ twice and set $\lambda = 0$; all that survives is $\int_\Omega \boldsymbol{u}_1 \times l_1 = \mathbf{0}$ since $l''(0) = l_2 \in \mathcal{L}_e \left(\text{so} \int_\Omega I_\Omega \times l_2 = 0\right)$ and $l(0) = 0$. ∎

Remarks

1. Note that $l_1 \in \mathcal{L}_e$ is a necessary condition for integrability.

2. A basic question to be asked is when the compatability conditions (C) are sufficient for integrability and how much freedom there is in our choice of $l(\lambda)$. This is the spirit of the classical work, where $\phi(\lambda)$ and $l(\lambda)$ are expanded in power series. See Truesdell and Noll [1965] for extensive discussions.

Problem 3.6 Show that these compatability conditions coincide with those derived in Truesdell and Noll [1965].

The following major theorem of Marsden and Wan [1983], whose proof is omitted here, establishes a key link with and substantially improves upon the classical power series methods.

3.39 Theorem *Suppose* (u_1, l_1) *satisfy* (L) *and* (C). *Then* (u_1, l_1) *is linearization stable.*

In this result one cannot simply take $l(\lambda) = \lambda l_1$, the second term in the expansion $l(\lambda) = \lambda l_1 + \lambda^2 l_2 + \ldots$ plays a key role.

3. To give an example of a non-integrable $l_1 \in \mathcal{L}_e$, one can find an l_1 such that for any $\boldsymbol{u}_1$ satisfying (L), condition (C) is violated. Such an example of Signorini is discussed in §9 of Capriz and Podio–Guidugli [1974].

4. One can carry out an analysis similar to this around a stressed state as well. The details of the computations and the possible bifurcation diagrams can be more complex, as one in effect has to deal with "genuine" three-dimensional buckling. This aspect is treated by Wan [1983]. The perturbation series approach of Signorini has been carried out in this case by Bharatha and Levinson [1978].

7.4 BASIC IDEAS OF DYNAMIC BIFURCATION THEORY

Dynamic bifurcation theory differs from the static theory in that we now concentrate on qualitative changes in phase portraits, such as the sudden appearance of periodic orbits. The static theory of Section 7.1 may be regarded as a subtheory, namely, the study of bifurcation of equilibrium points. One of the basic theorems in this subject is the "Hopf bifurcation theorem" on the

appearance of closed orbits. We present a self-contained proof of this theorem in Box 4.1.

The dynamical framework in which we operate is described as follows. Let $\mathcal{Y} \subset \mathcal{X}$ be Banach spaces (or manifolds) and let

$$f\colon \mathcal{Y} \times \mathbb{R}^p \longrightarrow \mathcal{X}$$

be a given C^k mapping. Here $\mathbb{R}^p$ is the parameter space and f may be defined only on an open subset of $\mathcal{Y} \times \mathbb{R}^p$. The dynamics is determined by the evolution equation $dx/dt = f(x, \lambda)$, which will be assumed to define a local semiflow $F_t^\lambda\colon \mathcal{Y} \longrightarrow \mathcal{Y}$ by letting $F_t^\lambda(x_0)$ be the solution of $\dot{x} = f(x, \lambda)$ with initial condition $x(0) = x_0$. See Section 6.5 for instances when this is valid.

A *fixed point* is a point (x_0, λ) such that $f(x_0, \lambda) = 0$. Therefore, $F_t^\lambda(x_0) = x_0$; that is, x_0 is an equilibrium point of the dynamics.

A fixed point (x_0, λ) is called $\mathcal{X}$- (resp. $\mathcal{Y}$-) *stable* if there is an $\mathcal{X}$- (resp. $\mathcal{Y}$-) neighborhood $\mathcal{U}_0$ of x_0 such that for $x \in \mathcal{U}_0 \cap \mathcal{Y}$, $F_t^\lambda(x)$ is defined for all $t \geq 0$, and if for any neighborhood $\mathcal{U} \subset \mathcal{U}_0$, there is a neighborhood $\mathcal{V} \subset \mathcal{U}_0$ such that $F_t^\lambda(x) \in \mathcal{U}$ if $x \in \mathcal{V}$ and $t \geq 0$. The fixed point is called *asymptotically stable* if, in addition, $F_t^\lambda(x) \longrightarrow x_0$ in the $\mathcal{X}$-norm (resp. $\mathcal{Y}$-norm) as $t \longrightarrow +\infty$, for x in a neighborhood of x_0.

> ***Problem 4.1*** Discuss the relationship between this notion of stability and that in Section 6.6 (see Definition 6.2).

Many semilinear hyperbolic and most parabolic equations satisfy an additional smoothness condition; we say F_t^λ is a $\mathcal{Y}$-C^k *semiflow* if for each t and λ, $F_t^\lambda\colon \mathcal{Y} \longrightarrow \mathcal{Y}$ (where defined) is a C^k map and its derivatives are strongly continuous in t, λ. Similarly, we say F_t^λ is $\mathcal{X}$—C^k if it extends to a C^k map of $\mathcal{X}$ to $\mathcal{X}$. One especially simple case occurs when

$$f(x, \lambda) = A_\lambda x + B(x, \lambda),$$

where $A_\lambda\colon \mathcal{Y} \longrightarrow \mathcal{X}$ is a linear generator depending continuously on λ and $B\colon \mathcal{X} \times \mathbb{R}^p \longrightarrow \mathcal{X}$ is a C^k map. Then F_t^λ is C^k from $\mathcal{X}$ to $\mathcal{X}$ and if B is C^k from $\mathcal{Y}$ to $\mathcal{Y}$, so is F_t^λ. This result is readily proved by the variation of constants formula

$$x(t) = e^{tA_\lambda} x_0 + \int_0^t e^{(t-s)A_\lambda} B(x(s), \lambda)\, ds.$$

See Section 6.5 for details. For more general conditions under which a semiflow is smooth, see Marsden and McCracken [1976]; see also Box 5.1, Section 6.5. The stability of fixed points may often be determined by the following basic result. For example, it applies to the Navier–Stokes equations, reproducing Prodi [1962] as a special case.

4.1 Liapunov's Theorem *Suppose F_t is an $\mathcal{X}$–C^1 flow, x_0 is a fixed point and the spectrum of the linear semigroup*

$$\mathcal{U}_t = D_x F_t(x_0)\colon \mathcal{X} \longrightarrow \mathcal{X}$$

(the Fréchet derivative with respect to $x \in \mathfrak{X}$) is $e^{t\sigma}$, where σ lies in the left half-plane a distance $> \delta > 0$ from the imaginary axis. Then x_0 is asymptotically stable and for x sufficiently close to x_0 we have the estimate

$$\| F_t(x) - x_0 \| \leq Ce^{-t\delta}.$$

Proof We shall need to accept from spectral and semigroup theory that there is an $\epsilon > 0$ and an equivalent norm $|||\cdot|||$ on $\mathfrak{X}$ such that

$$||| DF_t(x_0) ||| < e^{-\epsilon t}.$$

(Indeed, if $\mathfrak{U}_t$ is a semigroup with spectral radius e^{rt}, set

$$||| x ||| = \sup_{t \geq 0} \| \mathfrak{U}_t x \| / e^{rt};$$

see Hille and Phillips [1957].) Thus, if $0 < \epsilon' < \epsilon$,

$$||| DF_t(x) ||| \leq \exp(-\epsilon' t) \quad \text{for} \quad 0 \leq t \leq 1$$

and x in a neighborhood of x_0, say $\mathfrak{U} = \{x \mid ||| x - x_0 ||| < r\}$. This is because F_t is C^1 with derivative continuous in t.

We claim that if $x \in \mathfrak{U}$, and t is small, then $F_t x \in \mathfrak{U}$ and

$$||| F_t(x) - x_0 ||| \leq \exp(-\epsilon' t) ||| x - x_0 |||.$$

But it follows from this estimate:

$$\begin{aligned} ||| F_t(x) - x_0 ||| &= ||| F_t(x) - F_t(x_0) ||| \\ &= \left|\left|\left| \int_0^1 DF_t(sx + (1-s)x_0) \cdot (x - x_0)\, ds \right|\right|\right| \\ &< \int_0^1 ||| DF_t(sx + (1-s)x_0 ||| \, ||| (x - x_0) ||| \, ds \\ &< \exp(-\epsilon' t) ||| x - x_0 |||. \end{aligned}$$

This result now holds for large t by using the facts that $F_t = F_{t/n}^n$ and $\exp(-\epsilon' t) = [\exp(-\epsilon' t/n)]^n$. Changing back to the original norm, the theorem is proved. ∎

Observe that the hypotheses do not explicitly involve the generator A, so the theorem can be used for $\mathfrak{Y}$-smooth flows as well. As we noted in Box 5.1, Section 6.5, the full equations of nonlinear elasticity cannot be expected to define smooth flows. However, 4.1 can be expected to apply when a semilinear model is used.

To locate fixed points in a bifurcation problem, we solve the equation $f(x, \lambda) = 0$. The stability of a fixed point x_0 is usually determined by the spectrum σ of the linearization at x_0:

$$A_\lambda = D_x f(x_0, \lambda).$$

(If the operator A_λ and its semigroup are non-pathological—for example, they have discrete spectrum—then $\sigma(e^{tA}\lambda) = e^{t\sigma(A_\lambda)}$ or the closure of this set; see Carr [1981] and Roh [1982] for additional results.) Thus, if σ lies in the left half-plane, x_0 is stable. In critical cases where the spectrum lies on the imagi-

nary axis, stability has to be determined by other means (see Problem 5.4, Section 6.5 for an example). It is at criticality where, for example, a curve of fixed points $x_0(\lambda)$ changes from being stable to unstable, a bifurcation can occur.

The second major point we wish to make is that within the context of smooth semiflows, the invariant manifold theorems from ordinary differential equations carry over.

In bifurcation theory it is often useful to apply the invariant manifold theorems to the *suspended flow*

$$F_t\colon \mathfrak{X} \times \mathbb{R}^p \longrightarrow \mathfrak{X} \times \mathbb{R}^p \quad \text{defined by} \quad (x, \lambda) \mapsto (F_t^\lambda(x), \lambda).$$

The invariant manifold theorem states that if the spectrum of the linearization A_λ at a fixed point (x_0, λ) splits into $\sigma_s \cup \sigma_c$, where σ_s lies in the left half-plane and σ_c is on the imaginary axis, then the flow F_t leaves invariant manifolds $\mathcal{W}^s$ and $\mathcal{W}^c$ tangent to the eigenspaces corresponding to σ_s and σ_c, respectively; $\mathcal{W}^s$ is the *stable* and $\mathcal{W}^c$ is the *center* manifold. (One can allow an *unstable* manifold too if that part of the spectrum is finite.) Orbits on $\mathcal{W}^s$ converge to (x_0, λ) exponentially. For suspended systems, note that we always have $1 \in \sigma_c$.

For bifurcation problems the center manifold theorem is the most relevant, so we summarize the situation. (See Marsden and McCracken [1976] and Hassard, Kazarinoff and Wan [1981] for details.)

4.2 Center Manifold Theorem for Flows *Let $\mathcal{Z}$ be a Banach space admitting a C^∞ norm away from 0 and let F_t be a C^0 semiflow defined on a neighborhood of 0 for $0 \le t \le \tau$. Assume $F_t(0) = 0$ and for each $t > 0$, $F_t\colon \mathcal{Z} \longrightarrow \mathcal{Z}$ is a C^{k-1} map whose derivatives are strongly continuous in t. Assume that the spectrum of the linear semigroup $DF_t(0)\colon \mathcal{Z} \longrightarrow \mathcal{Z}$ is of the form $e^{t(\sigma_s \cup \sigma_c)}$, where $e^{t\sigma_c}$ lies on the unit circle (i.e., σ_c lies on the imaginary axis) and $e^{t\sigma_s}$ lies inside the unit circle a nonzero distance from it, for $t > 0$; that is, σ_s is in the left half-plane. Let C be the (generalized) eigenspace corresponding to the part of the spectrum on the unit circle. Assume* $\dim C = d < \infty$.

Then there exists a neighborhood $\mathcal{U}$ of 0 in $\mathcal{Z}$ and a C^k submanifold $\mathcal{W}^c \subset \mathcal{U}$ of dimension d passing through 0 and tangent to C at 0 such that;

(a) *If $x \in \mathcal{W}^c$, $t > 0$ and $F_t(x) \in \mathcal{U}$, then $F_t(x) \in \mathcal{W}^c$.*
(b) *If $t > 0$ and $F_t^n(x)$ remains defined and in $\mathcal{U}$ for all $n = 0, 1, 2, \ldots$, then $F_t^n(x) \longrightarrow \mathcal{W}_c$ as $n \longrightarrow \infty$.*

See Figure 7.4.1 for a sketch of the situation.

For example, in the pitchfork bifurcation from Section 7.1, we have a curve of fixed points $x_0(\lambda)$ and $\lambda \in \mathbb{R}$, which become unstable as λ crosses λ_0 and two stable fixed points branch off. All three points lie on the center manifold for the suspended system. Taking $\lambda =$ constant slices yields an invariant manifold $\mathcal{W}^c$ for the parametrized system; see Figure 7.4.2.

Although the center manifold is only known implicity, it can greatly simplify the problem qualitatively by reducing an initially infinite-dimensional problem

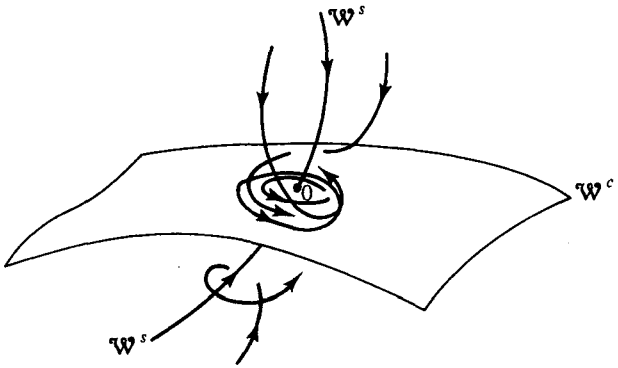

Figure 7.4.1

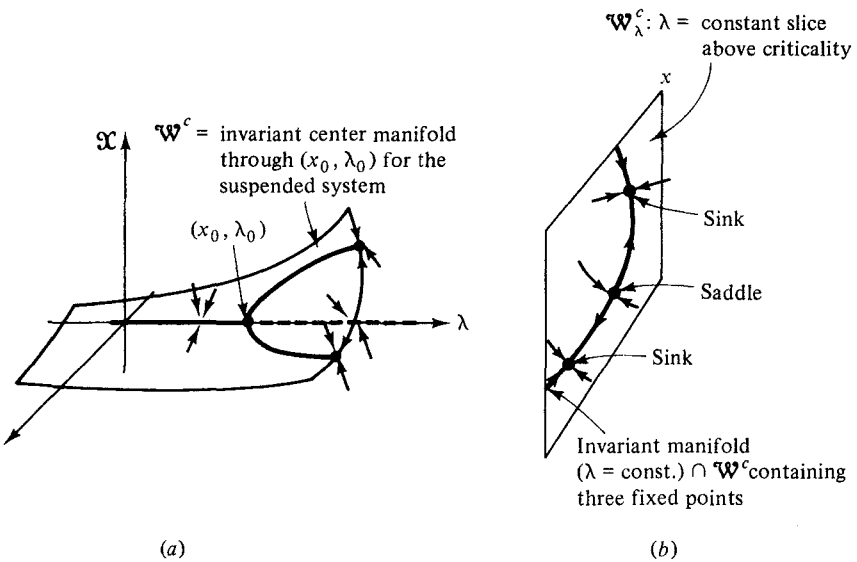

Figure 7.4.2

to a finite-dimensional one. Likewise, questions of stability become questions on the center manifold itself. Thus, the center manifold theorem plays the same role in the dynamic theory that the Liapunov–Schmidt procedure plays in the static theory. However, as we shall see in the proof of Hopf's theorem in Box 4.1, sometimes the Liapunov–Schmidt procedure is applied directly in dynamic problems.

It turns out to be true rather generally that stability calculations done via the Liapunov-Schmidt procedure and via the center manifold approach are

equivalent. This allows one to make dynamic deductions from the Liapunov-Schmidt procedure, which is convenient for calculations. See Schaeffer and Golubitsky [1981, §6] for details.

There are some important points to be made on the applicability of the preceeding theorems to nonlinear elasticity. First of all, dynamic elastic bifurcation phenomena often involve dissipation and forcing as well as the conservative elastic model. The equations of hyperelastodynamics (without dissipation) are such that the flow determined by them is probably not smooth. This has been indicated already in Section 6.5. On the other hand it is also not clear what dissipative mechanisms (such as viscoelasticity or thermo-elasticity) will produce smooth semiflows. As we already know, the situation is tractable for typical rod, beam, and plate models, for they give semilinear equations. Similar difficulties in delay equations can be overcome; cf. Hale [1981].

In short, for the full equations of three-dimensional nonlinear elasticity a dynamical bifurcation theory does not yet exist, for "technical reasons." For typical rod, beam, and plate models, however, the theory presented here does apply. (Some examples are discussed in the next section.)

We now turn our attention to a description of some of the basic dynamic bifurcations. Bifurcation theory for dynamical systems is more subtle than that for fixed points. Indeed the variety of bifurcations possible—their structure and an imperfection-sensitivity analysis—is much more complex. We begin by describing the simplest bifurcations for *one*-parameter system.

4.3 Saddle Node or Limit Point This is a bifurcation of fixed points; a saddle and a sink come together and annihilate one another, as shown in Figure 7.4.3. A simple real eigenvalue of the sink crosses the imaginary axis at the moment of bifurcation; one for the saddle crosses in the opposite direction. The suspended center manifold is two dimensional. The saddle-source bifurcation is similarly described.

If an axis of symmetry is present, then a symmetric pitchfork bifurcation can

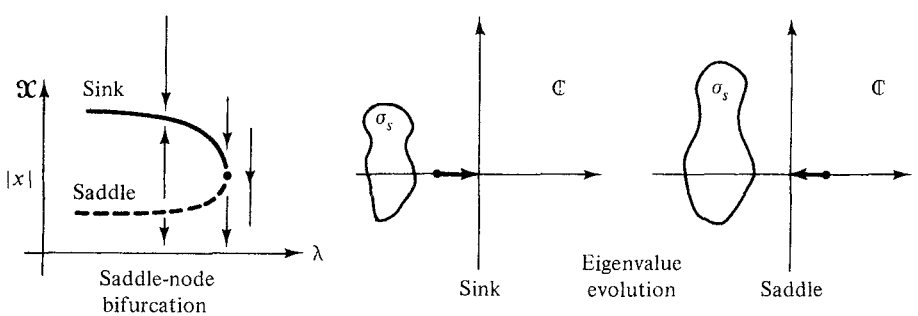

Figure 7.4.3

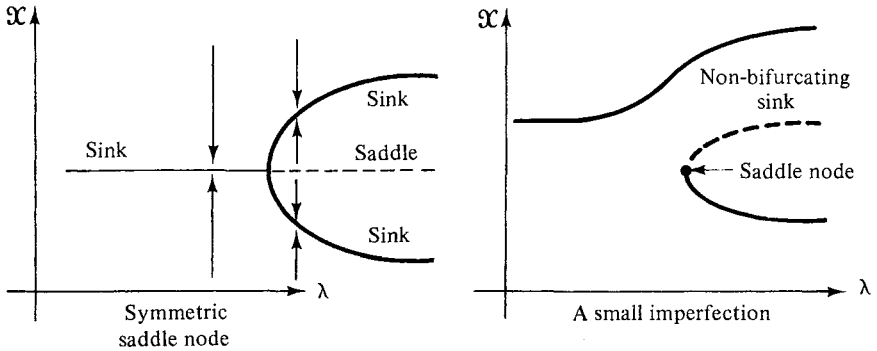

Figure 7.4.4

occur, as in Figure 7.4.4. As in our discussion of Euler buckling, in Section 7.1, small asymmetric perturbation or imperfection can "unfold" this in several ways, one of which is a simple non-bifurcating path and a saddle node.

4.4 Hopf Bifurcation This is a bifurcation of a fixed point to a periodic orbit; here a sink becomes a saddle by two complex conjugate non-real eigenvalues crossing the imaginary axis. As with the pitchfork, the bifurcation can be sub-critical (unstable closed orbits) or super-critical (stable closed orbits). Figure 7.4.5 depicts the supercritical attracting case in $\mathfrak{X} = \mathbb{R}^2$. Here the suspended center manifold is three dimensional.

The proof of the Hopf theorem will be sketched in Box 4.1. The use of center manifolds to prove it is due to Ruelle and Takens [1971]. For PDE's, many approaches are available; see the books of Marsden and McCracken [1976], Iooss and Joseph [1980], Henry [1981], and Hassard, Kazarinoff, and Wan [1981] for references and discussion.

These two bifurcations are local in the sense that they can be analyzed by linearization about a fixed point. There are, however, some *global* bifurcations that can be more difficult to detect. A *saddle connection* is shown in Figure 7.4.6. Here the stable and unstable separatrices of the saddle point pass through a state of tangency (when they are identical) and thus cause the annihilation of the attracting closed orbit.

These global bifurcations can occur as part of local bifurcations of systems with additional parameters. This approach has been developed by Takens [1974a, b], who has classified generic or "stable" bifurcations of two-parameter families of vector fields on the plane. This is an outgrowth of extensive work of the Russian school led by Andronov and Pontryagin [1937]. An example of one of Taken's bifurcations with a symmetry imposed is shown in Figure 7.4.7. (The labels will be used for reference in the next section.) In this bifurcation, rather

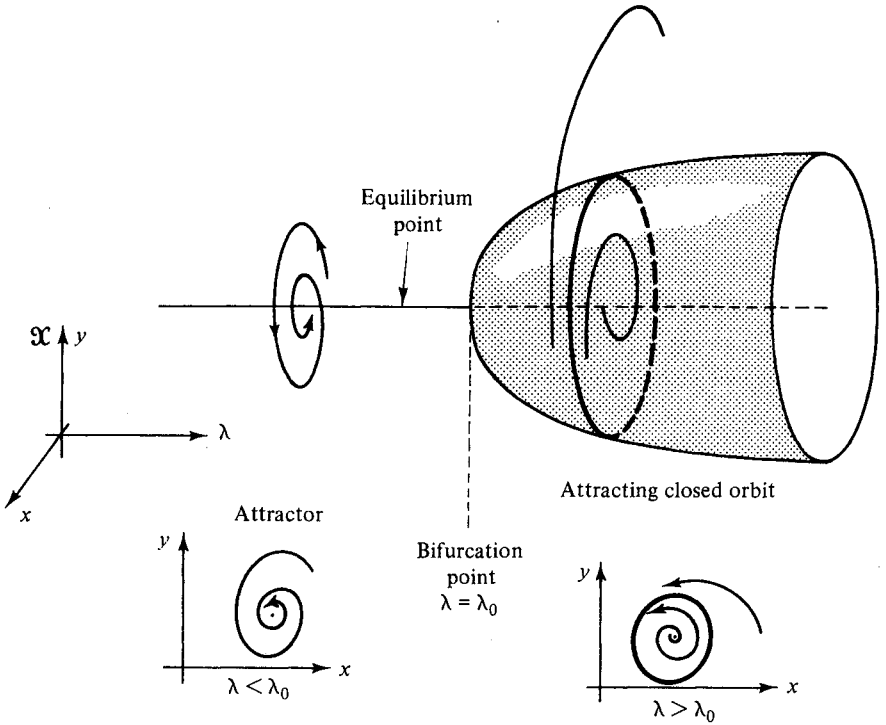

Figure 7.4.5

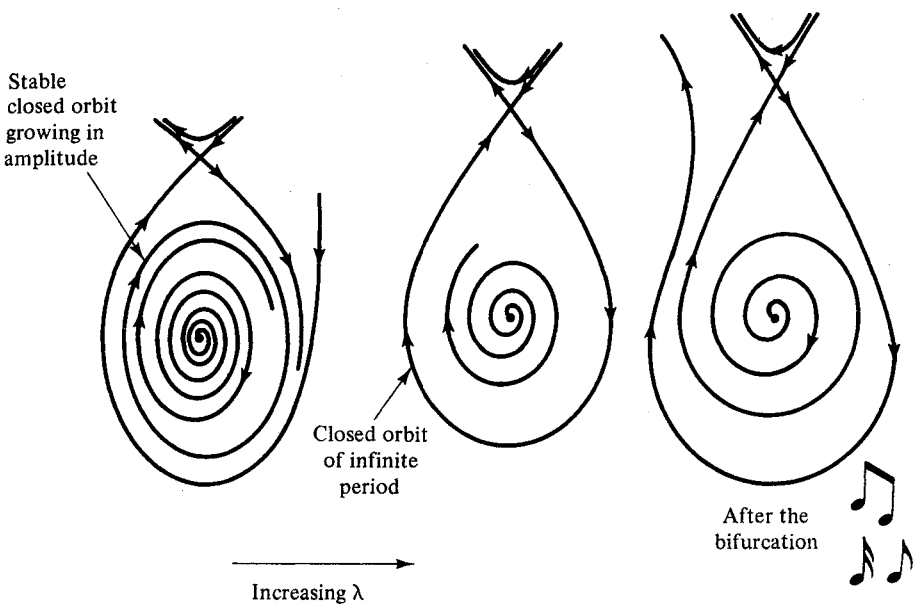

Figure 7.4.6

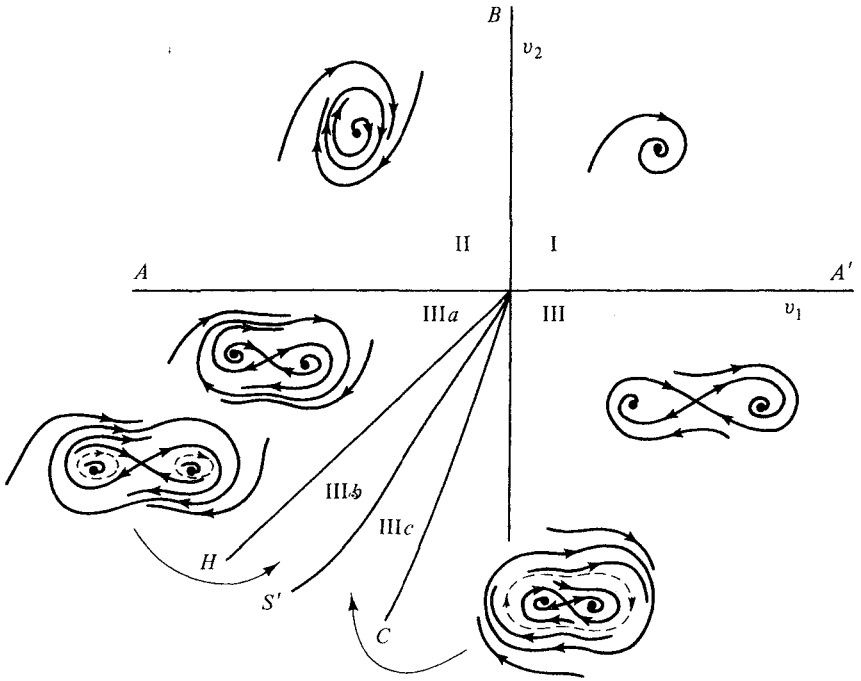

Figure 7.4.7 Takens' "(2, −) normal form" showing the local phase portrait in each region of parameter space.

than a single eigenvalue or a complex conjugate pair crossing the imaginary axis, a real double eigenvalue crosses at zero.

Many similar complex bifurcations are the subject of current research. For example, the eigenvalue configurations (a) one complex conjugate pair and one real zero and (b) two complex conjugate pairs, crossing the imaginary axis, are of interest in many problems. See, for example, Jost and Zehnder [1972], Cohen [1977], Takens [1973], Holmes [1980c], Guckenheimer [1980], and Langford and Iooss [1980]. A number of general features of dynamic bifurcation theory and additional examples are described in Abraham and Marsden [1978] and in Thompson [1982].

Some of the phenomena captured by the bifurcations outlined above have been known to engineers for many years. In particular, we might mention the jump phenomenon of Duffing's equation (see Timoshenko [1974], Holmes and Rand [1976]) and the more complex bifurcational behavior of the forced van der Pol oscillator (Hayashi [1964], Holmes and Rand [1978]; the latter contains a proof that the planar variational equation of the latter oscillator undergoes a saddle connection bifurcation as in Figure 7.4.6).

Box 4.1 ***The Hopf Bifurcation***

The references cited in the text contain many proofs of the Hopf bifurcation theorem. Here we give one that directly utilizes the Liapunov–Schmidt procedure rather than center manifolds. (It is similar to expositions of proofs known to Hale and Cesari, amongst others. The present version was told to us by G. Iooss, M. Golubitsky and W. Langford, whom we thank.)

Let $f\colon \mathbb{R}^n \times \mathbb{R} \longrightarrow \mathbb{R}^n$ be a smooth mapping satisfying $f(0, \lambda) = 0$ for all λ. We are interested in finding periodic solutions for

$$\frac{dx}{dt} = f(x, \lambda). \tag{1}$$

Let $A_\lambda = D_x f(0, \lambda)$ be the linearization of f at the equilibrium point $(0, \lambda)$. For simplicity we can assume our bifurcation point will be $\lambda_0 = 0$ and we write $A = A_{\lambda_0}$.

Our search for periodic orbits for (1) begins with the assumption that the linearization equation

$$\frac{dv}{dt} = Av \tag{2}$$

has some. Normalizing the periods of (2) to be 2π, and eliminating resonance leads to the following condition:

(H1) *A has simple eigenvalues $\pm i$ and no eigenvalues equal to ki, where k is an integer other than ± 1.*

The period of a putative periodic orbit of (1) will drift from 2π to an unknown period when the nonlinear terms are turned on. Thus we can introduce a new variable s by rescaling time:

$$s = (1 + \tau)t \tag{3}$$

In terms of s, (1) becomes

$$(1 + \tau)\frac{dx}{ds} = f(x, \lambda). \tag{4}$$

We now seek a 2π-periodic function $x(s)$ and a number τ such that (4) holds. Thus, we let

$$\Lambda^0 = \text{all continuous } 2\pi\text{-periodic functions } x(s) \text{ in } \mathbb{R}^n$$

and Λ^1 be the corresponding C^1 functions. Now set

$$F\colon \Lambda^1 \times \mathbb{R} \times \mathbb{R} \longrightarrow \Lambda^0 \qquad F(x, \tau, \lambda) = (1 + \tau)\frac{dx}{ds} - f(x, \lambda).$$

We seek zeros of F; these will be periodic orbits of period $(1 + \tau)2\pi$ (or in case $x = 0$, fixed points).

Now we apply the Liapunov–Schmidt procedure to F. The derivative of F with respect to its first argument at the trivial solution $(0, 0, 0)$ is denoted L:

$$Lu = D_1F(0, 0, 0)\cdot u = \frac{du}{ds} - Au. \tag{5}$$

From (H1) we see that the kernel of L is spanned by two functions, say $\phi_1, \phi_2 \in \Lambda^1$. In fact, if $Aw = iw$, then we can choose $\phi_1(s) = \mathrm{Re}(e^{is}w)$ and $\phi_2(s) = \mathrm{Im}(e^{is}w)$. The space spanned by ϕ_1 and ϕ_2 can be identified with $\mathbb{R}^2$ by $(x, y) \leftrightarrow x\phi_1 + y\phi_2$. The kernel of the adjoint, L^*, which is orthogonal to the range of L (see Section 6.1) is likewise spanned by two functions, say $\phi_1^*, \phi_2^* \in \Lambda^1$; L^* is given by

$$L^*u = -\frac{du}{ds} + A^*. \tag{6}$$

The Liapunov–Schmidt procedure thus gives us an (implicitly defined) map

$$g\colon \mathbb{R}^2 \times \mathbb{R} \times \mathbb{R} \longrightarrow \mathbb{R}^2$$

whose zeros we seek. The first $\mathbb{R}^2$ is the space spanned by ϕ_1 and ϕ_2 and the second is that spanned by ϕ_1^* and ϕ_2^*.

Now the circle S^1 acts on Λ^1 by $x(s) \mapsto \theta x(s) = x(s - \theta)$, where $\theta \in S^1$ (S^1 is regarded as real numbers modulo 2π). The function F is covariant with respect to this action, as is easily checked: $F(\theta x, \tau, \lambda) = \theta F(x, \tau, \lambda)$. Now in general when a function whose zeros we seek is covariant (or equivariant) with respect to a group action, preserving the norm, the function produced by the Liapunov–Schmidt procedure is also covariant.

Problem 4.2 Prove this assertion. (See Sattinger [1979] if you get stuck.)

From the form of ϕ_1 and ϕ_2, the action of S^1 on $\mathbb{R}^2$ is just given by rotations through an angle θ. Now a rotationally covariant function from $\mathbb{R}^2$ to $\mathbb{R}^2$ is determined by its restriction to a line through the origin in its domain. Thus, we can write g in the form

$$g(x, y, \tau, \lambda) = \begin{pmatrix} x & -y \\ y & x \end{pmatrix} \begin{pmatrix} \mu \\ \beta \end{pmatrix}, \tag{7}$$

where μ and β are smooth[10] functions of $u = \epsilon^2 = x^2 + y^2$, τ, and λ. We have $\mu(0, \tau, \lambda) = 0 = \beta(0, \tau, \lambda)$ corresponding to the trivial solu-

[10]It is clear that μ and β are smooth functions of $\epsilon = \sqrt{x^2 + y^2}$; one can show that their evenness on reflection through the origin implies they are smooth functions of ϵ^2, a classical result of Whitney; cf. Schwarz [1975] for a general study of such phenomena.

tions. If we find a zero of (μ, β) other than at $x = 0$, $y = 0$, we have a periodic orbit. Roughly speaking, (μ, β) defines the perturbations of the amplitude and period of the periodic orbits we seek. From the fact that the variable τ is directly proportional to the changes in period, we find that $(\partial\beta/\partial\tau)(0, 0, 0) = 1$.

Problem 4.3 Prove the preceeding assertion.

Thus, by the implicit function theorem we can solve $\beta = 0$ for $\tau(\epsilon^2, \lambda)$.

We still need to solve $\mu = 0$. By S^1 covariance it is enough to look at the function $\mu(u, \lambda) = \mu(u, \lambda, \tau(u, \lambda))$; that is, we can restrict to $y = 0$ and take $x \geq 0$; here $u = \epsilon^2$.

(H2) $\dfrac{\partial\mu}{\partial\lambda}(0, 0) \neq 0.$

This is often called the "Hopf condition." As stated, it is not very easy to check. However, it holds iff the eigenvalues of A_λ cross the imaginary axis with non-zero speed (with respect to the parameter λ).

Problem 4.4 Prove this assertion. Consult Marsden and McCracken [1976] or Iooss and Joseph [1980] if you get stuck.

The condition (H2) implies that $\mu = 0$ is solvable for $\lambda(u)$. Thus we have proved some key parts of the following important result of Hopf [1942]:

4.5 Hopf Theorem *If (H1) and (H2) hold, then there is a unique one-parameter family of periodic orbits of (1) in $\mathbb{R}^n \times \mathbb{R}$, that are tangent to $\mathbb{R}^n \times \{0\}$ at $\lambda = 0$. Moreover, if*

(H3) $\dfrac{\partial\mu}{\partial u}(0, 0) \neq 0,$

then $g(\epsilon, \lambda, \tau) = a(\epsilon^2, \lambda)\epsilon$ is contact equivalent (with a $\mathbb{Z}_2$-symmetry) to $(x^2 \pm \lambda)x$. [In the + case ($\partial\mu/\partial u > 0$) the periodic orbits are supercritical and are stable and in the − case ($\partial\mu/\partial u < 0$) they are subcritical and are unstable.] The Hopf and the saddle-node bifurcation are, in a sense, analogous to that explained in Box 1.1, the only one-parameter structurally stable dynamic bifurcations.

For the completion of the proof, methods for computing $\mu_2 = \partial\mu/\partial u$, and infinite-dimensional generalizations, we refer to one of the references already given. (See also Crandall and Rabinowitz [1978], Hassard, Kazarinoff and Wan [1981], and Gurel and Rossler [1979]. We also refer to Takens [1973] and Golubitsky and Langford [1981] for an

imperfection-sensitivity analysis when (H2) or (H3) fail and, to Thompson and Lunn [1981a] for Hopf bifurcation with forcing, to Langford and Iooss [1980] for the interaction of the Hopf and pitchfork bifurcations and to Langford [1979] for the interaction of the Hopf and transcritical bifurcations. A "catalogue" of some of the important dynamic bifurcations is given in Abraham and Marsden [1978].

Box 4.2 ***Summary of Important Formulas for Section 7.4***

Dynamic Bifurcation

A bifurcation in a parameter-dependent dynamical system means a qualitative change in the phase portrait as the parameter(s) varies.

Liapunov's Theorem

A fixed point is stable if the eigenvalue of the linearized system lie in the left half-plane.

Bifurcation at a fixed point can occur only when eigenvalues cross the imaginary axis.

Center Manifold

An invariant manifold corresponding to the purely imaginary eigenvalues captures all the bifurcation behavior.

Limit Point

Bifurcation of fixed points occurring when a saddle and a sink self-destruct (or are spontaneously created).

Hopf Bifurcation

If conditions (H1), (H2), (H3) hold (see the previous box), then the fixed point bifurcates to a family of periodic orbits that are either supercritical (stable) or are subcritical (unstable); see Figure 7.4.5 for the stable case.

7.5 A SURVEY OF SOME APPLICATIONS TO ELASTODYNAMICS[11]

As with Section 7.2, we shall give a biased and incomplete survey. The number of papers dealing with dynamical bifurcation in systems related to elasticity is astronomical. Two examples are Hsu [1977] and Reiss and Matkowsky [1971].

[11]This section was written in collaboration with Philip Holmes.

We shall concentrate on the phenomena of *flutter* in various engineering systems. We begin by describing some general features of flutter.

A dynamical system is said to be *fluttering* if it has a stable closed orbit. Often flutter is suggested if a system linearized about a fixed point has two complex conjugate eigenvalues with positive real part. However, a general proclamation of this sort is certainly false, as shown in Figure 7.5.1. A theorem that can

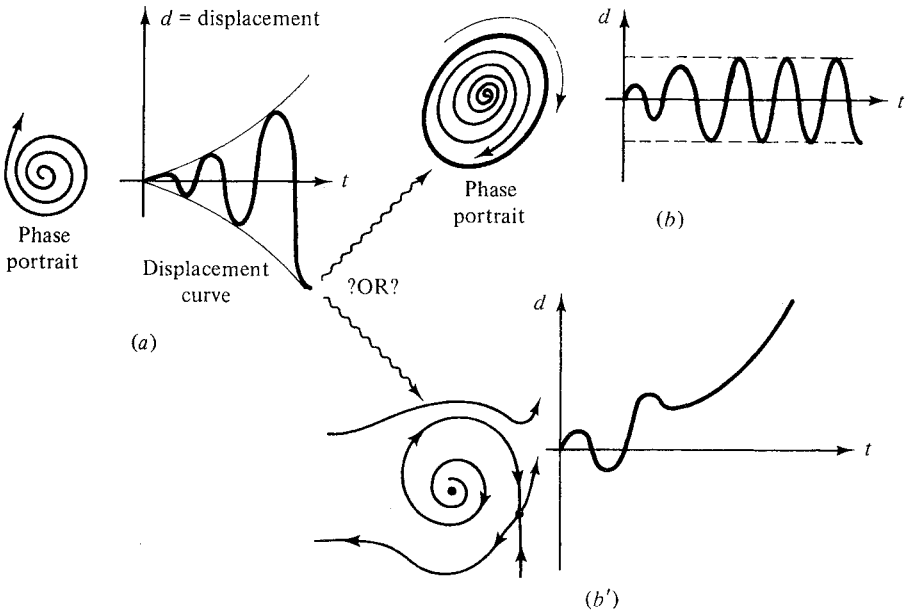

Figure 7.5.1 (a) Linear "flutter." (b) Nonlinear flutter (limit cycle). (b′) An example of linear, but not nonlinear, flutter (no limit cycle).

be used to substantiate such a claim is the Hopf bifurcation theorem, which was proved in the preceding section.

Similar remarks may be made about divergence (a saddle point or source) as shown in Figure 7.5.2.

There are, in broad terms, three kinds of flutter of interest to the engineer. Here we briefly discuss these types. Our bibliography is not intended to be exhaustive, but merely to provide a starting point for the interested reader.

5.1 Airfoil or Whole Wing Flutter on Aircraft Here linear stability methods *do* seem appropriate since virtually any oscillations are catastrophic. Control surface flutter probably comes under this heading also. See Bisplinghoff and Ashley [1962] and Fung [1955] for examples and discussion.

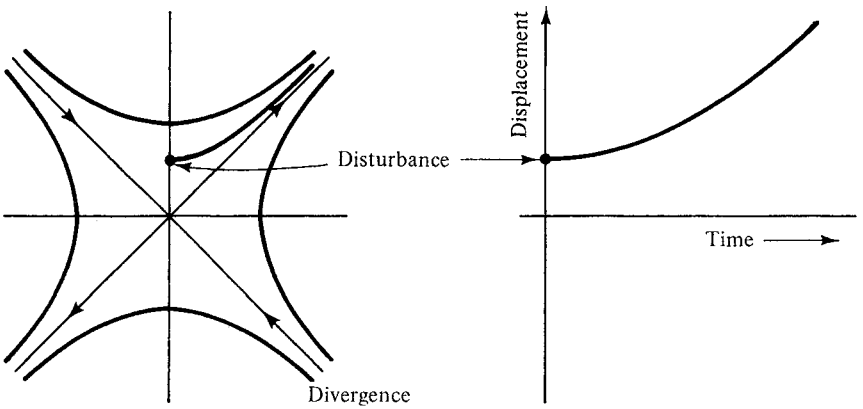

(a)

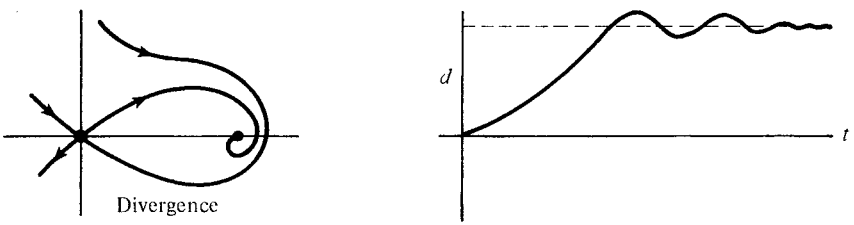

(b)

Figure 7.5.2 (a) Linear theory. (b) A nonlinear possibility.

5.2 Cross-Flow Oscillations The familiar flutter of sun-blinds in a breeze comes under this heading. The "galloping" of power transmission lines and of tall buildings and suspension bridges provide examples that are of more direct concern to engineers: the famous Tacoma Narrows bridge disaster was caused by cross-flow oscillations. In such cases (small) limit cycle oscillations are acceptable (indeed, they are inevitable), and so a nonlinear analysis is appropriate.

Cross-flow flutter is believed to be due to the oscillating force caused by "von Karman" vortex shedding behind the body; see Figure 7.5.3. The alter-

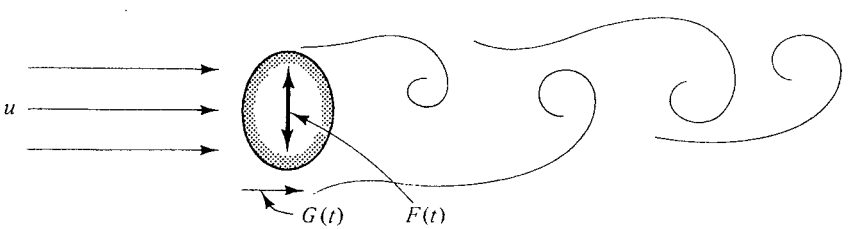

Figure 7.5.3

nating stream of vortices leads to an almost periodic force $F(t)$ transverse to the flow in addition to the in-line force $G(t)$; $G(t)$ varies less strongly than $F(t)$. The flexible body responds to $F(t)$ and, when the shedding frequency (a function of fluid velocity, u, and the body's dimensions) and the body's natural (or resonance) frequency are close, then "lock on" or "entrainment" can occur and large amplitude oscillations are observed. Experiments strongly suggest a limit cycle mechanism and engineers have traditionally modeled the situation by a van der Pol oscillator or perhaps a pair of coupled oscillators. See the symposium edited by Naudascher [1974] for a number of good survey articles; the review by Parkinson is especially relevant. In a typical treatment, Novak [1969] discusses a specific example in which the behavior is modeled by a free van der Pol type oscillator with nonlinear damping terms of the form

$$a_1\dot{x} + a_2\dot{x}^2 + a_3\dot{x}^3 + \cdots.$$

Such equations possess a fixed point at the origin $x = \dot{x} = 0$ and can also possess multiple stable and unstable limit cycles. These cycles are created in bifurcations as the parameters $a_1, a_2, \ldots$, which contain windspeed terms, vary. Bifurcations involving the fixed-point and global bifurcations in which pairs of limit cycles are created both occur. Parkinson also discusses the phenomenon of entrainment that can be modeled by the *forced* van der Pol oscillator.

Landl [1975] discusses such an example that displays both "hard" and "soft" excitation, or, in Arnold's [1972] term, *strong* and *weak* bifurcations. The model is

$$\ddot{x} + \delta\dot{x} + x = a\Omega^2 C_L,$$
$$\ddot{C}_L + (\alpha - \beta C_L^2 + \gamma C_L^4)\dot{C}_L + \Omega^2 C_L = b\dot{x}.$$

Here $\dot{x} \equiv d/dt$ and α, β, γ, δ, a, b are generally positive constants for a given problem (they depend upon structural dimensions, fluid properties, etc.) and Ω is the vortex shedding frequency. As Ω varies the system can develop limit cycles leading to a periodic variation in C_L, the *lift coefficient*. The term $a\Omega^2 C_L$ then acts as a periodic driving force for the first equation, which represents one mode of vibration of the structure. This model, and that of Novak, appear to display generalized Hopf bifurcations (see Takens [1973] and Golubitsky and Langford [1981]).

In related treatments, allowance has been made for the effects of (broad band) turbulence in the fluid stream by including stochastic excitations. Vacaitis et al. [1973] proposed such a model for the oscillations of a two degree of freedom structure and carried out some numerical and analogue computer studies. Holmes and Lin [1978] applied qualitative dynamical techniques to a deterministic version of this model prior to stochastic stability studies of the full model (Lin and Holmes [1978]). The Vacaitis model assumes that the von Karman vortex excitation can be replaced by a term

$$F(t) \equiv F\cos(\Omega t + \Psi(t)),$$

where Ω is the (approximate) vortex shedding frequency and $\Psi(t)$ is a random phase term. In common with all the treatments cited above, the actual mechanism of vortex generation is ignored and "dummy" drag and lift coefficients are introduced. These provide discrete analogues of the actual fluid forces on the body. Iwan and Blevins [1974] and St. Hilaire [1976] have gone a little further in attempting to relate such force coefficients to the fluid motion, but the problem appears so difficult that a rigorous treatment is still impossible. The major problem is, of course, our present inability to solve the Navier–Stokes equations for viscous flow around a body. Potential flow solutions are of no help here, but recent advances in numerical techniques may be useful. Ideally a rigorous analysis of the fluid motion should be coupled with a continuum mechanical analysis of the structure. For the latter, see the elegant Hamiltonian formulation of Marietta [1976], for example.

The common feature of all these treatments (with the exception of Marietta's) is the implicit reduction of an infinite-dimensional problem to one of finite dimensions, generally to a simple nonlinear oscillator. The use of center manifold theory and the concept structural stability suggests that in some cases this reduction might be rigorously justified. To illustrate this we turn to the third broad class of flutter, which we discuss in more detail.

5.3 Axial Flow-Induced Oscillations In this class of problems, oscillations are set up directly through the interaction between a fluid and a surface across which it is moving. Examples are oscillations in pipes and (supersonic) panel flutter; the latter is analyzed in 5.6 below. Experimental measurements (vibration records from nuclear reactor fuel pins, for example) indicate that axial flow-induced oscillations present a problem as severe as the more obvious one of cross-flow oscillations. See the monograph by Dowell [1975] for an account of panel flutter and for a wealth of further references. Oscillations of beams in axial flow and of pipes conveying fluid have been studied by Benjamin [1961], Paidoussis [1966], Paidoussis and Issid [1974] and Holmes [1980d]. Figure 7.5.4 shows the three situations. In addition to the effects of the fluid flow velocity ρ, the structural element might also be subject to mechanical tensile or compressive forces Γ, which can lead to buckling instabilities even in the absence of fluid forces.

The equations of motion of such systems, written in one-dimensional form and with all coefficients suitably nondimensionalized, can be shown to be of the type

$$\alpha\dot{v}'''' + v'''' - \left(K\int_0^1 (v'(\xi))^2\,d\xi + \sigma\int_0^1 (v'(\xi)\dot{v}'(\xi))\,d\xi\right)v'' + \ddot{v}$$
$$+ [\text{linear fluid and mechanical loading terms in } v'', \dot{v}', v', \dot{v}] = 0 \qquad (0)$$

Here α, $\sigma > 0$ are structural viscoelastic damping coefficients and $K > 0$ is a (nonlinear) measure of membrane stiffness; $v = v(z, t)$ and $\cdot = \partial/\partial t$; $' = \partial/\partial z$. (Holmes [1977a], Benjamin [1961], Paidoussis [1966], and Dowell [1975], for

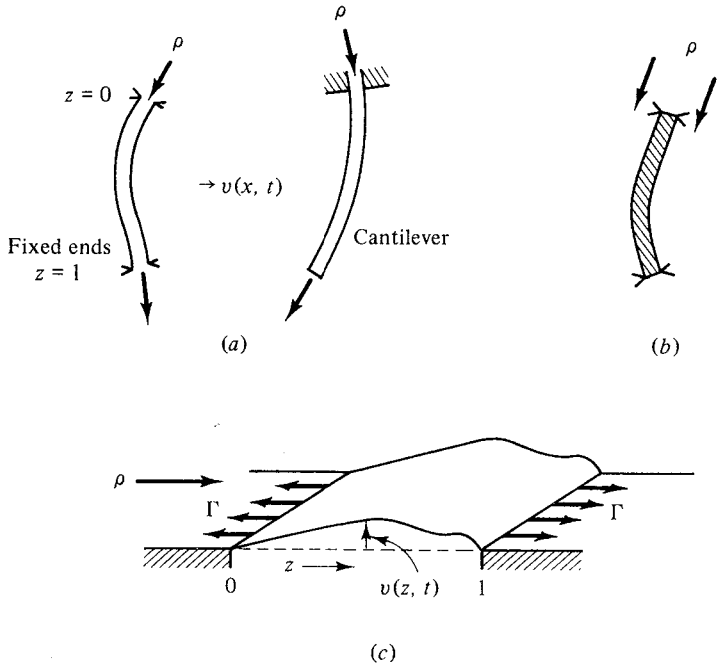

Figure 7.5.4 (a) Pipes conveying fluid. (b) Beam in axial flow. (c) Panel flutter.

example, provide derivations of specific equations of this type.) The fluid forces are again approximated, but in a more respectable manner.

In the case of panel flutter, if a static pressure differential exists across the panel, the right-hand side carries an additional parameter P. Similarly, if mechanical imperfections exist so that compressive loads are not symmetric, then the "cubic" symmetry of (0) is destroyed.

Problems such as those of Figure 7.5.4 have been widely studied both theoretically and experimentally, although, with the exception of Dowell and a number of other workers in the panel flutter area, engineers have for the most part concentrated on linear stability analyses. Such analyses can give misleading results. In many of these problems, engineers have also used low-dimensional models, even though the full problem has infinitely many degrees of freedom. Such a procedure can sometimes be justified if careful use is made of the center manifold theorem.

Often the location of fixed points and the evolution of spectra about them have to be computed by making a Galerkin or other approximation and then using numerical techniques. There are obvious convergence problems (see Holmes and Marsden [1978a]), but once this is done, the organizing centers and dimension of the center manifolds can be determined relatively simply.

5.4 Pipes Conveying Fluid and Supported at Both Ends Pipe flutter is an excellent illustration of the difference between the linear prediction of flutter and what actually happens in the nonlinear PDE model. The phase portrait on the center manifold in the nonlinear case is shown in Figure 7.5.5 at parameter values for which the linear theory predicts "coupled mode" flutter (cf. Paidoussis and Issid [1974] and Plaut and Huseyin [1975]). In fact, we see that the pipe merely settles to one of the stable buckled rest points with no nonlinear flutter. The presence of imperfections should not substantially change this situation.

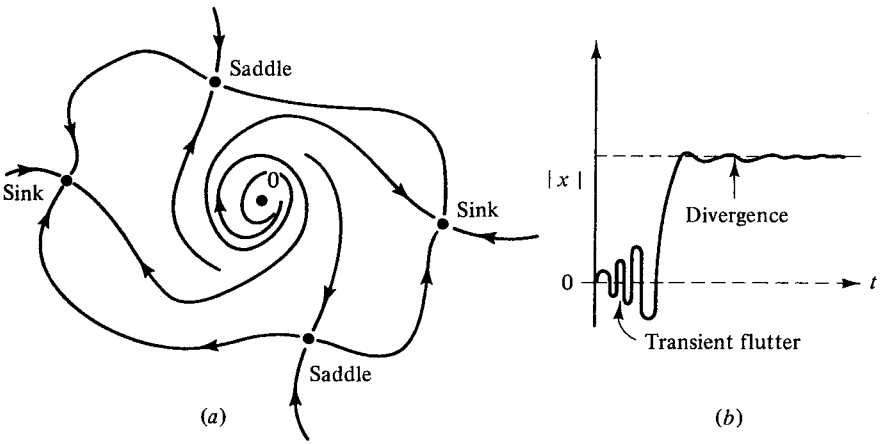

Figure 7.5.5 (a) Vector field. (b) Time evolution of a solution starting near {0}.

The absence of flutter in the nonlinear case can be seen by differentiating a suitable Liapunov function along solution curves of the PDE. In the pipe flutter case the PDE is

$$\alpha\dot{v}'''' + v'''' - \{\Gamma - \rho^2 + \gamma(1 - z) + K\|v'\|^2 + \sigma\langle v', \dot{v}'\rangle\}v'' + 2\sqrt{\beta}\,\rho\dot{v}' + \gamma v' + \delta\dot{v} + \ddot{v} = 0.$$

Here $\|\cdot\|$ and $\langle\cdot,\cdot\rangle$ denote the usual L^2- norm and inner product and solutions $x = (v, \dot{v})$ lie in a Hilbert space $\mathfrak{X} = H_\delta^2([0, 1]) \times L^2([0, 1])$. (See Section 6.5 for the specific analytic framework for such a problem.) For our Liapunov function we choose the energy, in this case given by

$$H(x(t)) = \tfrac{1}{2}\|\dot{v}\|^2 + \tfrac{1}{2}\|v''\|^2 + \frac{\Gamma - \rho^2}{2}\|v'\|^2 + \frac{K}{4}\|v'\|^4 + \frac{\gamma}{2}\langle[1 - z]v', v'\rangle.$$

Differentiating $H(x(t))$ along solution curves yields

$$\frac{dH}{dt} = -\delta\|\dot{v}\|^2 - \alpha\|\dot{v}''\|^2 - \sigma\langle v', \dot{v}'\rangle^2 - 2\sqrt{\beta}\,\rho\langle\dot{v}', \dot{v}\rangle.$$

Since $\langle \dot{v}', \dot{v} \rangle = 0$ and δ, α, $\sigma > 0$, dH/dt is negative for all $v > 0$ and thus al solutions must approach rest points. In particular, for $\Gamma < \Gamma_0$, the first Eule buckling load, all solutions approach $x_0 = \{0\} \in \mathfrak{X}$ and the pipe remain straight. Thus a term of the type $p\dot{v}'$ cannot lead to nonlinear flutter. In the cas of a beam in axial flow, terms of this type *and* of the type p^2v' both occur an nonlinear flutter evidently *can* take place (see Paidoussis [1966] for a linea analysis). Experimental observations actually indicate that fluttering motion more complex than limit cycles can occur.

5.5 Cantilevered Pipes Flexible pipes free at one end can flutter. Anyon who has played with a hose knows this. Benjamin [1961] has some excellen photographs of a two-link model. Here flutter is caused by the so-called followe force at the free end, which introduces an additional term into the energ equation.

Recently, Sethna [1980], and references therein, has shown how the Hop bifurcation can be used to obtain the flutter in this problem. His model allow only planar motions of the pipe. The three-dimensional problem is especiall interesting because of the S^1 symmetry about the axis of the pipe. This leads on to guess that the flutter will become modulated in a subsequent bifurcation, a in the analysis of Rand [1982] for the Taylor problem in fluid mechanics. Se also Thompson and Lunn [1981b].

5.6 Panel Flutter Now we turn to an analysis of panel flutter. We conside the "one-dimensional" panel shown in Figure 7.5.4(c) and we shall be interested in bifurcations near the trivial zero solution. The equation of motion of such a thin panel, fixed at both ends and undergoing "cylindrical" bending (or spanwis bending) can be written as

$$\alpha\dot{v}'''' + v'''' - \left(\Gamma + K\int_0^1 (v'(\xi))^2\, d\xi + \sigma\int_0^1 (v'(\xi)\dot{v}'(\xi))\, d\xi\right)v'' + \rho v'' + \sqrt{\rho}\,\delta\dot{v} + \ddot{v} = 0. \tag{1}$$

See Dowell [1975] and Holmes [1977a]. Here $\cdot \equiv \partial/\partial t$, $' = \partial/\partial z$, and we have included viscoelastic structural damping terms α, σ as well as aerodynamic damping $\sqrt{\rho}\,\delta$. K represents nonlinear (membrane) stiffness, ρ the dynamic pressure, and Γ an in-plane tensile load. All quantities are nondimensionalized and associated with (1). We have boundary conditions at $z = 0, 1$, which might typically be simply supported ($v = v'' = 0$) or clamped ($v = v' = 0$). In the following we make the physically reasonable assumption that α, σ, δ, K are fixed > 0 and let the control parameter $\mu = \{(\rho, \Gamma) \mid \rho \geq 0\}$ vary. In contrast to previous studies in which (1) and similar equations were analyzed for specific parameter values and initial conditions by numerical integration of a finite-dimensional Galerkin approximation, here we study the qualitative behavior of (1) under the action of μ.

As in Section 6.5, we first redefine (1) as an ODE on a Banach space, choosing

as our basic space $\mathfrak{X} = H_\partial^2([0, 1]) \times L^2([0, 1])$, where H_∂^2 denotes H^2 functions in $[0, 1]$ that vanish at 0, 1. Set $\|\{v, \dot{v}\}\|_{\mathfrak{X}} = (\|\dot{v}\|^2 + \|v''\|^2)^{1/2}$, where $\|\cdot\|$ denotes the usual L^2-norm and define the linear operator

$$A_\mu = \begin{pmatrix} 0 & I \\ C_\mu & D_\mu \end{pmatrix} \qquad \begin{aligned} C_\mu v &= -v'''' + \Gamma v'' - \rho v', \\ D_\mu \dot{v} &= -\alpha \dot{v}'''' - \sqrt{\rho}\,\delta \dot{v}. \end{aligned} \tag{2}$$

The basic domain $\mathfrak{D}(A_\mu)$ of A_μ, consists of $(v, \dot{v}) \in \mathfrak{X}$ such that $\dot{v} \in H_\partial^2$ and $v + \alpha\dot{v} \in H^4$; particular boundary conditions necessitate further restrictions. After defining the nonlinear operator $B(v, \dot{v}) = (0, [K\|v'\|^2 + \sigma\langle v', \dot{v}'\rangle]v'')$, where $\langle\ ,\ \rangle$ denotes the L^2 inner product, (1) can be rewritten as

$$\frac{dx}{dt} = A_\mu x + B(x) \equiv G_\mu(x) \qquad x = (v, \dot{v}) \qquad x(t) \in \mathfrak{D}(A_\mu). \tag{3}$$

From Section 6.5 recall that we have an energy function $H\colon \mathfrak{X} \to \mathbb{R}$ defined by

$$H(v, \dot{v}) = \tfrac{1}{2}\|\dot{v}\|^2 + \tfrac{1}{2}\|v''\|^2 + \frac{\Gamma}{2}\|v'\|^2 + \frac{K}{4}\|v'\|^4 \tag{4}$$

and

$$\frac{dH}{dt} = -\rho\langle v', \dot{v}\rangle - \sqrt{\rho}\,\delta\|\dot{v}\|^2 - \alpha\|\dot{v}''\|^2 - \sigma\langle v', \dot{v}\rangle^2.$$

In Section 6.5 we showed that (3) and hence (1) defines a unique smooth global semi-flow F_t^μ on $\mathfrak{X}$.

By making two-mode and four-mode approximations, one finds that for $\sigma = 0.0005$, $\delta = 0.1$, the operator A_μ has a double zero eigenvalue at $\mu = (\rho, \Gamma) \approx (110, -22.6)$ (the point 0 in Figure 7.5.6), the remaining eigenvalues

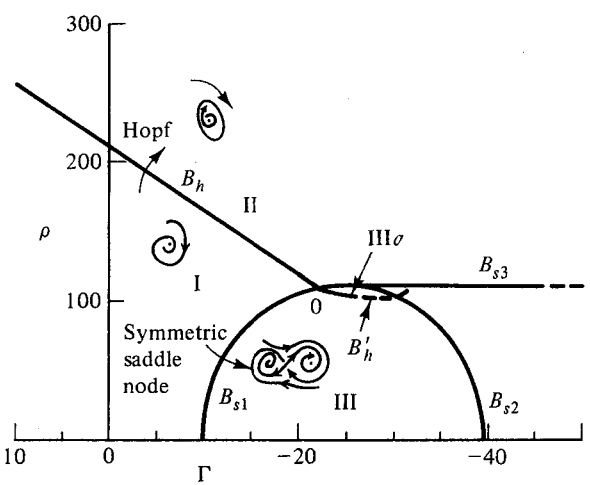

Figure 7.5.6 Partial bifurcation set for the two-mode panel ($\alpha = 0.005$, $\delta = 0.1$).

being in the left half-plane. (See Holmes [1977a] and Holmes and Marsden [1978a].) Thus around the zero solution we obtain a four-dimensional suspended center manifold. (Note that the control parameter μ is now two dimensional.) Referring to the eigenvalue evolution at the zero solution in Figure 7.5.7, which is obtained numerically, we are able to fill in the portions of the bifurcation diagram shown in Figure 7.5.6.

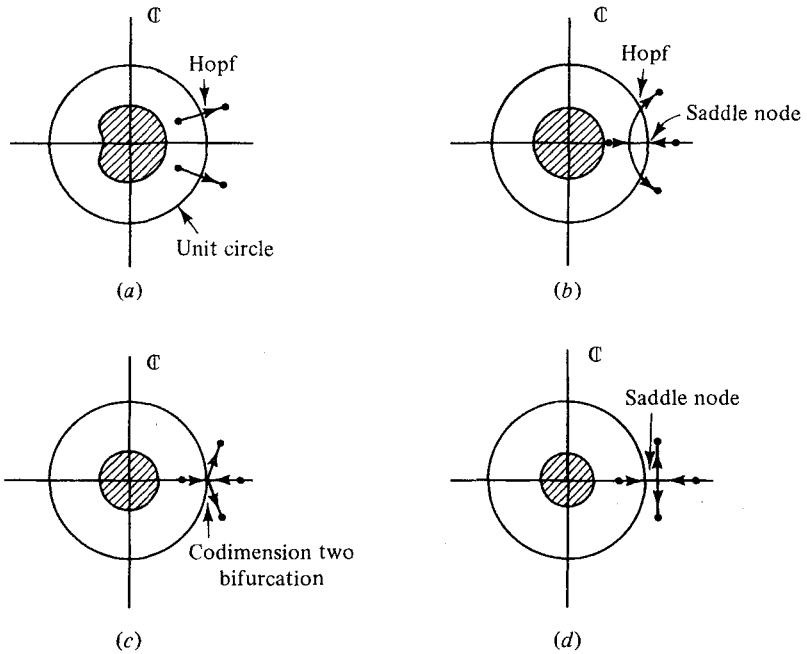

Figure 7.5.7 Eigenvalue evolutions for $DF_t^{\mu}(0)\colon X \longrightarrow X$, Γ fixed, ρ increasing, estimated from two-mode model. (a) $\Gamma = 0$. (b) $\Gamma = -16$. (c) $\Gamma \simeq -21.91$. (d) $\Gamma = -24$.

A supercritical Hopf bifurcation occurs crossing B_h and a symmetrical saddle node on B_{s1}, as shown. These are the flutter and buckling or divergence instabilities detected in previous studies such as Dowell's. Moreover, finite-dimensional computations for the two fixed points $\{\pm x_0\}$ appearing on B_{s1} and existing in region III show that they are sinks ($|\text{spectrum } (DF_t^{\mu}(\pm x_0))| < 1$) below a curve B_h' originating at 0, which we also show on Figure 7.5.6. As μ crosses B_h' transversally, $\{\pm x_0\}$ undergo simultaneous Hopf bifurcations before coalescing with $\{0\}$ on B_{s1}. A fuller description of the bifurcations, including those occurring on B_{s2} and B_{s3}, is provided by Holmes [1977a]. First consider the case where μ crosses B_{s2} from region I to region III, not at 0. Here the eigenvalues indicate that a saddle-node bifurcation occurs. In Holmes [1977a] exact expressions are derived for the new fixed points $\{\pm x_0\}$ in the two-mode case. This then approxi-

mates the behavior of the full evolution equation and the associated semiflow $F_t^\mu: \mathfrak{X} \longrightarrow \mathfrak{X}$ and we can thus assert that a symmetric saddle-node bifurcation occurs on a one-dimensional manifold as shown in Figure 7.5.6 and that the "new" fixed points are sinks in region III. Next consider μ crossing $B_h \backslash O$. Here the eigenvalue evolution shows that a Hopf bifurcation occurs on a two-manifold and use of the stability calculations from Hassard [1979] show that the family of closed orbits existing in region II are attracting.

Now let μ cross $B_{s2} \backslash O$ from region II to region IIIa. Here the closed orbits presumably persist, since they lie at a finite distance from the bifurcating fixed point $\{0\}$. In fact, the new points $\{\pm x_0\}$ appearing on B_{s2} are saddles in region IIIa, with two eigenvalues of spectrum $(DG_\mu(\pm x_0))$ in the right half-plane and all others in the left half-plane. As this bifurcation occurs one of the eigenvalues of spectrum $DF_t^\mu(0)$ passes into the unit circle so that throughout regions IIIa and III $\{0\}$ remains a saddle. Finally, consider what happens when μ crosses B_h' from region IIIa to III. Here $\{\pm x_0\}$ undergo simultaneous Hopf bifurcations and the stability calculations show that the resultant sinks in region III are surrounded by a family of repelling closed orbits. We do not yet know how the multiple closed orbits of region III interact or whether any other bifurcations occur, but we now have a *partial* picture of behavior near 0 derived from the two-mode approximation and from use of the stability criterion. The key to completing this analysis lies in the point 0, the "organizing center" of the bifurcation set at which B_{s2}, B_h, and B_h' meet.

According to our general scheme, we now postulate that our bifurcation diagram near 0 is stable to small perturbations in our (approximate) equations. Takens' bifurcation shown in Figure 7.4.7 is consistent with the information found in Figure 7.5.6. Thus we are led to the complete bifurcation diagram shown in Figure 7.5.8 with the oscillations in various regions as shown in Figure 7.4.7.

One can actually check this rigorously by proving that our vector field on

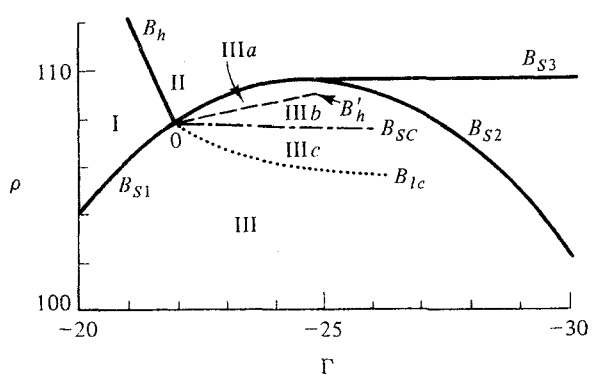

Figure 7.5.8 A local model for bifurcations of the panel near 0, $(\rho, \Gamma) \simeq (107.8, -21.91)$; $\alpha = 0.005$, $\delta = 0.1$.

the center manifold has the appropriate normal form. This calculation is rather long. See Holmes [1982].

Although the eigenvalue computations used in this analysis were derived from two and four mode models (in which A_μ of (2) is replaced by a 4×4 or 8×8 matrix and $\mathfrak{X}$ is replaced by a vector space isomorphic to $\mathbb{R}^4$ or $\mathbb{R}^8$), the convergence estimates of Holmes and Marsden [1978a] indicate that in the infinite-dimensional case the behavior remains qualitatively identical. In particular, for $\mu \in \mathfrak{U}$, a neighborhood of 0, all eigenvalues but two remain in the negative half-plane. Thus the dimension of the center manifold does not increase and our four-dimensional "essential model," a two-parameter vector field on a 2-manifold, provides a local model for the onset of flutter and divergence. We are therefore justified in locally replacing the infinite-dimensional semiflow F_t^μ: $\mathfrak{X} \to \mathfrak{X}$ by a finite-dimensional system. Moreover, the actual vector fields and bifurcation set shown in Figure 7.4.7. can be realized by the explicit nonlinear oscillator

$$\ddot{y} + \lambda_2\dot{y} + \lambda_1 y + \gamma y^2\dot{y} + \eta y^3 = 0 \qquad \gamma, \eta > 0$$

or

$$\dot{y}_1 = y_2 \qquad \dot{y}_2 = -\lambda_1 y_1 - \lambda_2 y_2 - \gamma y_1{}^2 y_2 - \eta y_1{}^3. \tag{5}$$

In engineering terms (5) might be thought of as a "nonlinear normal mode" of the system of Equation (1), with λ_1, λ_2 representing equivalent linear stiffness and damping. (See Rosenberg [1966].) Note, however, that the relationship between the coordinates y_1, y_2 and any conveniently chosen basis in the function space $\mathfrak{X}$ is likely to be nonlinear: in particular, a single "natural" normal mode model of the panel flutter problem *cannot* exhibit flutter, although it can diverge. (See Holmes [1977a]; flutter occurs through coupling between the natural (linear) normal modes.)

The bifurcation diagram in Figure 7.4.7 for panel flutter is derived under an assumption of symmetry. One would expect extremely complex dynamics to be possible if this symmetry is broken because the homoclinic orbits can be broken. The reason we say this is explained in the next section. In fact, Dowell [1980] has found numerically that in certain parameter regions, *chaotic* dynamics occurs in panel flutter. This indicates that breaking the symmetry in Figure 7.4.7—which amounts to an imperfection sensitivity analysis—gives a bifurcation to chaotic dynamics. A situation where one can actually prove such an assertion is described in the next section.

7.6 BIFURCATIONS IN THE FORCED OSCILLATIONS OF A BEAM[12]

In recent years many examples of dynamical systems have been found with the property that the equations of motion are relatively simple, yet the trajectories are very complex and depend very sensitively on the initial data. The literature

[12]This section was written jointly with Philip Holmes and is based on Holmes and Marsden [1981].

on this topic is vast, but some of the more accessible works are Temam [1976], Ratiu and Bernard [1977], Lorenz [1979], Gurel and Rossler [1979], Holmes [1980a], Collet and Eckman [1980], and Guckenheimer and Holmes [1983].

Our goal is to sketch a method that enables one to rigorously describe some of the complexity in the dynamics of a forced beam. Experimentally, aperiodic or apparently random motions have been observed by Tseng and Dugundjii [1971] and by Moon [1980a, b]. One sees in a power spectrum, periodicity (energy concentrated at certain frequencies) shift to aperiodicity (energy spread over a broad band of frequencies) as a parameter is increased. As we shall see, our analysis enables one to compute explicitly the bifurcation point where periodicity switches to aperiodicity for a special class of equations.

We shall consider a motivating example first and state the results for it. Following this we shall describe the methods by which they are obtained.

Consider a beam that is buckled by an external load Γ, so that there are two stable and one unstable equilibrium states (see Figure 7.6.1). The whole structure

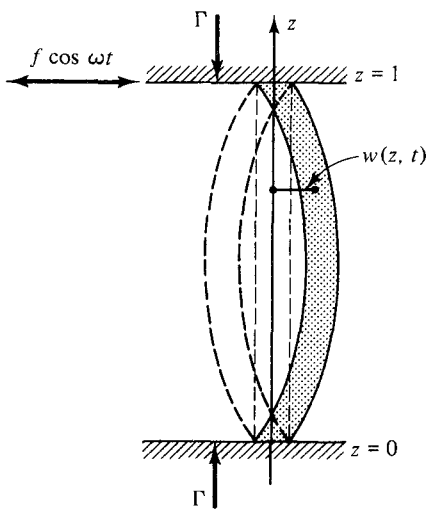

Figure 7.6.1 The forced, buckled beam.

is shaken with a transverse periodic displacement, $f \cos \omega t$ and the beam moves due to its inertia. One observes periodic motion about either of the two stable equilibria for small f, but as f is increased, the motion becomes aperiodic or chaotic.

A specific model for the transverse deflection $w(z, t)$ of the centerline of the beam is the following partial differential equation

$$\ddot{w} + w'''' + \Gamma w'' - \kappa\left(\int_0^1 [w']^2 \, d\zeta\right) w'' = \epsilon(f \cos \omega t - \delta \dot{w}), \tag{1}$$

where $\cdot = \partial/\partial t$, $' = \partial/\partial z$, Γ = external load, κ = stiffness due to "membrane' effects, δ = damping, and ϵ is a parameter used to measure the size of f and δ Among many possible boundary conditions we shall choose $w = w'' = 0$ a $z = 0, 1$—that is, simply supported, or hinged, ends. With these boundary con ditions, the eigenvalues of the linearized, unforced equations—that is, comple numbers λ such that

$$\lambda^2 w + w'''' + \Gamma w'' = 0$$

for some non-zero w satisfying $w = w'' = 0$ at $z = 0, 1$—form a countable se

$$\lambda_j = \pm \pi j \sqrt{\Gamma - \pi^2 j^2} \quad (j = 1, 2, \ldots).$$

Assume that $$\pi^2 < \Gamma < 4\pi^2,$$

in which case the solution $w = 0$ is unstable with one positive and one negative eigenvalue, and the nonlinear equation (1) with $\epsilon = 0$, $\kappa > 0$ has two nontrivial stable buckled equilibrium states.

A simplified model for the dynamics of (1) is obtained by seeking lowest mode solutions of the form

$$w(z, t) = x(t) \sin(\pi z).$$

Substitution into (1) and taking the inner product with the basis function $\sin(\pi z)$, gives a Duffing-type equation for the modal displacement $x(t)$:

$$\ddot{x} - \beta x + \alpha x^3 = \epsilon(\gamma \cos \omega t - \delta \dot{x}), \tag{2}$$

where $\beta = \pi^2(\Gamma - \pi^2) > 0$, $\alpha = \kappa\pi^4/2$, and $\gamma = 4f/\pi$.

Further assumptions we make on (1) follow:

1. (No resonance): $j^2\pi^2(j^2\pi^2 - \Gamma) \neq \omega^2$ $(j = 2, 3, 4, \ldots)$.
2. (Large forcing to damping ratio):

$$\frac{f}{\delta} > \frac{\pi}{3} \frac{\Gamma - \pi^2}{\omega\sqrt{\kappa}} \cosh\left(\frac{\omega}{2\sqrt{\Gamma - \pi^2}}\right) \quad \text{(bifurcation point).}$$

3. (Small forcing and damping): ϵ is sufficiently small.

By the results of Section 6.5, (1) has well-defined smooth global dynamics on the Banach space $\mathfrak{X} = H_\partial^2 \times L^2$ of pairs $(w, \dot{w})$. In particular, there is a time $2\pi/\omega$ map $P: \mathfrak{X} \longrightarrow \mathfrak{X}$ that takes initial data and advances it in time by one period of the forcing function. The main result shows that the map P has complicated dynamics in a very precise sense.

6.1 Theorem *Under the above hypotheses, there is some power P^N of P that has a compact invariant set $\Lambda \subset \mathfrak{X}$ on which P^N is conjugate to a shift on two symbols. In particular, (1) has infinitely many periodic orbits with arbitrarily high period.*

This set Λ arises in a way similar to Smale's famous "horseshoe" that is described below. The statement that P^N is conjugate to a shift on two symbols means that there is a homeomorphism $h: \Lambda \longrightarrow$ (space of bi-infinite sequences of

0's and 1's) $= \{(\ldots, a_{-2}, a_{-1}, a_0, a_1, a_2, \ldots) \mid a_j = 0 \text{ or } 1, j \in \mathbb{Z}\} = \{0, 1\}^{\mathbb{Z}}$ such that $h \circ P^N \circ h^{-1}$ is the shift map taking the sequence (a_j) to the sequence (b_j), where $b_j = a_{j-1}$. Any periodic sequence then gives a periodic point for P^N.

There are many results on periodic orbits for partial differential equations. Perhaps the best are due to Rabinowitz [1978]. However, the approach and results here are quite different.

Let us now explain briefly how the "horseshoe" comes about. We consider Equation (2) for simplicity although the basic idea is the same for (1). The key thing is that when $\epsilon = 0$ (no forcing or damping) the flow has homoclinic orbits—that is, an orbit connecting a saddle point to itself. See Figure 7.6.2. In fact, this equation is Hamiltonian on $\mathbb{R}^2$ with

$$H(x, \dot{x}) = \frac{(\dot{x})^2}{2} - \frac{\beta x^2}{2} + \frac{\alpha x^4}{4}.$$

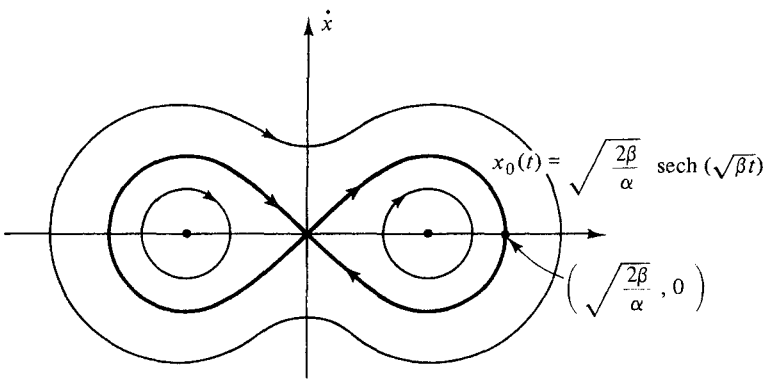

Figure 7.6.2

The flow of this system is the familiar figure eight pattern with a homoclinic orbit given by

$$x_0(t) = \sqrt{\frac{2\beta}{\alpha}} \operatorname{sech}(\sqrt{\beta}\, t).$$

When forcing and damping are turned on ($\epsilon > 0$) the idea is to use a technique of Melnikov [1963] (see also Arnold [1964]) to give a criterion for when the map P has stable and unstable manifolds that intersect transversally (see Figure 7.6.3). We shall go through this procedure shortly. Redrawing the situation, we have a map P of $\mathbb{R}^2$ to itself with stable and unstable manifolds as shown in Figure 7.6.4. It is plausible that the rectangle $\mathcal{R}$ is mapped as shown under a high power N of P. This is the reason for the name "horseshoe." Smale's basic work on this (Smale [1963], [1967]) was motivated by work of Cartwright,

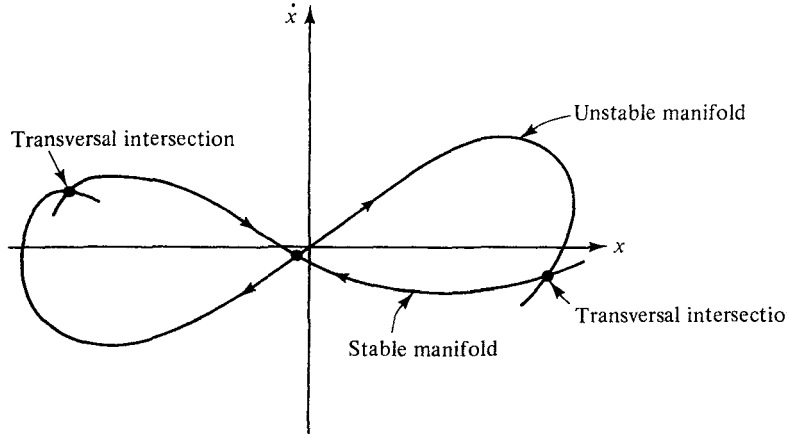

Figure 7.6.3

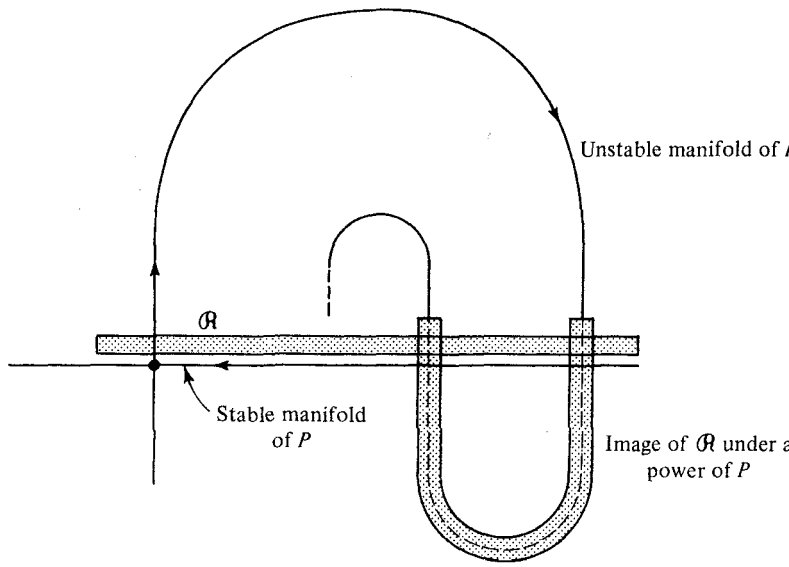

Figure 7.6.4

Littlewood, and Levinson on nonlinear oscillations. The invariant set Λ is obtained as $\Lambda = \bigcap_{n=-\infty}^{\infty}(P^N)^n(\mathcal{R})$.

For purposes of Equation (1) one requires an infinite-dimensional generalization of this situation. Using an elegant argument of Conley and Moser (see Moser [1973]) this was done by Holmes and Marsden [1981]. Some important refinements of this horseshoe picture for two-dimensional systems have been

obtained by Chow, Hale and Mallet–Paret [1980] and Greenspan and Holmes [1982].

It is known that the time t-maps of the Euler and Navier–Stokes equations written in Lagrangian coordinates are smooth (Ebin and Marsden [1970]). Thus the methods described here can apply to these equations, in principle. On regions with no boundary, one can regard the Navier–Stokes equations with forcing as a perturbation of a Hamiltonian system (the Euler eauations). Thus, if one knew a homoclinic orbit for the Euler equations, then the methods of this section would produce infinitely many periodic orbits with arbitrarily high period, indicative of turbulence. No specific examples of this are known to us (one could begin by looking on the two-torus T^2 and studying Arnold [1966]).

Similar situations probably arise in traveling waves and the current-driven Josephson junction. For example, an unforced sine-Gordon equation with damping studied by M. Levi seems to possess a homoclinic orbit (cf. Levi, Hoppenstadt, and Miranker [1978]). Presumably the ideas will be useful for the *KdV* equation as well.

There has been considerable interest recently in chaotic dynamics and strange attractors (cf. Gurel and Rossler [1979] and Hellman [1980]). The methods described here do not prove they exist for (1) or (2), but they do provide evidence that they are there. For a discussion in connection with (2), see Holmes [1979b]. The difference between our set Λ and a true strange attractor $\mathcal{S}$ is that $\mathcal{S}$ is an attracting set and the flow near $\mathcal{S}$ has well-defined statistical properties. However, Λ is not an attractor; the flow near Λ is statistical for a long time, but eventually this leaks out. For a discussion of horseshoes in Hamiltonian systems, see Holmes and Marsden [1982a] and Kopell and Washburn [1981].

We shall now outline the abstract methods by which the result on transversal intersection is proved.

We consider an evolution equation in a Banach space $\mathfrak{X}$ of the form

$$\dot{x} = f_0(x) + \epsilon f_1(x, t), \tag{3}$$

where f_1 is periodic of period T in t. Our hypotheses on (3) are as follows:

(H1) (a) *Assume* $f_0(x) = Ax + B(x)$, *where* A *is an (unbounded) linear operator that generates a* C^0 *one-parameter group of transformations on* $\mathfrak{X}$ *and where* $B: \mathfrak{X} \to \mathfrak{X}$ *is* C^∞. Assume that $B(0) = 0$ and $DB(0) = 0$.

(b) *Assume* $f_1: \mathfrak{X} \times S^1 \to \mathfrak{X}$ *is* C^∞, *where* $S^1 = \mathbb{R}/(T)$, *the circle of length* T.

From the results of Section 6.5, Assumption (1) implies that the associated suspended autonomous system on $\mathfrak{X} \times S^1$,

$$\left.\begin{aligned} \dot{x} &= f_0(x) + \epsilon f_1(x, \theta), \\ \dot{\theta} &= 1, \end{aligned}\right\} \tag{4}$$

has a smooth local flow, F_t^ϵ. This means that $F_t^\epsilon: \mathfrak{X} \times S^1 \to \mathfrak{X} \times S^1$ is a smooth map defined for small $|t|$, which is jointly continuous in all variables

ϵ, t, $x \in \mathfrak{X}$, $\theta \in S^1$, and for x_0 in the domain of A, $t \mapsto F_t^\epsilon(x_0, \theta_0)$ is the unique solution of (4) with initial condition x_0, θ_0.

The final part of Assumption (1) follows:

(c) *Assume that F_t^ϵ is defined for all $t \in \mathbb{R}$ for $\epsilon > 0$ sufficiently small.*

Our second assumption is that the unperturbed system is Hamiltonian. We recall from Chapter 5 that this means that $\mathfrak{X}$ carries a skew-symmetric continuous bilinear map Ω: $\mathfrak{X} \times \mathfrak{X} \longrightarrow \mathbb{R}$, which is weakly non-degenerate (i.e., $\Omega(u, v) = 0$ for all v implies $u = 0$), called the *symplectic form*, and there is a smooth function $H_0 : \mathfrak{X} \longrightarrow \mathbb{R}$ such that

$$\Omega(f_0(x), u) = dH_0(x) \cdot u$$

for all x in $\mathfrak{D}(A)$, the domain of A.

(H2) (a) *Assume that the unperturbed system $\dot{x} = f_0(x)$ is Hamiltonian with energy $H_0 : \mathfrak{X} \longrightarrow \mathbb{R}$.*

Problem 6.1 Verify that Equations (1) and (2) are Hamiltonian on $H_\partial^2 \times L^2$ and $\mathbb{R}^2$, respectively. The Hamiltonian for (1) is

$$H(w, \dot{w}) = \tfrac{1}{2} \| \dot{w} \|^2 - \frac{\Gamma}{2} \| w' \|^2 + \tfrac{1}{2} \| w'' \|^2 + \frac{\kappa}{4} \| w' \|^2.$$

(b) *Assume there is a symplectic 2-manifold $\Sigma \subset \mathfrak{X}$ invariant under the flow F_t^0 and that on Σ the fixed point $p_0 = 0$ has a homoclinic orbit $x_0(t)$;* that is:

$$\dot{x}_0(t) = f_0(x_0(t))$$

and

$$\lim_{t \to +\infty} x_0(t) = \lim_{t \to -\infty} x_0(t) = 0.$$

Next we introduce a non-resonance hypothesis.

(H3) (a) *Assume that the forcing term $f_1(x, t)$ in* (3) *has the form*

$$f_1(x, t) = A_1 x + f(t) + g(x, t), \tag{5}$$

where $A_1 : \mathfrak{X} \longrightarrow \mathfrak{X}$ is a bounded linear operator, f is periodic with period T, $g(x, t)$ is t-periodic with period T and satisfies $g(0, t) = 0$, $D_x g(0, t) = 0$, so g admits the estimate

$$\| g(x, t) \| \leq (\text{const.}) \| x \|^2 \tag{6}$$

for x in a neighborhood of 0.

(b) *Suppose that the "linearized" system*

$$\dot{x}_L = A x_L + \epsilon A_1 x_L + \epsilon f(t) \tag{7}$$

has a T-periodic solution $x_L(t, \epsilon)$ such that $x_L(t, \epsilon) = O(\epsilon)$.

For finite-dimensional systems, (H3) can be replaced by the assumption that 1 does not lie in the spectrum of e^{TA}; that is, none of the eigenvalues of A resonates with the forcing frequency.

Next, we need an assumption that A_1 contributes positive damping and that $p_0 = 0$ is a saddle.

(H4) (a) *For* $\epsilon = 0$, e^{TA} *has a spectrum consisting of two simple real eigenvalues* $e^{\pm\lambda T}$ $(\lambda \neq 0)$ *with the rest of the spectrum on the unit circle.*

(b) *For* $\epsilon > 0$, $e^{T(A+\epsilon A_1)}$ *has a spectrum consisting of two simple real eigenvalues* $e^{T\lambda_\epsilon^\pm}$ *(varying continuously in* ϵ *from perturbation theory of spectra) with the rest of the spectrum,* σ_R^ϵ, *inside the unit circle* $|z| = 1$ *and obeying the estimates*

$$C_2\epsilon \leq \text{distance}(\sigma_R^\epsilon, |z| = 1) \leq C_1\epsilon \tag{8}$$

for C_1, C_2 *positive constants.*

Finally, we need an extra hypothesis on the nonlinear term. We have already assumed B vanishes at least quadratically as does g. Now we assume B vanishes cubically.

(H5) $B(0) = 0$, $DB(0) = 0$, *and* $D^2B(0) = 0$.

This implies that in a neighborhood of 0, $\|B(x)\| \leq \text{const.}\, \|x\|^3$. (Actually $B(x) = o(\|x\|^2)$ would do.)

Consider the suspended system (4) with its flow $F_t^\epsilon: \mathfrak{X} \times S^1 \longrightarrow \mathfrak{X} \times S^1$. Let $P^\epsilon: \mathfrak{X} \longrightarrow \mathfrak{X}$ be defined by $P^\epsilon(x) = \pi_1 \cdot (F_T^\epsilon(x, 0))$, where $\pi_1: \mathfrak{X} \times S^1 \longrightarrow \mathfrak{X}$ is the projection onto the first factor. The map P^ϵ is just the Poincaré map for the flow F_t^ϵ. Note that $P^0(p_0) = p_0$, and that fixed points of P^ϵ correspond to periodic orbits of F_t^ϵ.

6.2 Lemma *For* $\epsilon > 0$ *small, there is a unique fixed point* p_ϵ *of* P^ϵ *near* $p_0 = 0$; *moreover,* $p_\epsilon - p_0 = O(\epsilon)$; *that is, there is a constant* K *such that* $\|p_\epsilon\| < K\epsilon$ *(for all small* ϵ*).*

For ordinary differential equations, Lemma 6.2 is a standard fact about persistence of fixed points, assuming 1 does not lie in the spectrum of e^{TA} (i.e., p_0 is hyperbolic). For general partial differential equations, the proof is similar in spirit, but is more delicate, requiring our assumptions. See Holmes and Marsden [1981] for details. An analysis of the spectrum yields the following.

6.3 Lemma *For* $\epsilon > 0$ *sufficiently small, the spectrum of* $DP^\epsilon(p_\epsilon)$ *lies strictly inside the unit circle with the exception of the single real eigenvalue* $e^{T\lambda_\epsilon^+} > 1$.

The next lemma deals with invariant manifolds.

6.4 Lemma *Corresponding to the eivengvalues* $e^{T\lambda_\epsilon^\pm}$, *there are unique invariant manifolds* $\mathfrak{W}^{ss}(p_\epsilon)$ *(the strong stable manifold) and* $\mathfrak{W}^u(p_\epsilon)$ *(the unstable manifold) of* p_ϵ *for the map* p_ϵ *such that:*

(i) $\mathfrak{W}^{ss}(p_\epsilon)$ *and* $\mathfrak{W}^u(p_\epsilon)$ *are tangent to the eigenspaces of* $e^{T\lambda_\epsilon^\pm}$, *respectively, at* p_ϵ.

(ii) *They are invariant under* P^ϵ.

(iii) *If* $x \in \mathcal{W}^{ss}(p_\epsilon)$, *then*

$$\lim_{n\to\infty} (P^\epsilon)^n(x) = p_\epsilon,$$

and if $x \in \mathcal{W}^u(p_\epsilon)$, *then*

$$\lim_{n\to-\infty} (P^\epsilon)^n(x) = p_\epsilon.$$

(iv) *For any finite* t^*, $\mathcal{W}^{ss}(p_\epsilon)$ *is* C^r *close as* $\epsilon \to 0$ *to the homoclinic orbit* $x_0(t)$ $(t^* \leq t < \infty)$ *and for any finite* t_*, $\mathcal{W}^u(p_\epsilon)$ *is* C^r *close to* $x_0(t)$ $(-\infty < t \leq t_*)$ *as* $\epsilon \to 0$. *Here,* r *is any fixed integer* $(0 \leq r < \infty)$.

The Poincaré map P^ϵ was associated to the section $\mathcal{X} \times \{0\}$ in $\mathcal{X} \times S^1$. Equally well, we can take the section $\mathcal{X} \times \{t_0\}$ to get Poincaré maps $P^\epsilon_{t_0}$. By definition, $P^\epsilon_{t_0}(x) = \pi_1(F^\epsilon_T(x, t_0))$. There is an analogue of Lemmas 6.2, 6.3, and 6.4 for $P^\epsilon_{t_0}$. Let $p_\epsilon(t_0)$ denote its unique fixed point and $\mathcal{W}^{ss}_\epsilon(p_\epsilon(t_0))$ and $\mathcal{W}^u_\epsilon(p_\epsilon(t_0))$ be its strong stable and unstable manifolds. Lemma 6.3 implies that the stable manifold $\mathcal{W}^s(p_\epsilon)$ of p_ϵ has codimension 1 in $\mathcal{X}$. The same is then true of $\mathcal{W}^s(p_\epsilon(t_0))$ as well.

Let $\gamma_\epsilon(t)$ denote the periodic orbit of the (suspended) system with $\gamma_\epsilon(0) = (p_\epsilon, 0)$. We have

$$\gamma_\epsilon(t) = (p_\epsilon(t), t).$$

The invariant manifolds for the periodic orbit γ_ϵ are denoted $\mathcal{W}^{ss}(\gamma_\epsilon)$, $\mathcal{W}^s(\gamma_\epsilon)$, and $\mathcal{W}^u(\gamma_\epsilon)$. We have

$$\mathcal{W}^s(p_\epsilon(t_0)) = \mathcal{W}^s(\gamma_\epsilon) \cap (\mathcal{X} \times \{t_0\}),$$
$$\mathcal{W}^{ss}(p_\epsilon(t_0)) = \mathcal{W}^{ss}(\gamma_\epsilon) \cap (\mathcal{X} \times \{t_0\}),$$
$$\mathcal{W}^u(p_\epsilon(t_0) = \mathcal{W}^u(\gamma_\epsilon) \cap (\mathcal{X} \times \{t_0\}).$$

See Figure 7.6.5.

We wish to study the structure of $\mathcal{W}^u_\epsilon(p_\epsilon(t_0))$ and $\mathcal{W}^s_\epsilon(p_\epsilon(t_0))$ and their intersections. To do this, we first study the perturbation of solution curves in $\mathcal{W}^{ss}_\epsilon(\gamma_\epsilon)$, $\mathcal{W}^s_\epsilon(\gamma_\epsilon)$, and $\mathcal{W}^u_\epsilon(\gamma_\epsilon)$.

Choose a point, say $x_0(0)$, on the homoclinic orbit for the unperturbed system. Choose a codimension 1 hyperplane H transverse to the homoclinic orbit at $x_0(0)$. Since $\mathcal{W}^{ss}_\epsilon(p_\epsilon(t_0))$ is C^r close to $x_0(0)$, it intersects H in a unique point, say $x^s_\epsilon(t_0, t_0)$. Define $(x^s_\epsilon(t, t_0), t)$ to be the unique integral curve of the suspended system (4) with initial condition $x^s_\epsilon(t_0, t_0)$. Define $x^u_\epsilon(t, t_0)$ in a similar way. We have

$$x^s_\epsilon(t_0, t_0) = x_0(0) + \epsilon v^s + O(\epsilon^2),$$
$$x^u_\epsilon(t_0, t_0) = x_0(0) + \epsilon v^u + O(\epsilon^2),$$

by construction, where $\|O(\epsilon^2)\| \leq \text{const.} \cdot \epsilon^2$ and v^s and v^u are fixed vectors. Notice that

$$(P^\epsilon_{t_0})^n x^s_\epsilon(t_0, t_0) = x^s_\epsilon(t_0 + nT, t_0) \to p_\epsilon(t_0) \quad \text{as} \quad n \to \infty.$$

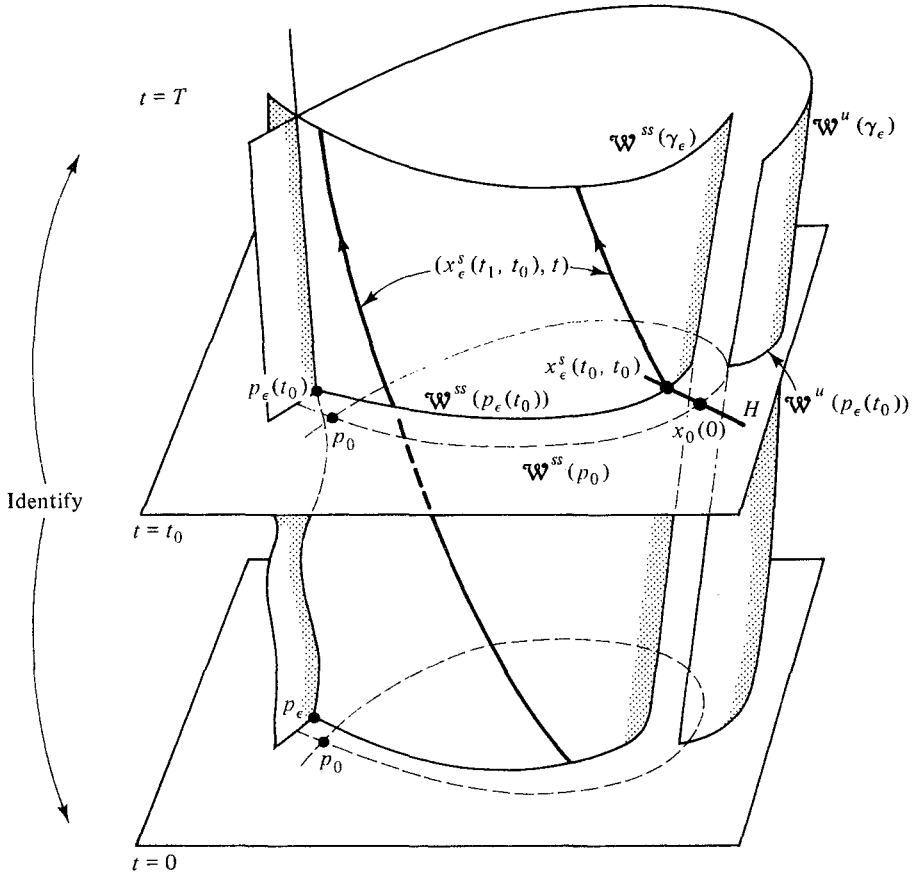

Figure 7.6.5

Since $x_\epsilon^s(t, t_0)$ is an integral curve of a perturbation, we can write

$$x_\epsilon^s(t, t_0) = x_0(t - t_0) + \epsilon x_1^s(t, t_0) + O(\epsilon^2),$$

where $x_1^s(t, y_0)$ is the solution of the first variation equation

$$\frac{d}{dt} x_1^s(t, t_0) = Df_0(x_0(t - t_0)) \cdot x_1^s(t, t_0) + f_1(x_0(t - t_0), t), \tag{9}$$

with $x_1^s(t_0, {}_{00}) = v^s$.

Define the *Melnikov function* by

$$\Delta_\epsilon(t, t_0) = \Omega(f_0(x_0(t - t_0)), x_\epsilon^s(t, t_0) - x_\epsilon^u(t, t_0))$$

and set $$\Delta_\epsilon(t_0) = \Delta_\epsilon(t_0, t_0).$$

6.5 Lemma *If ϵ is sufficiently small and $\Delta_\epsilon(t_0)$ has a simple zero at some t_0 and maxima and minima that are at least $O(\epsilon)$, then $\mathcal{W}^u_\epsilon(p_\epsilon(t_0))$ and $\mathcal{W}^s_\epsilon(p_\epsilon(t_0))$ intersect transversally near $x_0(0)$.*

The idea is that if $\Delta_\epsilon(t_0)$ changes sign, then $x^s_\epsilon(t_0, t_0) - x^u_\epsilon(t_0, t_0)$ changes orientation relative to $f_0(x_0(0))$. Indeed, this is what symplectic forms measure. If this is the case, then as t_0 increases, $x^s_\epsilon(t_0, t_0)$ and $x^u_\epsilon(t_0, t_0)$ "cross," producing the transversal intersection.

The next lemma gives a remarkable formula that enables one to explicitly compute the leading order terms in $\Delta_\epsilon(t_0)$ in examples.

6.6 Lemma *The following formula holds:*

$$\Delta_\epsilon(t_0) = -\epsilon \int_{-\infty}^{\infty} \Omega(f_0(x_0(t - t_0)), f_1(x_0(t - t_0), t))\, dt + O(\epsilon^2).$$

Proof Write $\Delta_\epsilon(t, t_0) = \Delta^+_\epsilon(t, t_0) - \Delta^-_\epsilon(t, t_0) + O(\epsilon^2)$,

where $$\Delta^+_\epsilon(t, t_0) = \Omega(f_0(x_0(t - t_0)), \epsilon x^s_1(t, t_0))$$

and $$\Delta^-_\epsilon(t, t_0) = \Omega(f_0(x_0(t - t_0)), \epsilon x^u_1(t, t_0)).$$

Using Equation (9), we get

$$\frac{d}{dt}\Delta^+_\epsilon(t, t_0) = \Omega(Df_0(x_0(t, t_0))\cdot f_0(x_0(t - t_0)), \epsilon x^s_1(t, t_0))$$
$$+ \Omega(f_0(x_0(t - t_0)), \epsilon\{Df_0(x_0(t - t_0))\cdot x^s_1(t, t_0) + f_1(x_0(t - t_0), t)\}).$$

Since f_0 is Hamiltonian, Df_0 is Ω-skew. Therefore, the terms involving x^s_1 drop out, leaving

$$\frac{d}{dt}\Delta^+_\epsilon(t, t_0) = \Omega(f_0(x_0(t - t_0)), \epsilon f_1(x_0(t - t_0), t)).$$

Integrating, we have

$$-\Delta^+_\epsilon(t_0, t_0) = \epsilon \int_{t_0}^{\infty} \Omega(f_0(x_0(t - t_0)), f_1(x_0(t - t_0), t))\, dt,$$

since

$$\Delta^+_\epsilon(\infty, t_0) = \Omega(f_0(p_0), \epsilon f_1(p_0, \infty)) = 0, \quad \text{because} \quad f_0(p_0) = 0.$$

Similarly, we obtain

$$\Delta^-_\epsilon(t_0, t_0) = \epsilon \int_{-\infty}^{t_0} \Omega(f_0(x_0(t - t_0)), f_1(x_0(t - t_0), t))\, dt$$

and adding gives the stated formula. ∎

We summarize the situation as follows:

6.7 Theorem *Let hypotheses (H1)–(H5) hold. Let*

$$M(t_0) = \int_{-\infty}^{\infty} \Omega(f_0(x_0(t - t_0)), f_1(x_0(t - t_0), t)\, dt.$$

Suppose that $M(t_0)$ has a simple zero as a function of t_0. Then for $\epsilon > 0$ sufficiently small, the stable manifold $\mathcal{W}^s_\epsilon(p_\epsilon(t_0))$ of p_ϵ for $P^\epsilon_{t_0}$ and the unstable manifold $\mathcal{W}^u_\epsilon(p_\epsilon(t_0))$ intersect transversally.

Having established the transversal intersection of the stable and unstable manifolds, one can now substitute into known results in dynamical systems (going back to Poincaré) to deduce that the dynamics must indeed be complex. In particular, Theorem 6.1 concerning Equation (1) may be deduced. The calculations needed for the examples are outlined in the following problems.

Problem 6.2 (Holmes [1980b]) Consider Equation (2). Show that the Melnikov function is given by

$$M(t_0) = \int_{-\infty}^{\infty} (\dot{x}\gamma \cos \omega t - \delta w)\, dt,$$

where x stands for $x_0(t - t_0) = (\sqrt{2\beta/\alpha})\operatorname{sech}\sqrt{\beta}\,(t - t_0)$. Evaluate the integral using residues:

$$M(t_0) = -2\gamma\pi\omega\sqrt{\frac{2}{\alpha}}\,\frac{\sin \omega t_0}{\cosh(\pi\omega/2\sqrt{\beta})} - \frac{4\delta\beta^{3/2}}{3\alpha}.$$

Thus, show that the critical value γ_c above which transversal intersection occurs is

$$\gamma_c = \frac{4\delta\beta^{3/2}}{3\omega\sqrt{2\alpha}}\cosh\left(\frac{\pi\omega}{2\sqrt{\beta}}\right).$$

Problem 6.3 Show that a homoclinic orbit for (1) is given by

$$w_0(z, t) = \frac{2}{\pi}\sqrt{\frac{\Gamma - \pi^2}{\kappa}}\sin(\pi z)\operatorname{sech}(t\pi\sqrt{\Gamma - \pi^2}).$$

Use Problem 6.2 to compute the Melnikov function and hence arrive at the bifurcation value given on p. 506.